The role of Circadian Rhythms in Epidermal Homeostasis

Peggy Janich

TESI DOCTORAL UPF / 2012

Thesis director: Dr. Salvador Aznar-Benitah

Department: Differentiation and Cancer
Epithelial Homeostasis and Cancer Group
Center for Genomic Regulation (CRG)

Für meine Großeltern,
die nie genau verstanden
was ich mache,
aber immer daran glaubten,
dass ich es kann.

ABSTRACT
RESUMEN

ABSTRACT

The natural daily cycles of light and dark have played a fundamental role in shaping the development of an adaptive intrinsic clock mechanism which allows organisms to coordinate the function of multiple organs by setting the correct circadian timing of cellular processes ensuring proper homeostasis. In mammalian skin, homeostasis is maintained by epidermal stem cells (epSCs). EpSCs localize to specialized niches where they undergo cycles of quiescence and proliferation. Several pathways are known to play essential roles in epSC function; however, how are these pathways spatiotemporally coordinated, and why not all stem cells within the niche behave in the same manner, is still poorly understood. We have analyzed the role of the molecular circadian clock in fine-tuning the behavior of epidermal stem cells. Using a fluorescent circadian reporter mouse model, we demonstrate that the dormant epidermal stem cell compartment contains two co-existing populations of stem cells in different clock states. Global comparative transcriptome analysis indicated that each clock population corresponds to a distinct predisposition state of response towards stem cell activating and dormancy cues. We provide evidence that the core circadian transcription factors BMAL1 and CLOCK bind to regulatory elements in the promoters of several of these stem cell homeostatic genes, thus being directly responsible for creating these two stem cell clock states. Unbalancing this clock driven equilibrium of epSCs *in vivo* resulted in progressive changes in the response of stem cells to activating or dormancy cues, which led to a progressive premature tissue aging, and a significant reduction in the development of cutaneous squamous cell carcinomas. Thus, our results indicate that the molecular clock machinery fine-tunes the spatiotemporal behavior of epidermal stem

cells within their niche, and that perturbation of this mechanism affects tissue homeostasis and the predisposition to neoplastic transformation.

RESUMEN

Los ciclos naturales de luz y oscuridad han sido determinantes en el desarrollo de un reloj molecular intrínseco que permite coordinar la función de múltiples órganos para mantener la homeostasis global del organismo. La homeostasis del compartimento queratinocítico de la piel depende de una población de células troncales adultas epidermales (epSCs). Las epSCs están localizadas en nichos específicos y especializados desde dónde responden a las necesidades de repoblación celular del tejido mediante la alternancia de fases de quiescencia y proliferación. Varias rutas de señalización regulan el comportamiento de las epSCs; sin embargo, aún no entendemos bien porqué no todas las epSCs se comportan de la misma manera dentro de un mismo nicho troncal, y cómo están coordinadas a nivel espacio-temporal. Hemos analizado el impacto del ritmo circadiano sobre las función de las epSCs. Mediante un ratón reportero fluorescente del ritmo circadiano hemos demostrado que el nicho troncal quiescente contiene dos poblaciones de epSCs en diferentes fases de su reloj molecular. El análisis comparativo global del transcriptoma de ambas poblaciones indicó que las dos poblaciones corresponden a dos estados opuestos de predisposición a responder a estímulos de activación y quiescencia. Mostramos resultados que demuestran que los factores de transcripción circadianos Bmal1 y Clock regulan directamente la expresión de genes que regulan el comportamiento de las epSCs. La arritmia in vivo en las epSCs resultó en una pérdida progresiva de la homeostasis tisular, un envejecimiento prematuro y una reducción significativa en el desarrollo de tumores escamosos de piel. Por lo tanto, nuestros resultados indican que la maquinaria del reloj molecular permite a las epSCs a anticiparse y coordinar su respuesta a estímulos

locales del nicho, lo que constituye un mecanismo esencial para su correcta función en el tejido.

PREFACE

The work presented in this doctoral thesis was supported by the AGAUR (Agencia de Gestio d'Adjuts Universitaris i de Recerca) and was carried out in the Epithelial Homeostasis and Cancer Group at the Center for Genomic Regulation (CRG) in Barcelona, Spain under the supervision of Dr. Salvador Aznar-Benitah.

The content of this thesis provides novel insights into how circadian rhythms regulate epidermal stem cell behavior during homeostasis and cancer and was published in Nature (2011), 480: 209-14.

TABLE OF CONTENTS

ABBREVIATIONS

APC	adenomatous polyposis coli
Arntl	aryl hydrocarbon receptor nuclear translocator-like 1
ATM	ataxia telangiectasia mutated
Axin	axis inhibition protein
Bhlhe41	basic helix-loop-helix family, member e41
BIO	6-Bromoindirubin-3-oxime
Blimp1	B lymphocyte induced maturation protein 1
Bmal1/2	brain and muscle ARNT-like 1/2 (Arntl/2)
BMP	bone morphogenetic protein
BrdU	5-Bromo-2-deoxyuridine
Ccna2	cyclin A2
Ccnb1	cyclin B1
Ccnd2	cyclin D2
Cdk4	cyclin-dependent kinase 4
Cdkn2b	cyclin-dependent kinase inhibitor 2B
Cd34	cluster designation 34
Cd71	cluster designation 71
ChIP	chromatin immunoprecipitation
Chek1/2	checkpoint kinase 1/2
CK1 α, γ, ε	casein kinase 1 α, γ, ε
Clock	circadian locomoter output cycles kaput protein
CMV	cytomegalovirus
c-Myc	v-myc myelocytomatosis viral oncogene homolog
Cry1/2	cryptochrome 1/2
CT	circadian time
Dab2	disabled homolog 2

Dbp	D-site binding protein
Dkk1/3	Dickkopf 1/3
dKO	double knock out
DMBA	7,12-dimethylbenzanthracene
DNA	deoxyribonucleic acid
Dsh	Dishevelled
EGF	epidermal growth factor
EGFR	epidermal growth factor receptor
EMEM	Eagle's minimum essential medium
epSC	epidermal stem cell
EPU	epidermal proliferative unit
EtOH	ethanol
FACS	fluorescent activated cell sorting
FBS	fetal bovine serum
FGF	fibroblast growth factor
Flg2	filaggrin family member 2
Fzd2	frizzled homolog 2
Gadd45a/b	growth arrest and DNA damage-inducible protein α/β
GFP	green fluorescent protein
GSK3	glycogen synthase kinase 3
H19	H19 fetal liver mRNA
HAT	histone acetyltransferase
HF	hair follicle
IFE	interfollicular epidermis
Itga6	integrin alpha 6
Jarid1a	jumonji, AT rich interactive domain 1A
K14	keratin 14
K5	keratin 5

ABBREVIATIONS

Ki67/Mki67	antigen identified by monoclonal antibody Ki 67
KO	knock out
Lce	late cornified envelope
Lef1	lymphoid enhancer-binding protein 1
Lefty	left-right determination factor 1
Lgr5/6	leucine-rich repeat containing G protein-coupled receptor
Lhx2	LIM homeobox 2
Lor	loricrin
LRC	label retaining cell
Lrig1	leucine-rich repeats and immunoglobulin-like domains 1
Lrp5/6	low-density lipoprotein receptor-related protein 5/6
Ltbp2	latent TGF-β binding protein 2
Mdm-2	Mdm2 p53 binding protein homolog
Notch2	Notch gene homolog 2
Nr1d1	nuclear receptor subfamily 1, group D, member 1
p53	transformation related protein 53
PCR	polymerase chain reaction
Per1/2/3	Period 1/2/3
PMA	phorbol-12-myristate-13-acetate
Pum1	Pumilio 1
Rad9	DNA repair exonuclease rad9 homolog
Rev-Erbα	nuclear receptor subfamily 1, group D, member 1 (Nr1d1)
RIPA	radio immunoprecipitation assay
Rorα	RAR-related orphan receptor alpha
rpm	rotations per minute
SC	stem cell
SCC	squamous cell carcinoma
SCN	suprachiasmatic nuclei

SDS	sodium dodecyl sulfate
SHH	sonic hedgehog
Sfrp	secreted Frizzled-related protein
Sin3a	SIN3 transcription regulator homolog A
Sirt1	Sirtuin-1
Smad2/3/4/7	SMAD family member 2/3/4/7
Smurf	SMAD specific E3 ubiquitin protein ligase 1
Sos	Son of Sevenless
Sox9	SRY-box containing gene 9
Sppr1	sphingosine-1 phosphate receptor 5
TA	transit amplifying
Tcf3/4	T-cell factor 3/4
TGFβ	transforming growth factor beta
Tgfbr2	transforming growth factor beta receptor II
Tgm3	transglutaminase 3
TPA	12-O-tetradecanoylphorbol-13-acetate
UV	ultra violet
Wnt	wingless
Wnt3/3a/10a	wingless-related MMTV integration site 3/3a/10a
WT	wild type
ZT	Zeitgeber time

INTRODUCTION

I INTRODUCTION

1. Introduction to epidermal stem cells

1.1 The skin

The skin is a complex organ that comprises the dermis, epidermis and therein embedded appendages like hair follicles, sebaceous glands, sweat glands, nerves, blood and lymph vessels. It seals our body from the outside and serves as a protection barrier against pathogens, UV radiation and water loss. It is also essential for temperature regulation, sensation, secretion and absorption.

Mammalian skin, like other epithelial tissues, has a high turnover rate that maintains life-long homeostasis and ensures proper regeneration upon damage. The outermost layer of the skin, the epidermis, is a multilayered epithelium organized in various differentiation specific layers (Fig. 1). Since terminally differentiated cells are permanently shed from the surface of the epidermis, new cells must be constantly replenished from the subjacent cell layers. In addition, skin appendages like the hair follicles and sebaceous glands undergo rhythmically re-occurring cycles of growth and regression throughout the lifetime of the organism. This cellular turnover is guaranteed by a population of well-defined epidermal stem cells (epSCs) that undergo constant self-renewal in order to maintain tissue function. These epSCs localize to specialized niches where they remain quiescent and undifferentiated, but become proliferative and egress their niche in the need of epidermal replenishment, during the hair cycle, and wound repair.

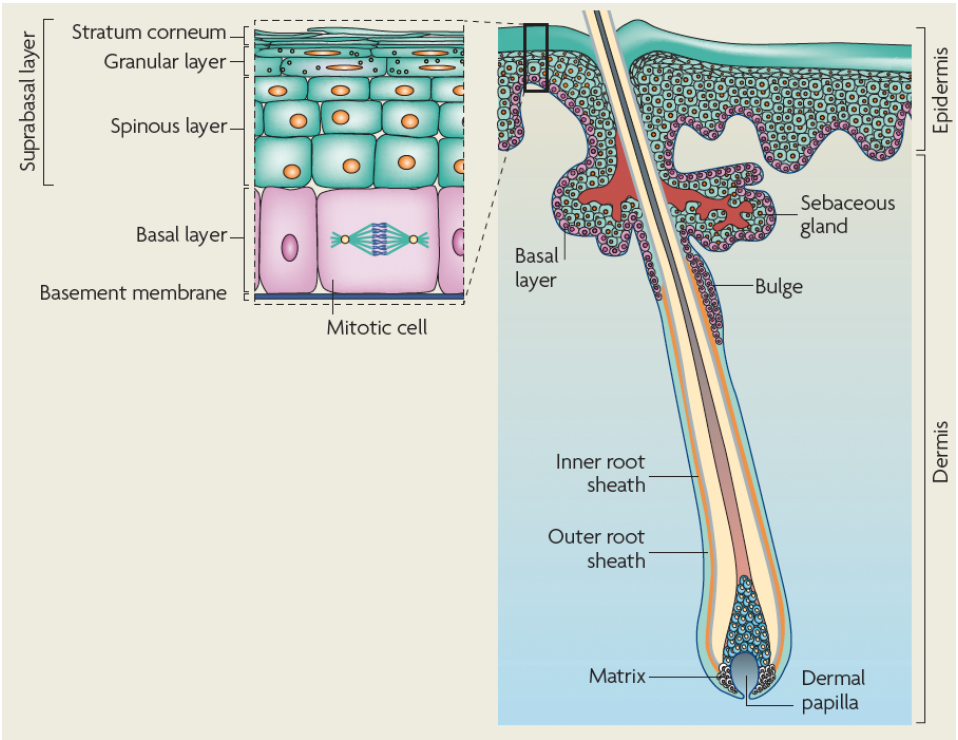

Figure 1: Architecture of the mammalian epidermis (adapted from Jones and Simons, 2008).

1.2 Epidermal stem cells

Epidermal stem cells have been identified in different compartments e.g. the interfollicular epidermis (IFE), sebaceous gland, and in the upper isthmus and bulge region of the hair follicle (Fig. 2). Under normal homeostatic conditions epSCs become periodically activated, give rise to actively proliferating transit amplifying (TA) cells, which subsequently exit the cell cycle and form all the differentiated lineages of the individual compartment. Under challenging conditions, such as wounding, epSCs can leave their compartment and give also rise to the cell progeny of the other compartments, thus showing their multipotency (Levy et al., 2005; 2007;

Horsley et al., 2006; Ito et al., 2007). So far the best-studied epSCs are those of the interfollicular epidermis and the bulge region of the hair follicle.

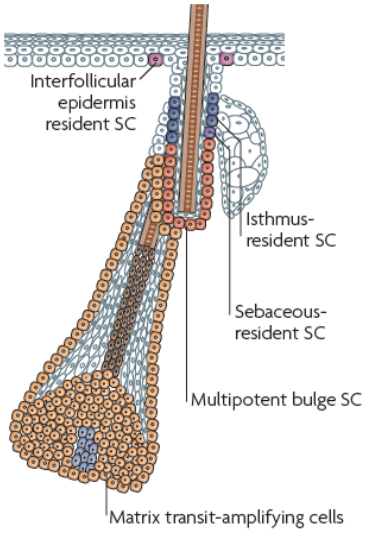

Figure 2: Localization of epidermal stem cells in the skin (adapted from Blanpain and Fuchs, 2009)

1.2.1 Interfollicular stem cells

The murine interfollicular epithelium is organized in epidermal proliferative units (EPUs) formed by a stack of hexagonally packed cells comprising approximately 10 cells at its base in the basal layer (Mackenzie, 1970; Potten, 1974). Interfollicular SCs are located in the basal layer in close contact with the underlying basement membrane and express high levels of adhesion molecules, such as α6- and β1-integrins (Jones et al., 1995). Unlike human interfollicular epidermis, where long term quiescent interfollicular SCs are responsible for homeostasis, murine interfollicular epidermis is maintained by stem cells that divide on a daily basis. The progeny of the SC (known as transit amplifying cell) then undergoes several rounds of division before it de-adheres from the basement membrane and differentiates along the suprabasal layers (Clayton et al., 2007; Jones and Simons, 2008). Upon commitment to terminal differentiation, keratinocytes

progress through several differentiation stages and form three distinct consecutive layers; the spinous, granular and cornified layer. The morphological and biochemical changes, characteristic for each stage of differentiation, reflect the sequential expression of several structural proteins. Cells of the spinous layer contain high levels of Involucrin, granular layer cells express Filaggrin, and Loricrin and Cornifin are characteristic for the cornified layer. The activation of transglutaminase in these layers leads to covalent crosslinking of the latter proteins and the formation of a protective cornified envelope. Once left the basal layer, keratinocytes also change their keratin decor; they start to loose the expression of Keratin 5 and 14 and express instead suprabasal keratins like Keratin 1 and 10, that localize to the spinous and granular layer (Candi et al., 2005).

1.2.2 Hair follicle stem cells and the hair cycle

Hair follicles are particularly well suited for exploring epSCs function since they undergo cyclical rounds of rest (telogen), growth (anagen) and degeneration (catagen), which are dependent on proper stem cell function. Furthermore, murine hair follicle development and cycling are strictly timed through the concerted action of hair follicle stem cells, allowing for population studies (Fig. 3).

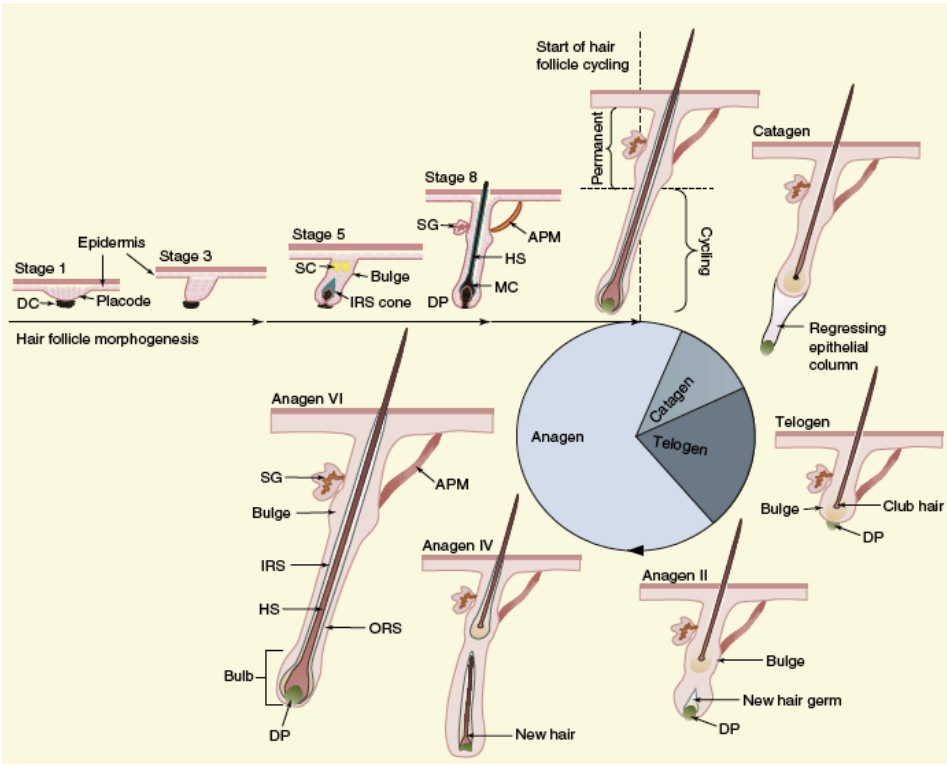

Figure 3: Hair follicle morphogenesis and key stages of the hair cycle (adapted from Schneider et al., 2009)

Hair follicles are formed in the embryo starting at E14.5 when a group of dermal fibroblasts called dermal papilla leads to the condensation and invagination of epidermal cells into the dermis to form the hair-originating placode (Fuchs, 2007; Schneider et al., 2009). The developing follicle extends downwards and encloses the dermal papilla, which sustains the cells at the base in a highly proliferative state. During hair follicle maturation proliferating matrix cells start to differentiate into the hair shaft and the outer and inner root sheath that are separated by the companion layer (Fuchs, 2007; Schneider et al., 2009). This entire phase is termed hair follicle morphogenesis and is completed 2 weeks after birth when hair

follicles enter the first hair cycle. At this time hair follicles reach a destructive phase (catagen) characterized by high levels of apoptosis and tissue remodeling in the lower two-thirds of the hair follicle. The subsequent first resting phase (telogen) lasts only 1-2 days before all hair follicles enter synchronously into the growth phase of the first hair cycle at around postnatal day P19-P21. During anagen onset SCs of the hair follicle, which reside in the outer root sheet in a region called the bulge (Fig. 2), become activated and migrate into the lower proliferative hair germ region, where they form a large pool of TA matrix progenitors that differentiate into the inner hair lineages (Greco et al., 2009; Zhang et al., 2009). Subsequently, at mid-anagen (P22-P28), the bulge undergoes a second round of activation, which replenishes bulge cells that were lost at the onset of anagen (Greco et al., 2009; Zhang et al., 2009). During late anagen (P29-P35), the percentage of proliferative bulge cells decreases and during subsequent catagen (P36-P42) and telogen (starting at P43) bulge cells enter a new phase of quiescence (Greco et al., 2009; Zhang et al., 2009). After each subsequent hair cycle the length of telogen phase extends, hair follicle growth occurs unsynchronized and in distinct patches throughout the body, and cycling frequency is reduced as animals age (Schneider et al., 2009). Nevertheless, synchronous entry into anagen can also be induced at later stages either by depilation or ectopically applied chemicals like the phorbol ester TPA that induces aberrant proliferation on treated skin areas.
In addition to the bulge cells, SCs with uni- and multipotent characteristics have also been described in the isthmus region, that is located between the bulge and the sebaceous gland (Nijhof, 2006; Jensen et al., 2009; Snippert et al., 2010), in the infundibulum (Jensen et al., 2008) and in the sebaceous gland (Horsley et al., 2006).

It is worth mentioning that the hair follicle does not only harbor epithelial stem cells, but also neural-crest-derived melanocyte SCs (Nishimura et al., 2005; 2010; Steingrímsson et al., 2005) and Nestin-expressing SCs (Amoh et al., 2005; Uchugonova et al., 2011) as well as mesenchymal SCs in the connective tissue sheath (Lako et al., 2002).

1.2.3 Epidermal stem cell markers

For basic research and potential medical purposes it is necessary to identify individual stem cell populations. Until now, two methods have been mainly used for the identification of epidermal SCs: i) approaches to mark slow-cycling cells *in vivo*; and ii) the use of SC specific biomarkers (Blanpain and Fuchs, 2006; 2009; Pincelli and Marconi, 2010).

Slow cycling stem cells can be distinguished by means of label retention assays that use either BrdU (Bickenbach, 1981; Cotsarelis et al., 1990; Blanpain and Fuchs, 2006) or a tetracycline-controllable Histone H2B-GFP (Tumbar et al., 2004; Fuchs, 2009) to label these cells. Cells that continuously or repeatedly proliferate dilute their label as they divide, whereas slow cycling cells retain the label and are therefore termed label retaining cells (LRCs) (Bickenbach, 1981). It was speculated that LRCs constituted the *bonafide* stem cells, since they were the longest-lived cells within the epidermis. This has been demonstrated by several groups with elegant functional assays and lineage tracing experiments (Tumbar et al., 2004; Morris et al., 2004). However, it should be mentioned that quiescence is not the defining feature of stem cells since several tissues such as the intestinal epithelium, and as mentioned above the interfollicular epidermis, are maintained by pools of continuously proliferating stem cells (Blanpain and Fuchs, 2006; Haegebarth and Clevers, 2010).

A variety of stem cell specific proteins allow for discriminating the different epidermal SC populations found in the skin. During the last decade, several gene expression profiling studies identified Keratin-15, CD34 and α6-integrin as bulge specific SC markers (Fig. 4) (Tumbar et al., 2004; Morris et al., 2004; Blanpain et al., 2004).

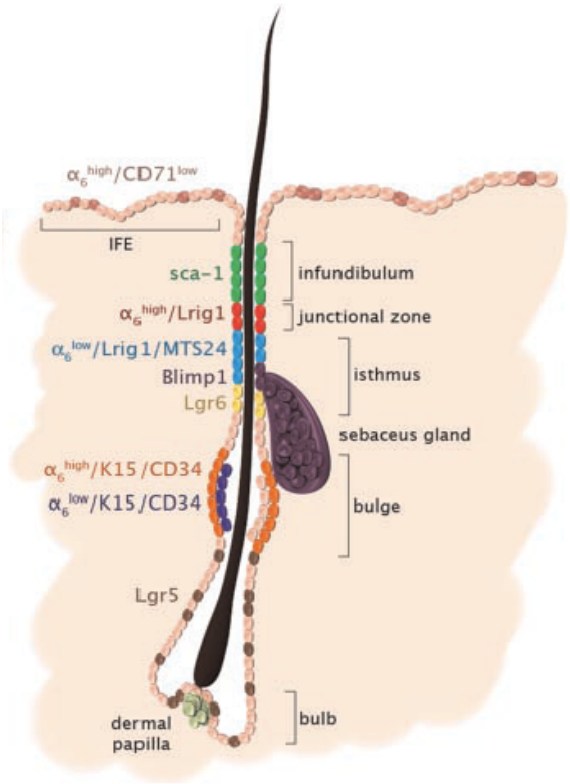

Figure 4: Epidermal stem cell marker (adapted from Pincelli and Marconi, 2010)

Bulge cells expressing CD34 co-localize widely with LRCs and show high colony-forming ability *in vitro*. In combination with α6-integrin, $CD34^{+}$ bulge SCs can be further divided into $CD34^{+}/\alpha6\text{-integrin}^{bright}$ and $CD34^{+}/\alpha6\text{-integrin}^{low}$ populations, which correspond to the basal and the suprabasal cells of the bulge (Fig. 4) (Blanpain et al., 2004). The $CD34^{+}/\alpha6\text{-integrin}^{low}$

cells appear only after the first hair cycle and are considered as the more quiescent progeny of the basal bulge SCs (Blanpain et al., 2004). A subpopulation of bulge SCs, located in the lower part of the bulge, can be marked by the expression of Lgr5, and is thought to constitute a more frequently proliferating fraction of hair follicle stem cells (Jaks et al., 2008). Isthmus resident SCs can be distinguished and purified through their high levels of Lgr6 and high expression of MTS24 and Lrig1 (Snippert et al., 2010; Nijhof, 2006; Jensen et al., 2008; 2009). The unipotent SC populations of the infundibulum and the sebaceous gland were shown to express Sca-1 and BLIMP1, respectively (Jensen et al., 2008; Horsley et al., 2006). And as mentioned beforehand, SCs of the interfollicular epidermis are characterized by their high expression of α6-integrin and low levels of transferrin receptor CD71 (Fig. 4) (Tani et al., 2000).

Candidate stem cells, which have been selected by the presence or absence of different markers are used frequently in colony forming assays to assess their stem cell potential *in vitro* (Barrandon and Green, 1987). However, not only cell intrinsic factors account for the characteristics of a stem cell, but also its interactions with the microenvironment (stem cell niche), which is defined by cell-cell and cell-matrix contacts, and by different growth factors and cytokines.

1.3 Relevant pathways important for epSC regulation

Several pathways have been shown to act directly on stem cells or on the niche to modulate stem cell fate. Pathways required for maintenance/quiescence, activation and specification of epidermal and HF stem cells during development and in adult mice are Wnt/β-catenin, bone morphogenetic protein (BMP), transforming growth factor-beta (TGF-β),

fibroblast growth factor (FGF), sonic hedgehog (SHH), epidermal growth factor (EGF) and Notch signaling pathway, among others (Fuchs, 2007; Schneider et al., 2009). The spatiotemporal interplay and the relative amounts of multiple molecular regulators of these pathways control cellular decisions to ensure proper epidermal homeostasis.

1.3.1 The Wnt/β-catenin pathway

The Wnt signaling pathway is critical for neonatal HF morphogenesis and the activation of bulge SCs during HF cycling in the adult. In particular, canonical Wnt signaling in which the transcriptional regulation of Wnt target genes is mediated through β-catenin is essential for hair follicle stem cell activation and onset of differentiation (Fig. 5). In the absence of WNT ligands, β-catenin is phosphorylated in the cytoplasm by a 'destruction complex' containing Axin, APC, glycogen synthase kinase 3β (GSK3β) and casein kinase 1α (CK1α). This leads to the degradation of β-catenin by the proteasome and prevents its entry to the nucleus. Thus, prospective target genes are kept 'OFF' through the binding of T-cell factor (TCF) and lymphoid enhancer-binding protein (LEF) and associated co-repressors. In addition, several extracellular Wnt inhibitors aid to maintain the pathway inactive, including Dickkopfs (DKKs) and secreted Frizzled-related proteins (SFRPs) (Fig. 5a) (Moon et al., 2004; Klaus and Birchmeier, 2008; MacDonald et al., 2009).

The Wnt/β-catenin pathway is activated when WNT ligands interact with seven-transmembrane Frizzled receptors (FZDs) and their co-receptor, the low-density lipoprotein receptor-related protein 5 and 6 (LRP5/6). The binding of WNT to the Frizzled/LRP5/6 complex leads to phosphorylation of LRP5/6 by GSK3β and casein kinase 1γ (CK1γ) and interaction of the

phosphoprotein Dishevelled (DSH) with Frizzled receptors. These events mediate the translocation of the 'destruction complex' to the plasma membrane, where Axin directly binds to the cytoplasmic domain of LRP5/6. The inhibition of the 'destruction complex' allows stabilization of β-catenin, which travels to the nucleus and interacts with DNA-bound TCF/LEF to activate the transcription of Wnt target genes (Fig. 5b) (Moon et al., 2004; Klaus and Birchmeier, 2008; MacDonald et al., 2009).

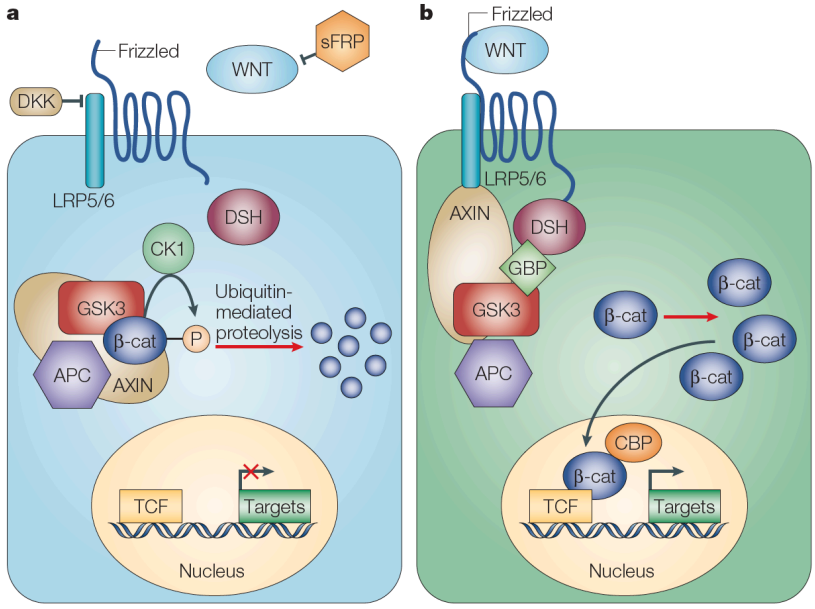

Figure 5: a) Inactive Wnt/β-catenin pathway. **b)** Active Wnt/β-catenin pathway (adapted from Moon et al., 2004).

In the embryo, it was shown that conditional ablation of β-catenin or overexpression of the Wnt inhibitor DKK1 blocks hair placode formation during development, which leads consequently to the loss of specification of the HF stem cell niche (Huelsken et al., 2001; Andl et al., 2002). Similarly, deletion of Lef1 arrests HF development and causes alopecia (van Genderen et al., 1994). Conversely, ectopic expression of β-catenin leads to de novo

hair follicle morphogenesis and tumor formation (Gat et al., 1998; Celso, 2004). Transient expression of active β-catenin in telogen HFs of adult mice induces precocious activation of bulge stem cells and subsequent proliferation and differentiation (Van Mater, 2003; Lowry et al., 2005). Further, Wnt/β-catenin/Lef1 are important to induce differentiation in matrix cells, which generate the hair shaft (DasGupta and Fuchs, 1999). Tcf3 and Tcf4 are essential for long-term maintenance of epSCs and for wound repair, although some of the functions mediated by Tcf3 and Tcf4 have been shown to be Wnt-independent (Merrill, 2001; Nguyen et al., 2009). Also the Wnt-regulated transcription factors Sox9 and Lhx2 have been shown to be important for HF morphogenesis, bulge SC maintenance and HF cycling (Vidal et al., 2005; Nowak et al., 2008; Rhee et al., 2006; Törnqvist et al., 2010).

1.3.2 The TGF-β pathway

Transforming growth factor-beta (TGF-β) is a multifunctional cytokine that is important to maintain homeostasis by controlling essential cellular functions, including growth arrest, apoptosis, migration, adhesion and other physiological and pathological responses (Siegel and Massagué, 2003; Massagué and Gomis, 2006; Ikushima and Miyazono, 2010). In mammals, three isoforms of TGF-β exist (TGF-β1, 2 and 3) that signal through TGF-β type I and II receptors and transmit the signal through intracellular SMAD proteins that regulate the transcription of a large number of target genes. In brief, TGF-β ligands bind to the type II receptor, which leads to the immediate recruitment of the TGF-β type I receptor and the formation of a heterotetrameric complex, in which the type II receptor phosphorylates the type I receptor close to its kinase domain. The activated type I receptor then

phosphorylates receptor associated SMADs (SMAD2/3), which releases them from cytoplasmic anchoring proteins and allows their interaction with SMAD4. Subsequently, heteromeric SMAD complexes enter the nucleus, bind together with other DNA-binding transcription factors, as well as co-activators or co-repressors, to SMAD-responsive promoter elements in their target genes, leading to gene activation or repression (Fig. 6).

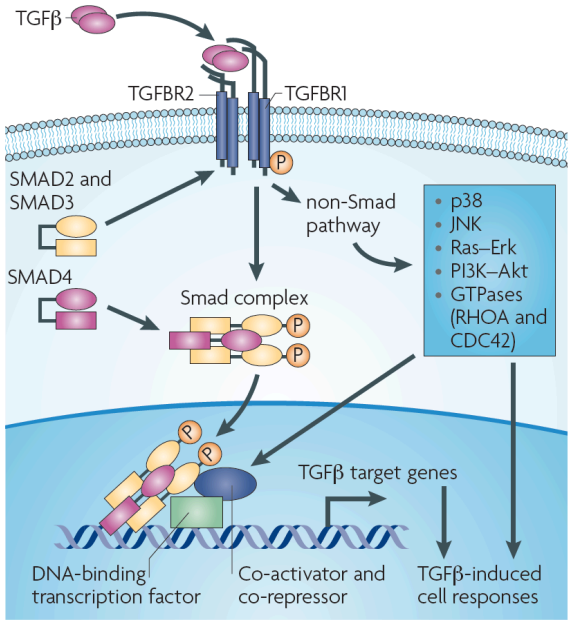

Figure 6: TGF-β signaling pathway (adapted from Ikushima and Miyazono, 2010).

SMAD proteins become dephosphorylated and shuttle back to the cytoplasm as soon as the TGF-β stimulus disappears (Siegel and Massagué, 2003; Massagué and Gomis, 2006). The activated TGF-β receptor complex can also induce the mobilization of a protein complex composed of SMAD7, which is an inhibitory SMAD, and SMURF, which acts as an E3 ubiquitin ligase, from the nucleus to the cytoplasm (Ebisawa, 2001; Tajima, 2003;

Siegel and Massagué, 2003). This complex ubiquitylates the activated TGF-β receptor and mediates its internalization thereby terminating the TGF-β signal (Di guglielmo 2003)(Siegel and Massagué, 2003). In addition, SMAD7 can compete for DNA binding and repress the transcriptional activity of signaling SMADs (Zhang et al., 2007). TGF-β signaling is further regulated by the action of LTBPs (latent TGF-β binding proteins). LTBPs are covalently attached to TGF-β molecules and, unless cleaved, keep them in an inactive complex, which prevents binding of the ligands to their receptors (Annes, 2003).

In the skin, several TGF-β signaling components, including TGF-β2, LTBPs and activated SMAD2, are enriched in dormant bulge SCs of the hair follicle (Tumbar et al., 2004). TGF-β1 is highly expressed in the bulge and ORS of cycling HFs and has been shown to inhibit cell proliferation and to control hair follicle regression through the induction of apoptosis (Foitzik et al., 2000). Transient overexpression of TGF-β1 in adult mice blocks re-entry of telogen HFs into anagen and causes resistance to PMA (phorbol 12-myristate 13-acetate) and TPA-induced hyperplasia (Cui et al., 1995; Wang et al., 1999; Liu et al., 2001). Conversely, expression of a dominant negative type II TGF-β receptor abolishes TGF-β induced growth arrest and causes epidermal hyperplasia (Wang et al., 1997). Hence, TGF-β signaling pathway, next to BMP signaling, is one of the pathways that transmit quiescent signals to epSCs and their niche. A role of TGF-β in SC quiescence has also been described in other stem cell populations, including hematopoietic SCs (Batard et al., 2000; Larsson, 2003; Karlsson et al., 2007; Yamazaki et al., 2009), melanocyte SCs (Kim et al., 2004; Nishimura et al., 2010), and neuronal SCs (Falk et al., 2008).

1.4 Skin cancer

Loss of function or continuous aberrant regulation of essential pathways disturbs tissue homeostasis and can lead to the process of tumorigenesis. One of the most frequent skin cancers, which arises mainly in sun-exposed regions of the skin is the squamous cell carcinoma (SCC). Normally, SCC can be cured by surgical excision if detected at early stages, but patients that present with metastatic SCC have only a 10-20% survival rate (Alam and Ratner, 2001). In order to investigate the molecular causes of SCC development, cancer mouse models are frequently studied in medical research.

In mice, SCC can be induced either chemically by continuous treatments with mutagenic agents (DMBA/TPA) (Kemp, 2005) or by gain or loss of function mutations of key genes implicated in critical signaling pathways. In this study, we used Keratin-5-SOS mice as a cancer mouse model for squamous tumors. These mice express oncogenic Son of Sevenless (SOS) under the regulation of the Keratin 5 promoter (K5-SOS) (Sibilia et al., 2000). SOS signals downstream of the epidermal growth factor receptor (EGFR), and acts as a guanine exchange factor activator of Ras GTPase, an oncogen that is frequently mutated and hyperactive in SCC (van der Schroeff et al., 1990; Spencer et al., 1995). In a EGFR mutant-heterozygous or wildtype background, K5-SOS mice spontaneously develop squamous tumors, primarily in the tail, with 100% penetrance (Sibilia et al., 2000; Lichtenberger et al., 2010). K5-SOS mice have the advantage that they develop neoplastic lesions as early as 2-3 weeks of age, whereas mutagenic-induced SCC will only appear after several months of treatment (Kemp, 2005).

2. Introduction to circadian rhythms

2.1 General aspects of circadian rhythms

The natural day and night cycles caused by the earth's rotation around its axis have played a fundamental role in shaping the evolutionary development of an intrinsic clock mechanism in most light-sensitive organisms. This intrinsic clock enables organisms to anticipate and synchronize physiological and metabolic processes to the appropriate time of the day. In mammals, many aspects of physiology follow circadian rhythms, including sleep-wake cycles, hormone production, blood pressure, renal function, body temperature, and food intake. Circadian rhythms show oscillations with a periodicity of around 24 hours (from the Latin *circa diem*, "about a day"). They are entrained by several environmental *Zeitgeber* (time giver) signals, among which light is the most dominant synchronizer. Light stimulates specialized photoreceptive neuronal ganglion cells in the retina of the eye, which transmit the stimulus via the optic nerve to the central circadian pacemaker, the suprachiasmatic nuclei (SCN) (Panda, 2007). The SCN is composed of 10,000-20,000 neurons and locates to the anterior hypothalamus of the brain. It transmits the rhythmic information through neuronal and hormonal signals to all cells of the body and simultaneously integrates information from peripheral organs to generate consistent rhythms in the organism. Circadian clocks are present in almost all peripheral tissues, including liver, heart, lungs, kidney and skin, where they maintain circadian rhythmicity within the tissue and modulate tissue-specific gene expression in concert with transcription factors and chromatin remodelers (Asher et al., 2008; 2010; Duong et al., 2011a; DiTacchio et al., 2011). Several genome wide transcriptome profiling studies revealed that up to 15% of all transcripts are rhythmically expressed throughout the day

depending on the tissue analyzed (Panda et al., 2002; Storch et al., 2002). These oscillations allow the cell to time biological functions chronologically and to segregate antagonistic biological processes, which is energetically favorable for the organism.

Circadian rhythms are self-sustained, meaning that oscillations can persist even in the absence of an external Zeitgeber, e.g. when mice are maintained under constant darkness for a longer period of time. Further, they are cell-autonomous, since even cells in culture that have been propagated for years possess robust circadian oscillations when synchronized by a serum or dexamethasone shock (Balsalobre et al., 1998; Balsalobre, 2000). On the molecular level circadian rhythms are controlled by transcriptional and translational feedback loops of several positive and negative regulators.

2.2 The mammalian molecular circadian clock machinery

The mechanism of interconnected negative feedback loops by which circadian rhythms are orchestrated is conserved from cyanobacteria to mammals. In mammals, the main positive regulators are BMAL1 and CLOCK, or its homologue NPAS2, which are basic-helix-loop-helix (bHLH) transcription factors, that heterodimerize and bind to E-box elements in promoters of target genes to induce their expression (Fig. 7). Among clock-controlled target genes are Cryptochrome 1 and 2 (Cry1/2), Period 1-3 (Per1, Per2 and Per3), Rorα and Rev-Erbα, which are an integral part of the circadian core machinery. As PER proteins accumulate in the cytoplasm, they are phosphorylated by CKIε and GSK3, which targets them for ubiquitin mediated protein degradation. However, when CRY protein levels rise in the cytoplasm, they form stable complexes with PER proteins and translocate to nucleus. Once it the nucleus, CRY/PER complexes repress BMAL1/CLOCK activity, resulting in the arrest of their own transcription

(Fig. 7). The circadian core is further stabilized by opposing functions of RORα and REV-ERBα, which are both transcription factors, that bind to RRE-elements in the Bmal1 promoter. RORα activates the transcription of Bmal1, whereas REV-ERBα inhibits it (Fu and Lee, 2003; Gallego and Virshup, 2007; Sahar and Sassone-Corsi, 2009). Besides phosphorylation, other post-translational modifications, including sumoylation and acetylation, have been shown to participate in the functional regulation of clock protein activity (Cardone et al., 2005; Hirayama et al., 2007). Furthermore, several chromatin-remodeling enzymes are associated with BMAL1/CLOCK complexes to modulate gene transcription, e.g. SIRT1, JARID1a and SIN3A (Asher et al., 2008; DiTacchio et al., 2011; Duong et al., 2011b). In addition, the CLOCK protein itself has been shown to possess an intrinsic histone acetyltransferase (HAT) activity (Doi et al., 2006).

Circadian oscillations, which are fine-tuned at different transcriptional and translational levels, create a network of clock controlled signaling pathways. Several cycle regulators, such as c-Myc, Cyclin D1, Mdm-2 and Wee1, are under circadian regulation (Fu et al., 2002; Matsuo et al., 2003). Metabolic genes involved in energy homeostasis, detoxification, fatty acid and glucose metabolism show cyclic transcript patterns in a tissue-specific manner (Turek et al., 2005; Yang et al., 2006b; Eckel-Mahan and Sassone-Corsi, 2009; Hatanaka et al., 2010). Moreover, PER1 directly interacts with the check-point proteins ATM and CHEK2, which mediate double-strand break repair in response to DNA damage (Gery et al., 2006).

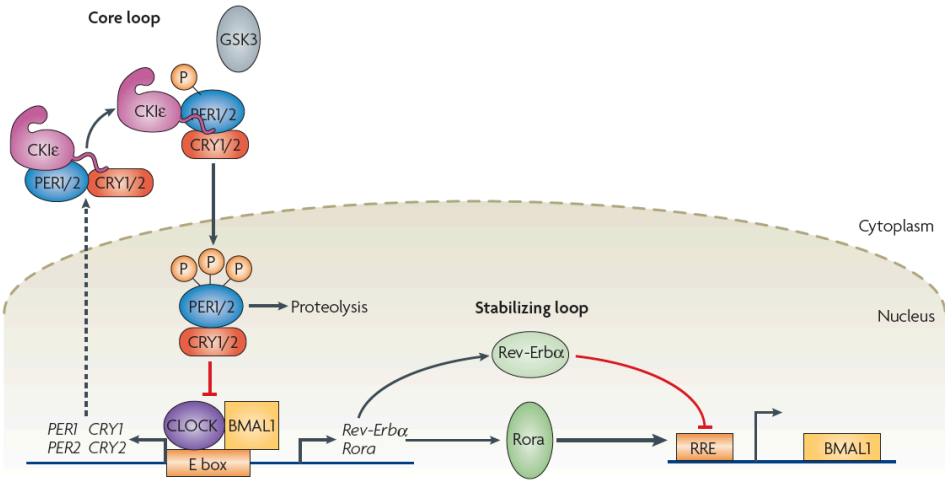

Figure 7: The mammalian circadian clock is regulated by feedback loops (adapted from Gallego and Virshup, 2007).

2.3 Disruption of circadian rhythmicity in humans

Since circadian rhythms coordinate many physiological and metabolic processes, it is not surprising that perturbations of this clock mechanism lead to the development of several pathological diseases, including neurological illnesses (e.g. depression), sleep- and metabolic disorders, and cancer.

In humans the simplest form of clock perturbation occurs by travelling to a different time zone. This de-synchronization of the SCN causes transient disturbances of sleep behavior, gastrointestinal and renal tract function, generally described as jet lag. A chronic form of jet lag with long term consequences on health, is shift work. Several studies have shown that extended shift work increases the risk to develop breast, prostate and colorectal cancers (Davis et al., 2001; Schernhammer et al., 2003; Megdal et al., 2005; Kubo, 2006; Gery and Koeffler, 2010). Further, it was shown that the expression of Per genes is lost or down-regulated in several types of cancer, including breast, lung, colorectal and prostate cancer, as well as

leukemias and lymphomas, suggesting their role as tumor suppressors. Thereby, loss of Per gene function occurs mainly through epigenetic silencing due to DNA methylation or mutations in Per genes (Gery et al., 2005; Chen et al., 2005; Yang et al., 2006a; Winter et al., 2007; Kuo et al., 2009; Hoffman et al., 2009; Zhu et al., 2011). Gain of function experiments *in vitro* demonstrated that forced expression of Per1 and Per2 in cancer cells induces growth arrest and apoptosis (Gery et al., 2006; 2007; Yang et al., 2011). In addition, a sleep disorder observed in humans where individuals sleep and wake at very early times could be directly associated with a point mutation in the Per2 gene. This point mutation disrupts a phosphorylation site, affecting PER2 protein stability, which consequently leads to a shortening of the period length (Toh, 2001; Xu et al., 2007).

2.4 Disruption of circadian rhythmicity in mouse

To investigate the consequences of circadian clock perturbation in mammalian physiology, a variety of mouse models with one or more genetically ablated clock gene have been generated. Circadian phenotypes are generally assessed by monitoring the wheel running behavior of mice under free-running conditions (e.g. constant darkness), when external timing cues are absent and the organism has to rely on its intrinsic clock. The deletion of each single gene of the circadian core machinery, except Bmal1, has been shown to cause a shortened or lengthened period in wheel running activity (summarized in Ripperger et al., 2011). The ubiquitous deletion of Bmal1 leads to circadian arrhythmicity, meaning total disruption of circadian behavior without the need to perturb any other member of the circadian core machinery (Bunger et al., 2000). Furthermore, Bmal1 knock out mice have reduced body weight and shortened life-spans, and show signs of premature aging, including organ shrinkage, cataracts, reduced

subcutaneous fat and defects in hair follicle cycling (Kondratov et al., 2006; Lin et al., 2009). Interestingly, Bmal1 KO mice do not have a predisposition to tumor formation even when challenged by γ-radiation (Lee et al., 2010). Since complete genetic ablation of Bmal1 has notable consequences on many physiological processes, a conditional knock out model was generated (Storch et al., 2007). The tissue specific knock out of Bmal1 in the liver, retina, and pancreatic islets leads to hypoglycemia, disturbed visual processing and diabetes, respectively (Storch et al., 2007; Lamia et al., 2008; Marcheva et al., 2010). These studies have demonstrated that circadian rhythms are directly involved in the control of physiological processes in peripheral organs.

Similar to Bmal1 knock out mice, Period1 and Period2 double mutant mice (Per1/2dKO) become immediately arrhythmic under free-running conditions, whereas mice deficient for only one of these genes display only mild behavioral phenotypes (Zheng et al., 1999; 2001; Bae et al., 2001). Since all PER proteins are structurally similar there might be a certain degree of redundancy so that they can compensate for each other in their circadian function. Per1/2dKO mice show sustained expression of Bmal1 target genes, since PER proteins are components of the negative limb that normally inhibits BMAL1/CLOCK function (Zheng et al., 2001). Further, Per1/2dKO mice develop spontaneous and radiation induced tumors, comprising lymphomas, liver and ovarian tumors. It was shown that circadian clock perturbation in Per1/2dKO mice affects p53 signaling, which consequently leads to the activation of oncogenic c-Myc (Lee et al., 2010).

Also Per2 single mutant mice are more susceptible to lymphomas after γ-radiation and display altered expression of cell cycle regulators and tumor suppressors, including c-Myc, Cyclin D1 and Gadd45α and loss of p53

activity (Fu et al., 2002). Tumor incidence in Per1 single mutant mice has not yet been studied.

Another group of mouse models that allow the visualization of circadian rhythms in living animals are based on the expression of luciferase or fluorescent protein reporters. The expression of the reporter is either under the control of a clock gene specific promoter or it is expressed as fusion protein together with a clock protein (summarized in Ripperger et al., 2011). Therefore, transgenic reporter mice are well suited to explore the role of circadian rhythms during development, homeostasis and tumorigenesis.

OBJECTIVES

II OBJECTIVES

Several pathways are known to play essential roles in epSC function; nevertheless, little is still understood about their hierarchy, how they are coordinated, the reasons for stem cell heterogeneity within the niche, and how SCs are aberrantly regulated during aging or neoplastic transformation. In this thesis we study the role of circadian clock genes in epSC in order to shed some light on these issues. In particular, we addressed the following questions:

1. Do epSC possess circadian rhythms?
2. Do circadian rhythms control epSC function?
3. Does perturbation of the circadian clock affect epSC behavior?
4. Does clock perturbation have an impact on tumorigenesis?

RESULTS

III RESULTS

3.1 Experimental strategy

To study the role of circadian rhythms in epSCs we decided to use the mouse as model system and acquired several genetically modified mice targeting the molecular circadian clock machinery.

By means of two independent transgenic reporter mice, in which the expression of green fluorescent protein (GFP) or fluorescent Venus is under the regulation of a 3.1 kb fragment or the full-length promoter of the *Per1* gene, activity of the circadian clock could be monitored *in vivo* (Kuhlman et al., 2000; Cheng et al., 2009). GFP or Venus expression mirrors the endogenous oscillation of the Per1 protein, thereby establishing its *bonafide* circadian reporter activity (Kuhlman et al., 2000; LeSauter et al., 2003; Cheng et al., 2009).

To study the biological significance of circadian clocks in the epidermal compartment, we first investigated mice with a conditional deletion of *Bmal1*, which is a positive clock regulator, in Keratin-14 expressing basal cells of the interfollicular epidermis and the hair follicle (K14Cre/Bmal1$^{LoxP/LoxP}$). Second, we analyzed Period1 and Period2 double mutant mice, which lack the negative limb of the molecular clock, thus having augmented Bmal1 function (Zheng et al., 2001). Finally, we investigated the effect of circadian clock perturbation on carcinogenesis using a mouse model that develops cutaneous squamous tumors (Sibilia et al., 2000).

3.2 Epidermal SCs are heterogeneous in their clock

We first studied the behavior of the clock in the dorsal skin of Per1-Venus mice collected between postnatal days 19 (P19) and P31, when hair follicles

synchronously transit from the dormant (telogen) to the growth phase (anagen). Interestingly, immunohistochemistry for Venus (anti-GFP) revealed that the expression of Venus in the bulge stem cell compartment is not homogenous, but that Venus^{bright} and Venus^{dim} cells co-exist within the bulge at any of the analyzed ages (Fig. 8).

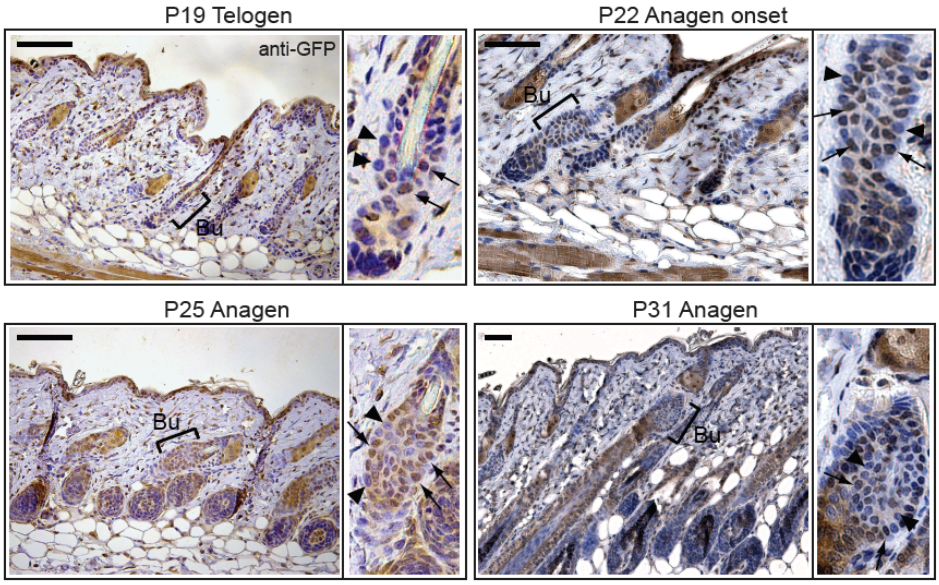

Figure 8: Bulge stem cells are heterogeneous in their clock.
Immunohistochemistry of Venus-GFP in Per1-Venus mouse backskin at different hair cycle stages (P19, P22, P25 and P31) shows Venus^{bright} (arrow) and Venus^{dim} (arrowhead) cells in the bulge (Bu, bulge). Scale bar, 100 μm.

To further quantify the number Venus^{bright} and Venus^{dim} cells in the bulge and basal epidermis of Per1-Venus mice, FACS analysis of Venus fluorescence was performed at different days between P19 and P31. At P19, a stage in which the bulge is predominantly dormant, the α6 integrin^{bright}/CD34^{+} bulge population contained approximately equal numbers of Venus^{bright} and Venus^{dim} stem cells (Fig. 9 a, c).

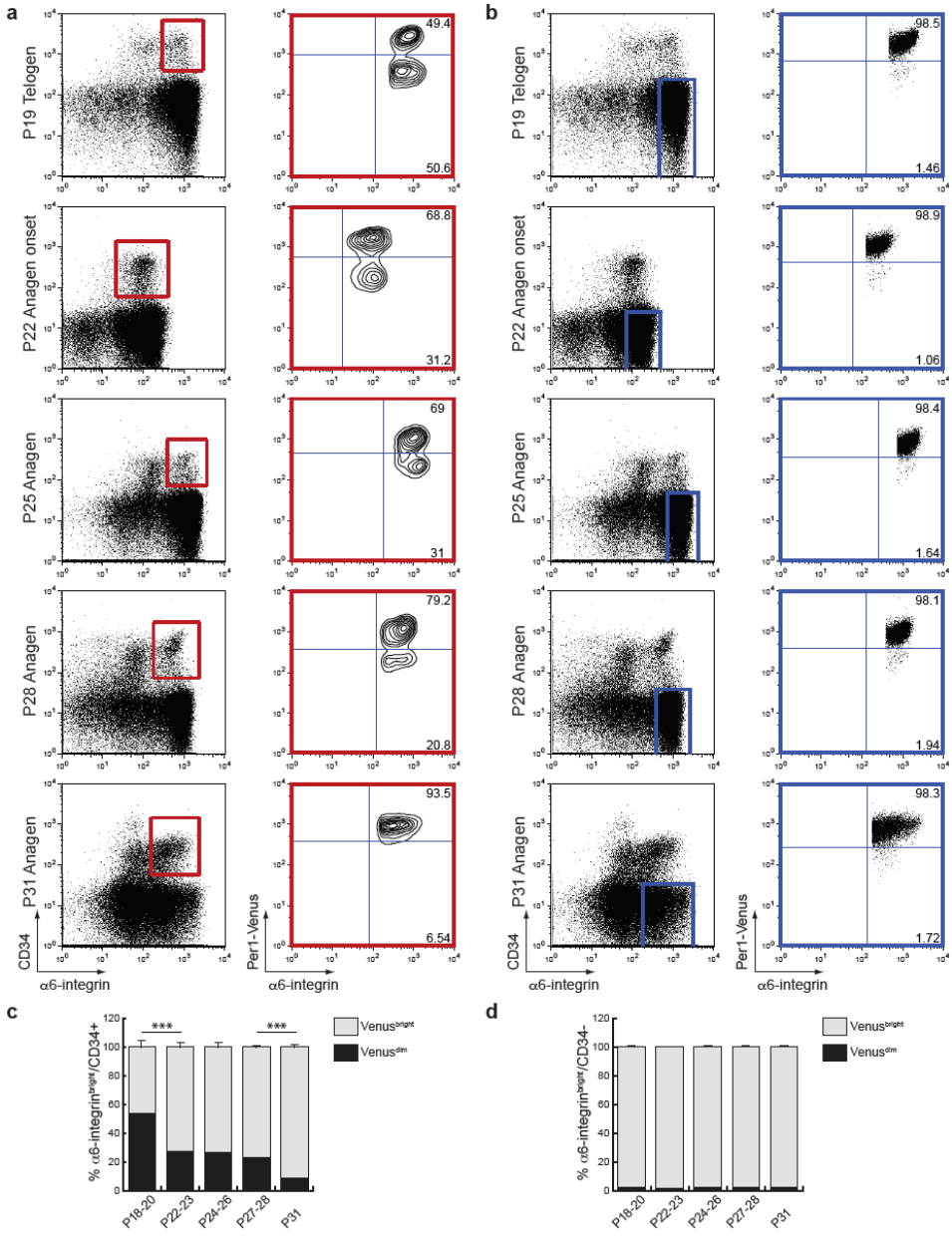

Figure 9: Per1-Venus expression during the hair cycle.
Quantification of Venus^{bright} and Venus^{dim} cells in the α6-integrin^{bright}/CD34+ bulge (**a**, **c**) and the α6-integrin^{bright}/CD34- epidermal population (**b**, **d**) of Per1-Venus mice at different stages of the hair cycle (P19, P22, P25, P28 and P31) by FACS (mean ± s.e.m.; n ≥ 6).

As hair follicles synchronously progressed into anagen (from P20 to P31), the proportion of Venus^{bright} bulge cells steadily increased, reaching a proportion of 90% Venus^{bright} to 10% Venus^{dim} at the peak of follicle growth (Fig. 9 a, c). Conversely, the basal layer of the interfollicular epidermis (α6 integrin^{bright}/CD34^{-}) displayed a homogenous pattern of clock activity with a ratio of approximately 95:5 Venus^{bright}:Venus^{dim} cells, irrespective of the day analyzed (Fig. 9 b, d).

Heterogeneity of the clock phase in bulge cells during the telogen to anagen transition was also observed with another independently generated reporter line, Per1-GFP, as shown by imaging direct GFP fluorescence or anti-GFP staining in 3D-wholemounts of tail epidermis (Fig. 10 a). Interestingly, immunostaining for GFP showed also robust GFP expression in the isthmus region, another niche for hair follicle stem cells that feed into the epidermis and sebaceous glands (Fig. 10 b) (Jensen et al., 2009).

Figure 10: Dynamic changes of clock gene expression during the hair cycle in Per1-GFP reporter mice.
a, Whole mount immunostaining of mouse tailskin from Per1-GFP mice at different stages of the hair cycle (P19, P22, P27 and P31) showed steady increase of GFP^{bright} cells in the bulge compartment during anagen. Upper panel, anti-GFP staining; lower panel, direct GFP fluorescence. Scale bar, 100 μm. **b**, Immunostaining for GFP (red) and Keratin 14 (K14; green) revealed strong GFP expression in the isthmus region, which contains epSCs that feed into the epidermis and sebaceous glands. Scale bar, 50 μm. Bu, bulge; SG, sebaceous gland; Ist, isthmus; UI, upper isthmus; and HG, hair germ.

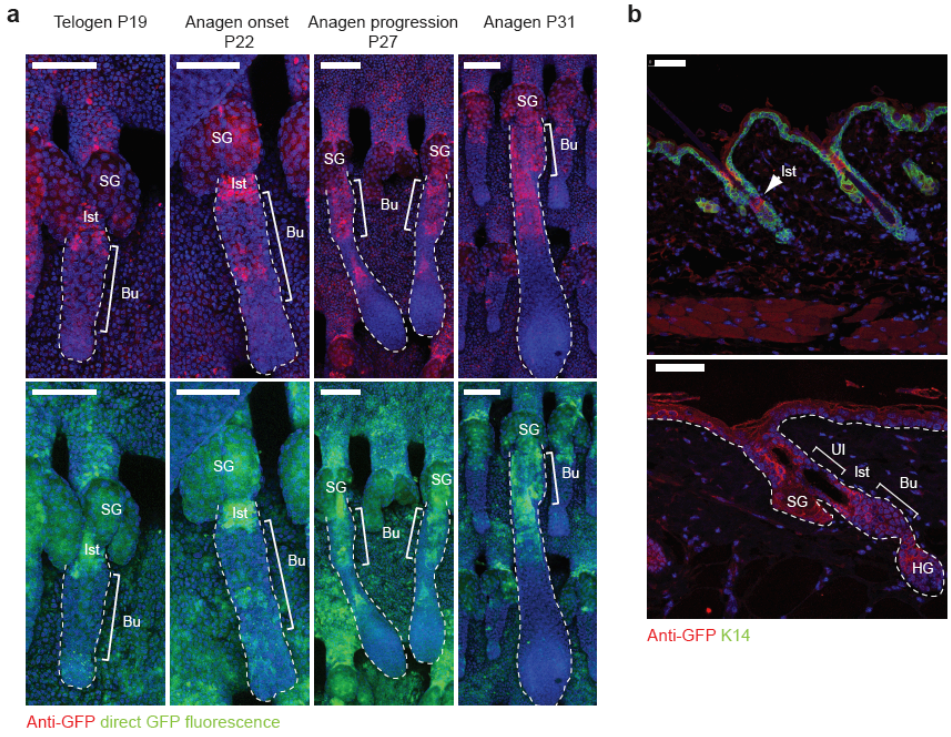

3.3 Epidermal stem cells show circadian oscillations

To verify whether these stem cells with high clock activity (Venus^{bright}) displayed circadian rhythmicity, FACS analysis was performed at 4 different time-points (every 6 hours) during a period of 24 hours in Per1-Venus mice in anagen (P27). Both, bulge and interfollicular epidermis cells, showed a circadian pattern of Venus expression with a peak in Venus mean fluorescence intensity at the onset of the dark phase (CT12), as it was reported previously for the suprachiasmatic nuclei of these mice (Fig. 11 a, b) (Cheng et al., 2009). This circadian variation in Venus expression occurred irrespective of whether the mice were maintained in 12 hour light/dark cycles (LD), or in the absence of light as an external circadian synchronizer when maintained in constant darkness under free running

conditions (DD) (Fig. 11 a, b).

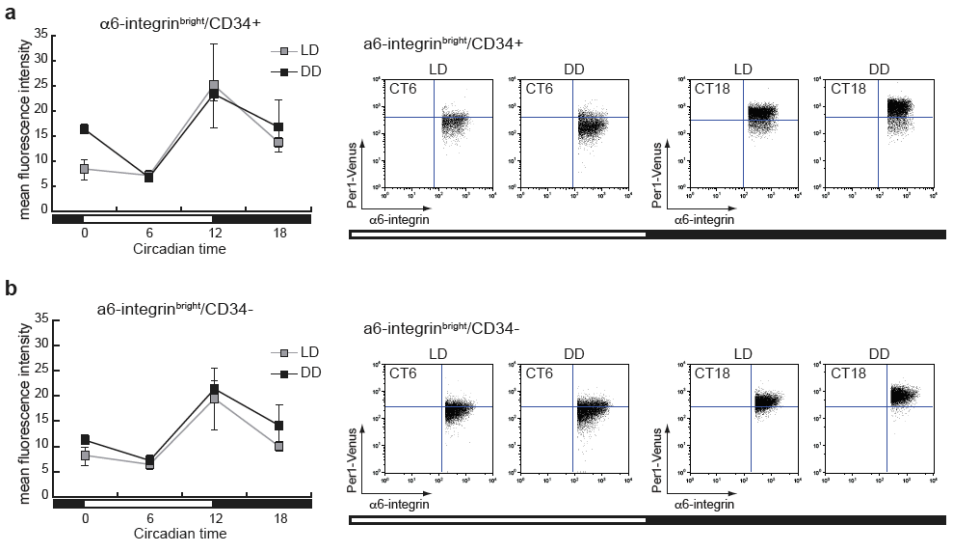

Figure 11: Venus expression changes in a circadian manner.
a, **b**, Comparison of Venus mean fluorescence intensity in α6-integrin^{bright}/CD34+ bulge (**a**) and α6-integrin^{bright}/CD34- epidermal cells (**b**) from P27 Per1-Venus mice kept under LD and DD conditions (one representative FACS profile is shown at CT6 and CT18 from each group; the gate to separate Venus^{bright} from Venus^{dim} cells was placed in all profiles according to the time point of brightest Venus fluorescence intensity at CT12). The graph in **a** and **b** shows the mean fluorescence quantification of 4 different time points (mean ± s.e.m.; n = 2). White and black bars represent subjective day and night. CT, circadian time; LD, 12 h light/12 h dark condition; DD, 12 h dark/12 h dark condition.

This circadian variation was further confirmed by a second approach using time-lapse *in vivo* confocal microscopy of whole dorsal skin explants that were biopsied from adult Per1-Venus mice and imaged in a heated chamber during 24 hours (Fig. 12 a). Fluorescence quantification of individual Venus^{bright} nuclei revealed an increase in Venus expression during the subjective night (ZT12-ZT24). Cosinor analysis, used for predicting rhythms in biological time series, confirmed circadian oscillations in Venus expressing bulge cells with a p-value < 0.001.

These circadian differences were also evident in the second reporter mouse

model shown by whole mount staining of tail epidermis isolated from Per1-GFP mice during the morning (ZT3) and evening (ZT12) (Fig 12 b).

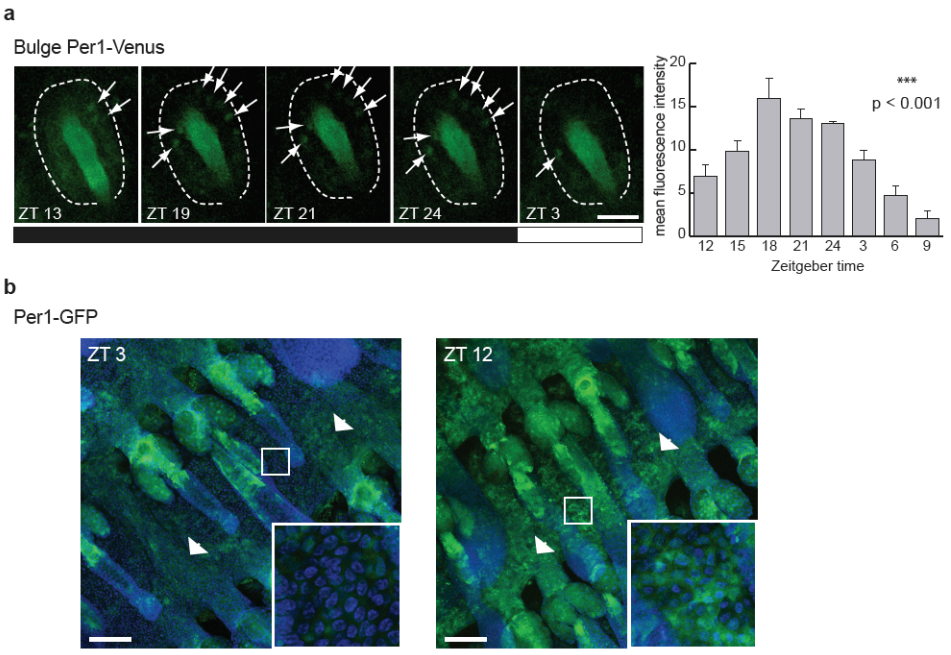

Figure 12: Venus/GFP expression changes in a circadian manner.
a, Time-lapse confocal imaging of telogen backskin of Per1-Venus mice reveals an increase in Venus^{bright} nuclei in the bulge over 24 hours (n = 5 nuclei; mean ± s.e.m.; *** $p < 0.001$ using Cosinor analysis). **b**, Whole mount immunostaining of mouse tailskin from Per1-GFP mice at Zeitgeber time ZT3 (3 hours of light) or ZT12 (12 hours of light) shows clear differences in GFP intensity in the basal epidermis (arrow and higher magnification) comparing morning (ZT3) to the evening (ZT12). Scale bars, 100 μm. ZT, Zeitgeber time.

3.4 Venus^{bright} and Venus^{dim} SCs display functional differences

In order to understand the impact of circadian clock differences in bulge SCs in-depth, we compared the global transcriptomes of FACS-purified Venus^{bright} and Venus^{dim} bulge cells from the dorsal skin of P18-19 mice using Affymetrix arrays. As expected, both populations showed differential expression of core circadian transcripts, such as Cry2, Per1, Nr1d1, Rorβ, Dec2, and E4BP4 (Fig. 13 and Table 1)[1]. Intriguingly, although the bulge is

inactive at P18-19, both populations differed in the expression of a significant number of genes previously shown to constitute the bulge signature (Morris et al., 2004; Tumbar et al., 2004; Zhang et al., 2009; Schneider et al., 2009). Venus^{bright} bulge SCs expressed higher levels (between 1.4- to 3-fold) of Wnt-signaling factors, including Tcf3, Fzd2/3, Sox9, Lhx2, Lgr5, Lef1, Dkk3, and Dab2, as well as TGFβ-inhibitory proteins such as Smad7, Ltbp2/3/4, Smurf, Lefty, and Cullin1 (Fig. 13 and Table 1)[1]. Other pathways differentially expressed and relevant for bulge behavior related to integrins, Notch, Bmp, and Shh, among others (Fig. 13). Thus, the co-existing clock states of dormant bulge SCs correlated with differential expression of key epidermal homeostasis genes.

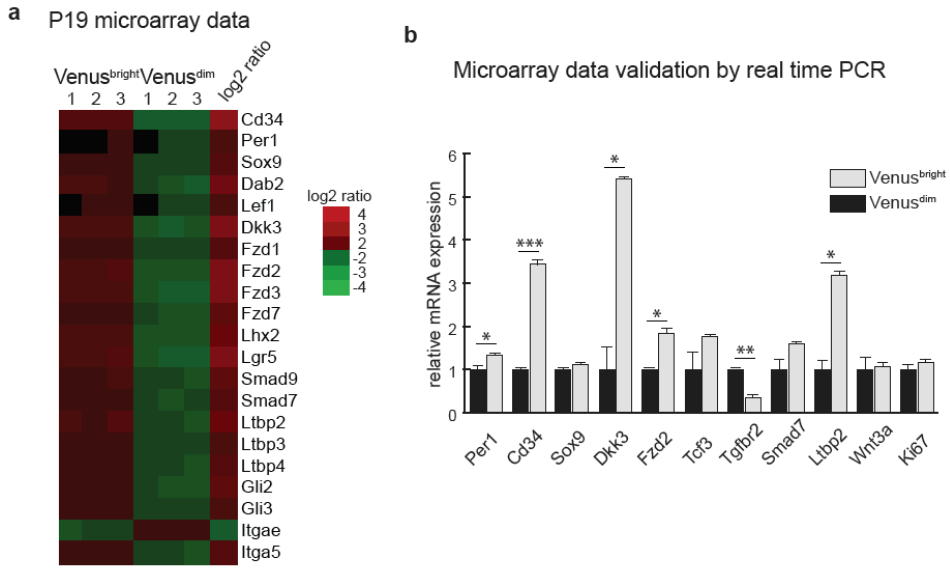

Figure 13: Profiling of Venus^{bright} and Venus^{dim} bulge cells.
a, Heatmap of selected genes from arrays of FACS-purified Venus^{bright} and Venus^{dim} bulge cells of P19 Per1-Venus mice (n = 3). **b**, Validation of microarray data by real-time PCR. Fold-change values are displayed as relative expression to Venus^{dim} cells after normalization to Pumilio1 (Pum1) (n = 2, pool of 6 mice per replicate). Results are shown as mean ± s.e.m.; * $p < 0.05$, ** $p < 0.01$, *** $p < 0.001$ (two-tailed Student's t-test).

The transcriptional differences of Venus^{bright} and Venus^{dim} cells translated also into functional differences of bulge and basal epidermal SCs, respectively (Fig. 14). When plated at clonal density, Per1-Venus^{bright} cells displayed a higher growth potential than the corresponding Venus^{dim} population, further suggesting that cells with high circadian clock activity (Venus^{bright} or clock^{high}) are more prone to become activated than the clock^{low} counterpart (Venus^{dim}).

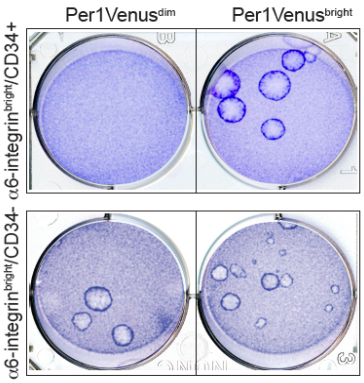

Figure 14: Clonogenic assay of Venus^{bright} and Venus^{dim} bulge and epidermal cells. Clonogenic assay of FACS-purified Venus^{bright} and Venus^{dim} α6-integrin^{bright}/CD34+ bulge and integrin^{bright}/CD34- epidermal cells from the backskin of P19 Per1-Venus mice ($7x10^3$ bulge and $1x10^5$ epidermal cells were plated).

3.5 Direct regulation of epSC genes by the circadian clock

Hence, we analyzed gene promoter sequences to understand whether epidermal homeostasis genes, encoding for proteins known to control bulge dormancy, activation, differentiation and niche interactions are directly regulated by the circadian transcriptional machinery. Promoter analysis revealed that several of these genes contain putative BMAL1/CLOCK-binding sites within their proximal and distal promoter regions (Table 2)[2]. These included the Wnt signaling factors, Dab2, Lef1, Dkk3, Fzd2, Sox9, Lhx2, and Tcf4; TGF-β regulators such as Smad7, Lefty, Smurf2, and Smad9; and integrin α6 as well as modulators of Bmp and Notch signaling (Table 2)[2]. We confirmed by chromatin immunoprecipitation (ChIP) that BMAL1

and CLOCK bind to these promoters in intact adult tail epidermis (Fig. 15 a), and by performing time-course ChIP experiments (every 3 hours during a period of 24 hours) that BMAL1 was recruited in a circadian manner to these promoters (Fig. 15 b). Chromatin occupancy of BMAL1 to these genes was also confirmed by ChIP analysis in FACS sorted bulge SCs (Fig. 15 c).

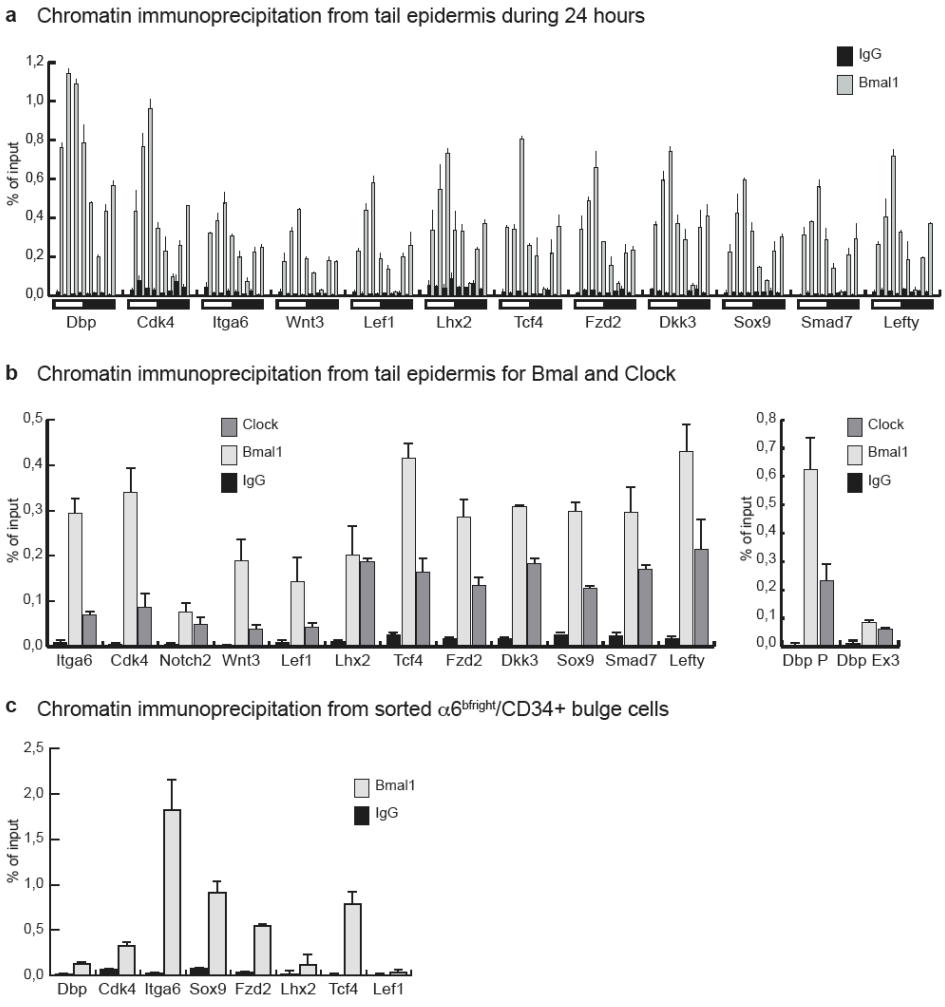

Figure 15: Bmal1 and Clock bind to the promoters of genes involved in adhesion, cell cycle, TGFβ and Wnt pathways.
a, Chromatin immunoprecipitation from tail epidermis of WT mice. Epidermis was collected every 3 hours during a period of 24 hours (white and black bar represent day and night) (n = 2). **b**, ChIP for Bmal1 and Clock from tail epidermis of WT mice. ChIP for Bmal1 and Clock in regions of the circadian-regulated gene Dbp was used as positive (P, promoter) and negative control (Ex3, exon 3) (n = 3). **c**, ChIP from FACS-purified bulge cells of WT mice. All graphs show the percentage of immunoprecipitated DNA over the input on the y-axis. The result from one representative experiment is shown as mean ± s.e.m.

3.6 Abrogation of clock function

We next sought to study the biological significance of this circadian clock mechanism in epidermal stem cells *in vivo*. To this end, we generated mice with a conditional deletion of Bmal1 in the Keratin-14+ basal keratinocyte compartment (K14Cre/Bmal1$^{LoxP/LoxP}$, hereafter referred as Bmal1KO) (Fig. 16 a). Deletion of Bmal1 was confirmed by PCR using gene specific primers for the engineered Bmal1 locus and by western blot for BMAL1 in epidermal cells isolated from Bmal1WT (K14Cre/Bmal1$^{Wt/Wt}$) and Bmal1KO mice (Fig. 16 b). In addition, we crossed Bmal1KO and Per1-Venus mice in order to verify that the circadian clock of bulge SCs and basal interfollicular epidermal cells was arrhythmic, and permanently skewed towards a clock^{low} (Venus^{dim}) state, irrespective of the time analyzed (Fig. 16 c).

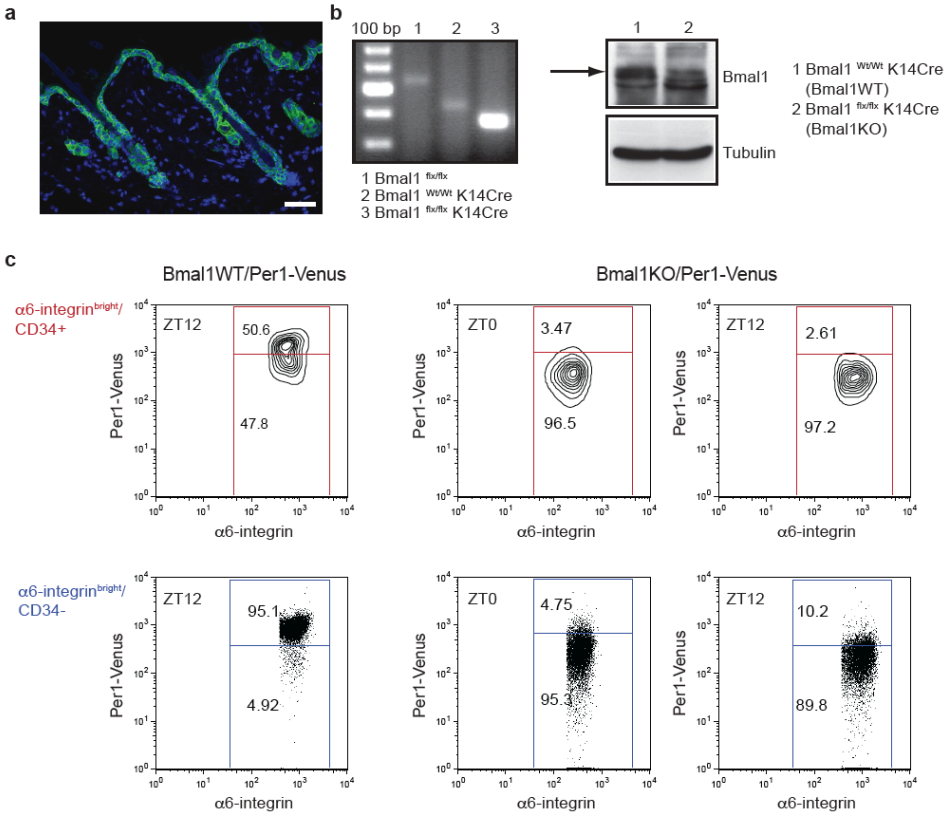

Figure 16: Conditional deletion of Bmal1 in the epidermis.
a, Immunostaining for Keratin 14 (green) to mark Cre-expressing cells in the epidermis. Scale bar, 50 μm. **b**, Efficiency of loxP recombination in the epidermis of K14Cre/Bmal1$^{flx/flx}$ (Bmal1KO) mice was assessed by PCR from genomic DNA of epidermal cells (left panel; lane 1, conditional allele; lane 2, WT allele; lane 3, recombined allele) and by western blot for Bmal1 in keratinocytes isolated from Bmal1WT or Bmal1KO mice (right panel; arrow). **c**, Conditional deletion of Bmal1 affects the expression of Venus in the epidermis of Bmal1KO/Per1-Venus mice. Quantification of Venus^{bright} and Venus^{dim} cells in the α6-integrin^{bright}/CD34+ bulge and α6-integrin^{bright}/CD34- epidermal population by FACS revealed a loss of Venus expression in Bmal1KO/Per1-Venus mice at ZT0 and ZT12 as compared to Bmal1WT/Per1Venus mice at ZT12 (numbers show percentages; n ≥ 3).

3.7 Effects of circadian clock perturbation

Cultured primary keratinocytes isolated from newborn Bmal1KO mice expressed lower transcript levels of Wnt related genes including Dab2, Dkk3, Lef1 and Wnt10a and higher amounts of TgfbR2 and Smad3 compared to WT cells (Fig. 17). All time-course experiments (n=3) showed a clear trend towards reduced Wnt and elevated TGFβ signaling in Bmal1KO cells, although it was not statistically significant (2-way ANOVA).

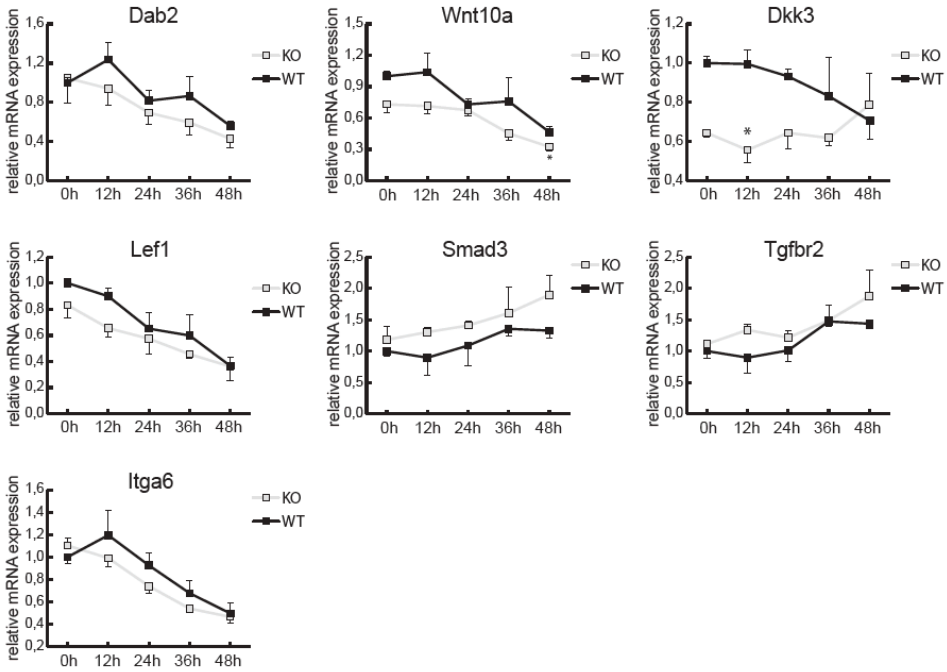

Figure 17: Real time PCR of adhesion, cell cycle, Wnt and TGFβ pathway genes in cultured mouse keratinocytes of Bmal1WT and Bmal1KO mice.
Fold-change values are displayed as relative mRNA expression levels to Bmal1WT cells at 0h after normalization to Pumilio1 (Pum1) (n = 3). Results are shown as mean ± s.e.m., * $p < 0.05$ (two-way ANOVA with Bonferroni post-test).

However, FACS-purified bulge stem cells from 10 months-old Bmal1WT and KO mice showed pronounced differences in the expression of genes implicated in Wnt and TGFβ signaling, some of which were indeed statistical significant (Fig. 18 a). Bmal1KO bulge SCs contained lower mRNA levels of Wnt related genes, including Sox9, Fzd2, Tcf3, Dab2, and Wnt10a and TGFβ inhibitors, like Smad7 and Ltbp2 and, as observed in cultured cells from newborn mice, higher amounts of TgfbR2 and Smad3 (Fig. 17 and 18 a). In addition, they showed reduced expression of Cd34, α6-integrin, Cdk4 and the circadian controlled gene Dbp. Moreover, the expression of several Wnt and TGFβ-related factors varied in purified bulge SCs within a 12 hour period in WT mice, but not Bmal1KO mice (Fig. 18 b).

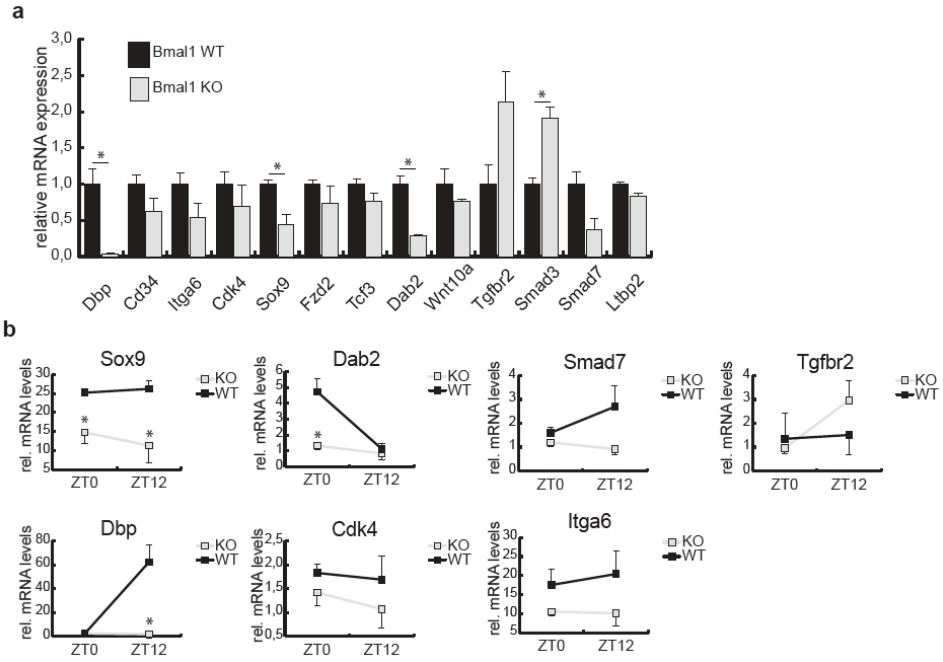

Figure 18: Bmal1 modulates the response of epidermal cells to activation and dormancy cues.
a, Real time PCR of FACS-purified bulge cells from 10-month-old Bmal1WT (WT) and Bmal1KO mice (KO). **b**, Real time PCR of FACS-purified bulge cells from 9-month-old Bmal1WT (WT) and Bmal1KO mice (KO) at 2 different time points (ZT0 and ZT12). Expression levels are shown as relative mRNA levels after normalization to Pumilio1 (Pum1) (n = 2). Results are shown as mean ± s.e.m., * $p < 0.05$ (two-tailed Student's t-test). ZT, Zeitgeber time.

Accordingly, the hair follicles of Bmal1KO mice showed the same differences at the protein level, as exemplified by immunohistochemical analysis of SOX9, LEF1, phospho-SMAD2 and TGFBR2 in dorsal skin sections of 10 months-old animals, and western blot from tail epidermis (Fig. 19).

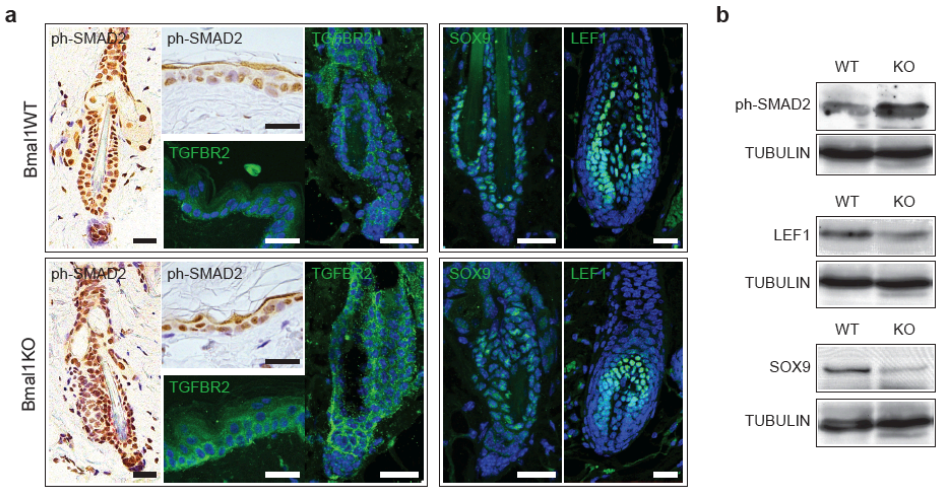

Figure 19: Bmal1KO mice show differences in the Wnt and TGFβ pathway.
a, Immunostaining for phospho-SMAD2, TGFBR2, LEF1 and SOX9 in the backskin of Bmal1WT and Bmal1KO mice (n ≥ 5). Scale bars, 25 μm. **b**, Western blot analysis for phospho-SMAD2, LEF1 and SOX9 in extracts from tail epidermis of 9-month-old Bmal1WT and Bmal1KO mice. Lanes represent extract from one WT and one KO animal; n = 3 mice were analyzed for each group; TUBULIN expression served as loading control.

Altogether these results suggested that the clock machinery might endow subpopulations of epidermal SCs with different predispositions to respond to dormancy or activation stimuli, such as TGFβ and Wnt. In line with this, the hair follicle bulge and interfollicular epidermis of Bmal1KO mice contained higher levels of active phospho-SMAD2 (Fig. 19). Moreover, Bmal1KO keratinocytes were more responsive to TGFβ than control keratinocytes when treated with TGFβ1 or 2 for 48 hours (Fig. 20).

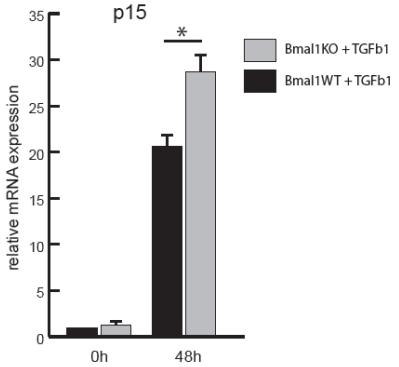

Figure 20: Primary mouse keratinocytes show enhanced responsiveness to TGFβ.
Primary mouse keratinocytes of Bmal1KO mice show increased levels of p15 expression when treated with TGFβ1 for 48 hours (n = 3).

To investigate to role of canonical Wnt signaling in Bmal1 deficient epidermal cells, we treated primary mouse keratinocytes with the GSK3b inhibitor BIO (6-Bromoindirubin-3-oxime) and measured Wnt activity by means of TOP-flash and FOP-flash reporter plasmids. These plasmids express luciferase under the control of intact (TOP) or mutated (FOP) TCF/Lef1 binding elements. In all performed experiments we could not detect any Wnt reporter TOP-Flash activity in our primary cultures of mouse keratinocytes stimulated with BIO for 24 hours (Fig. 21), which was in accordance with previous reports (Kameda and Sugiyama, 2005). This prevented us from further studying the effect of Bmal1 deletion on Wnt responsiveness.

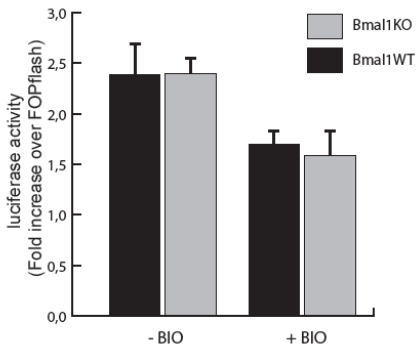

Figure 21: Primary mouse keratinocytes did not respond to activation through canonical Wnt signaling.
Primary mouse keratinocytes of Bmal1WT and Bmal1KO mice transfected with TOPflash and FOPflash reporter plasmids were incubated for 24 hours in the absence or presence of BIO (mean ± s.e.m.; n = 2).

3.8 Circadian clock arrhythmia affects homeostasis

Our hypothesis that epSCs at a clock^{high} state are more prone to become activated than the clock^{low} counterpart, as shown for Venus^{bright} and Venus^{dim} SCs of Per1-Venus mice (Fig. 13, 14), was confirmed by several additional data.

First, the hair follicle bulges of Bmal1KO mice, which were administered BrdU at one week of age and are permanently locked at the clock^{low} state, contained fewer proliferative cells (Ki67), and a higher number of long-term label retaining dormant stem cells (LRCs), when analyzed at 10 months of age (Fig. 22 a). Second, the epidermis of another model of circadian arrhythmia, Period1 and Period2 double mutant mice (Per1/2dKO), which lacks the negative limb of the molecular clock and is therefore locked at the clock^{high} state, displayed the opposite effects. These mice showed enhanced bulge proliferation (Ki67), reduced numbers of bulge LRCs at 10 weeks of age (Fig. 22 b). Of note, the observed differences in bulge proliferation did not affect the proportion of bulge SCs in adult Bmal1KO or Per1/2dKO mice compared to their WT controls (Fig. 23 a, b).

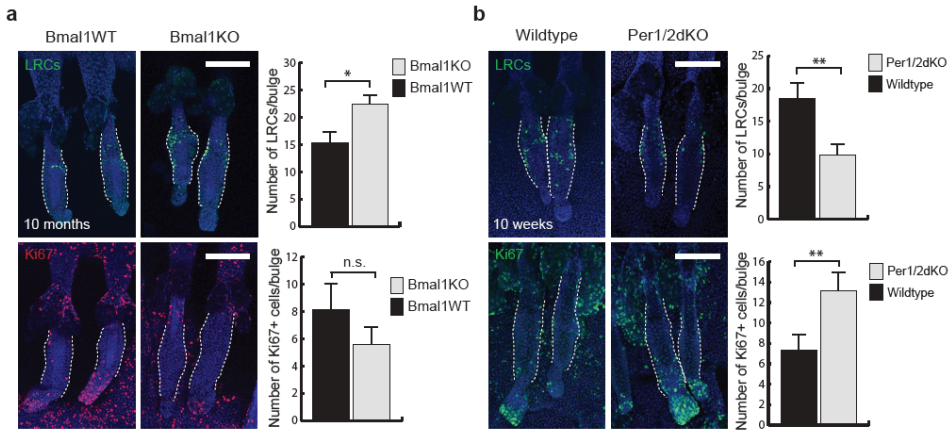

Figure 22: Clock perturbation in vivo affects the number of dormant bulge SCs.
a, **b**, Quantification of BrdU+ label retaining-cells (LRCs) and Ki67+ cells in the bulge of (**a**) 10-month-old Bmal1WT and Bmal1KO mice and (**b**) 10-week-old wildtype and Per1/2dKO mice, showing opposite phenotypes (n ≥ 4; 9 follicles per mouse were analyzed). Scale bars, 100 μm.

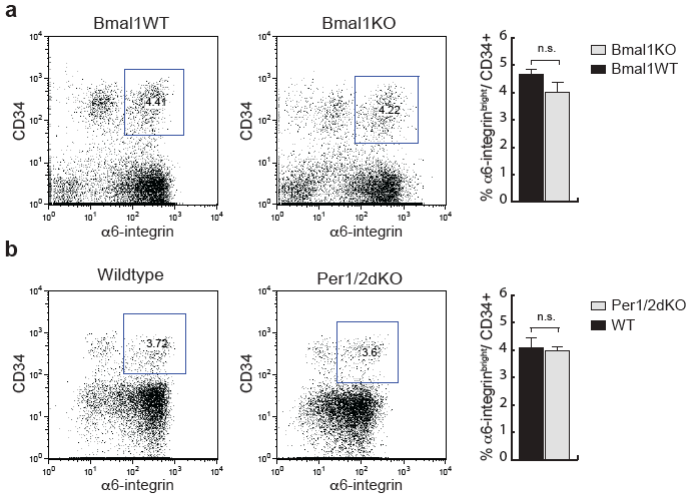

Figure 23: Percentage of bulge stem cells is not altered in Bmal1KO and Per1/2dKO mice.
a, **b**, FACS analysis of α6-integrin^{bright}/CD34+ bulge cells of (a) Bmal1WT and Bmal1KO mice or (b) Per1/2dKO mice and wildtype (WT) control show no differences in the percentage of bulge stem cells in 6-week-old animals (n = 4). Results are shown as mean ± s.e.m.; statistical significance was assessed by two-tailed Student's t-test. n.s., not significant.

Furthermore, Per1/2dKO mice, that display a sustained expression of epidermal clock target genes (Zheng et al., 2001), contained higher transcript levels of integrin α6, Wnt related genes including Dkk3 and Lef1 and lower amounts of TgfbR2 and Smad3 compared to WT cells (Fig. 24). The higher expression of Wnt related Bmal1 targets was also confirmed by immunohistochemistry and western blot for LEF1 and SOX9 (Fig. 25 a, b).

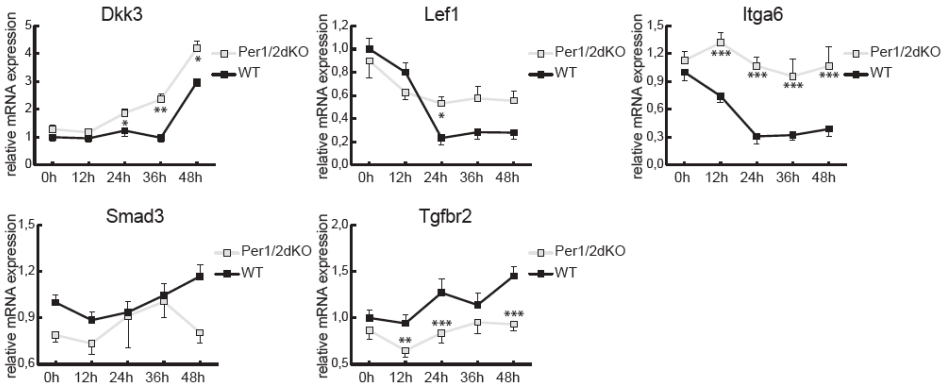

Figure 24: Per1/2dKO epidermal cells show enhanced expression of Bmal1 target genes.
Real time PCR of adhesion, Wnt and TGFβ pathway genes in primary keratinocytes of Per1/2dKO and wildtype control mice (WT). Fold-change values are displayed as relative mRNA expression levels to WT cells at 0h after normalization to Pumilio1 (Pum1) (n = 2). Results are shown as mean ± s.e.m., * $p < 0.05$, ** $p < 0.01$, *** $p < 0.001$ (two-way ANOVA with Bonferroni post-test).

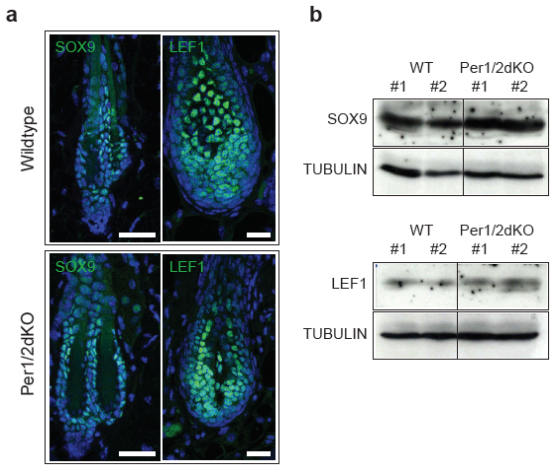

Figure 25: Per1/2dKO mice show enhanced expression of Bmal1 targets.
a, Backskin of Per1/2dKO mice and wiltype control animals was stained for LEF1 and SOX9 (n ≥ 6). Scale bars, 25 μm. **b**, Protein extracts from tail epidermis of 6-week-old Per1/2dKO mice and wiltype control animals were analyzed by western blot for the expression of LEF1 and SOX9. Lanes represent extracts from two WT and two KO animals (#1, #2). TUBULIN expression was analyzed as loading control.

In order to evaluate the ability of epSCs of Bmal1KO mice that reside in the clock^{low} state to respond to activating signals, we performed depilation experiments and treatment with the phorbol ester TPA, which enforce SC activation. The hair follicles of Bmal1KO mice were less efficient in becoming active upon depilation, comparing hair follicle length of WT and KO littermates 7 days post depilation by histological analysis (Fig. 26 a). Bmal1KO bulge cells were also less hyperproliferative than wild-type bulge cells in response to TPA treatment, thus delaying the entry of the hair follicles into anagen (Fig 26 b).

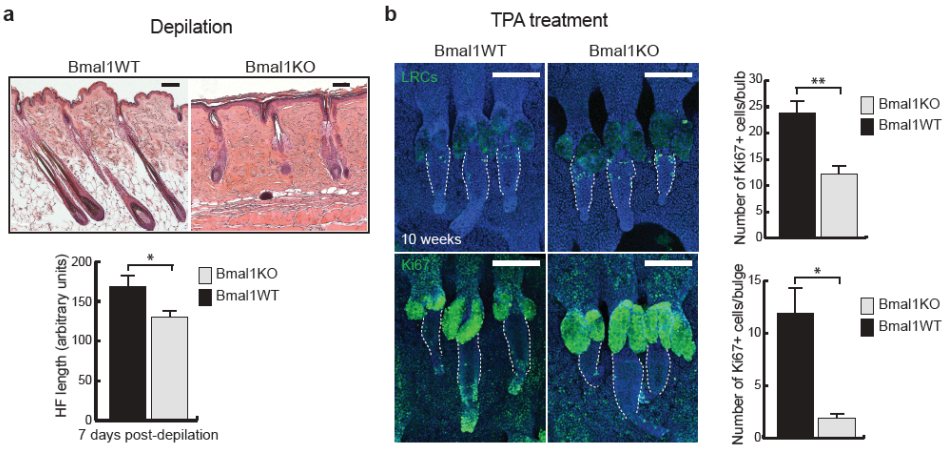

Figure 26: Bmal1KO mice show a delay in response upon ectopically induced stem cell activation.
a, Depilation-induced anagen entry shows a growth delay in Bmal1KO mice (n ≥ 5). **b**, Wholemount immunostaining for BrdU (LRCs) and the proliferation marker Ki67 of 10-week-old Bmal1WT and Bmal1KO after 1 week of TPA treatment (n =5). Scale bars, 100 μm. Results are shown as mean ± s.e.m., * $p < 0.05$, ** $p < 0.01$ (two-tailed Student's t-test).

In addition, reduced proliferation was also evident in the basal layer of the interfollicular epidermis of Bmal1KO, whereas Per1/2dKO mice showed enhanced proliferation compared to WT mice (Fig. 27). At last, these differences in proliferative potential were confirmed *in vitro* in clonogenic assays of epSCs purified from Bmal1KO and Per1/2dKO mice (Fig. 28 a, b).

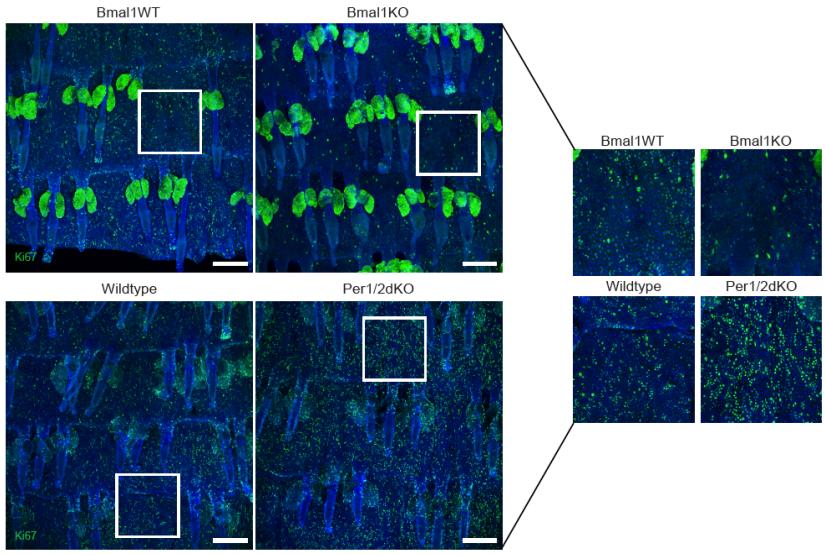

Figure 27: Bmal1KO and Per1/2dKO mice show opposite phenotypes with regard to epidermal proliferation.
Wholemount immunostaining for the proliferation marker Ki67 shows lower expression of Ki67 in the epidermis of Bmal1KO mice compared to Bmal1WT mice, and enhanced expression in the epidermis of Per1/2dKO mice with regard to their wildtype controls. Scale bars, 100 μm. (Upper panel: unspecific staining in sebaceous glands was Ki67 antibody batch dependent).

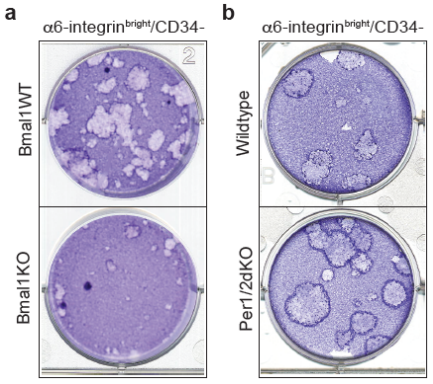

Figure 28: Clock^{high} epidermal keratinocytes have increased clonogenic potential.
a, **b**, Clonogenic assay of FACS-purified α6-integrin^{bright}/CD34- epidermal cells from the backskin of (**a**) Bmal1WT and Bmal1KO mice or (**b**) Per1/2dKO mice and wildtype control animals ($1x10^5$ cells were seeded).

3.9 Loss of Bmal1 induces epidermal aging

Bmal1KO mice displayed signs of inefficient epidermal self-renewal, with premature signs of aging as early as 5 months of age, such as the accumulation of terminally differentiated cornified cells shown by measuring the thickness of the cornified layer of 10-12 months-old animals and by immunohistochemistry for the terminal differentiation markers Filaggrin and Loricrin (Fig. 29). This was accompanied by increased expression of p16, which has been previously associated to increased epidermal aging (Barradas et al., 2009), but not p19, or apoptosis (Fig 30).

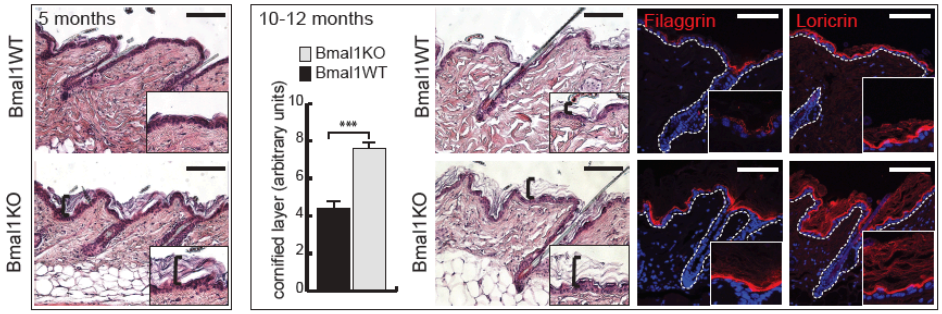

Figure 27: Clock perturbation in vivo results in premature tissue aging.
Histological analysis and immunostaining for the terminal differentiation markers Filaggrin and Loricrin (red) in Bmal1WT and Bmal1KO mice at 5 and 10-12 months of age. Graph shows thickness quantification of the cornified layer of 10-12-month-old mice (n = 13). Scale bars, 100 μm. Results are shown as mean ± s.e.m., *** $p < 0.001$ (two-tailed Student's t-test).

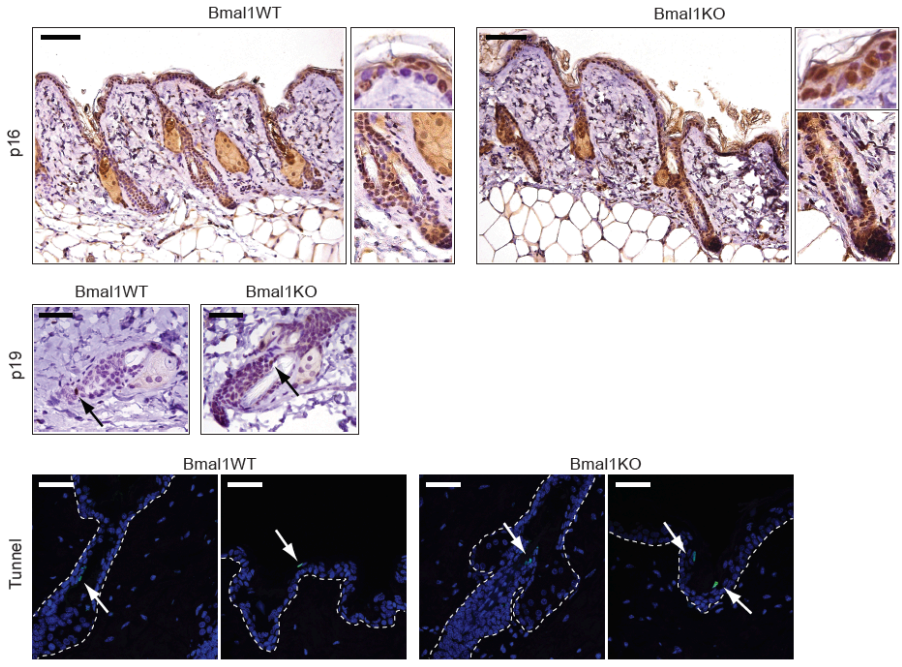

Figure 30: Analysis of aged Bmal1KO for the expression of p16, p19 and apoptosis.
Immunohistochemistry for p16 in 10-12-month-old Bmal1WT and Bmal1KO mice revealed enhanced expression of p16 in the epidermis and hair follicles of Bmal1KO mice. Cells positively stained for p19 (black arrows) were only occasionally observed in Bmal1WT and Bmal1KO mice in similar numbers. Similarly, apoptotic cells (Tunnel; green; white arrows) were only infrequently detected and located mainly to terminal differentiated areas of the hair follicle and the interfollicular epidermis. Scale bars, 50 μm.

Since bulge SCs do not contribute to epidermal maintenance in steady-state conditions (Ito et al., 2005), we sought to understand the molecular mechanisms underlying the defects of the interfollicular epidermis of Bmal1KO mice. We performed microarray analysis of purified basal interfollicular epidermal progenitors ($\alpha6^{bright}$/CD34^{-}) from 10 months-old Bmal1KO mice and their control littermates (Table 3)[3]. As expected, Bmal1KO cells showed strong differential expression of most of the core circadian transcripts, which were validated independently by RT-qPCR (Fig.

31 a and Table 3)[3]. Interestingly, Gene Ontology (GO) analysis indicated that cell cycle, energy and drug metabolism, calcium sensing proteins, DNA damage response, epidermal barrier response, and chromatin compaction, were significantly affected upon deletion of Bmal1 (Fig. 31 c). Intriguingly, although Bmal1KO mice displayed a hyperkeratotic phenotype, the viable epidermal layers expressed lower levels of terminal differentiation markers, including Flg, Lor, SPRR1, LCE genes, and Tgm (Fig. 31 b and Table 3)[3]. The reduced levels of epidermal differentiation genes likely reflects the lower efficiency of activation of basal interfollicular epidermal cells in Bmal1KO mice, suggesting that the hyperkeratotic phenotype developed as a compensatory mechanism to ensure a certain degree of epidermal barrier protection.

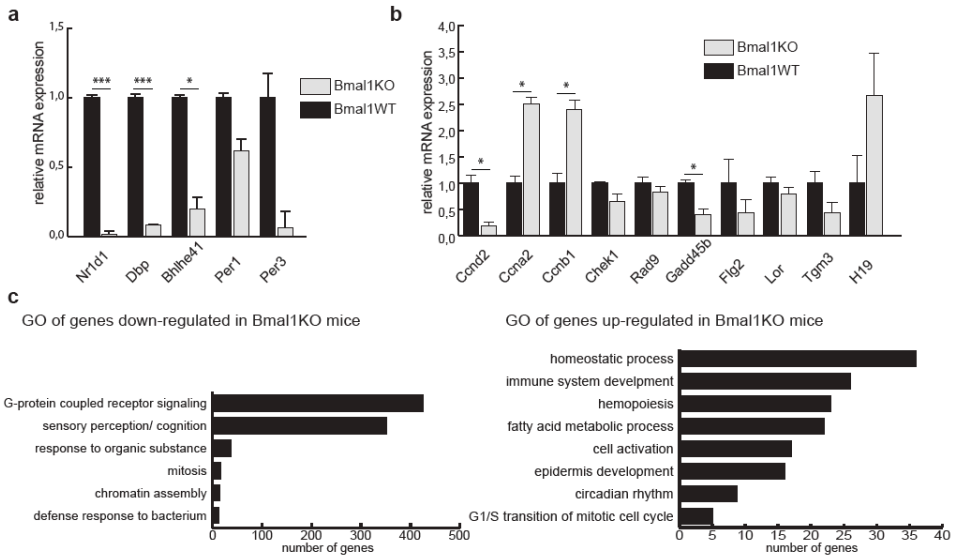

Figure 31: Validation of microarray data comparing aged Bmal1WT and Bmal1KO mice.

a, **b**, Validation of microarray data in FACS-isolated α6-integrinbright/CD34- epidermal cells from Bmal1KO and Bmal1WT mice by real time PCR (n = 2-3) shows differential expression of (**a**) several core circadian genes, (**b**) genes implicated in cell cycle, DNA damage and terminal differentiation. Fold-change values are displayed as relative expression to Bmal1WT cells after normalization to

Pumilio1 (Pum1). Results are shown as mean ± s.e.m., * $p < 0.05$, *** $p < 0.001$ (two-tailed Student's t-test). **d**, Graphic depicts GO enriched biological processes of genes up- and down-regulated in Bmal1KO mice. (Fold change ≥ 1.4 or ≤ -1.4; p-value ≤ 0.05).

Interestingly, Bmal1KO cells showed also differential expression of several non-coding RNAs and miRNAs, including the miR-122, that is expressed in a circadian manner and effects the rhythmic expression of its targets (Gatfield et al., 2009; Kojima et al., 2010). Bmal1KO cells also expressed lower amounts of the miRNA-23b/-27b/-24-1 cluster, which targets TGFbR2 and Smad transcripts (Rogler et al., 2009) (Fig. 32 a and Table 3)[3]. The differential expression of several cell cycle, DNA damage response, terminal differentiation and barrier function genes, as well as non-coding RNAs (H19) and miR-23b/-27b/-24-1 cluster was validated by RT-qPCR (Fig. 31 b and 32 a). Further, we were able to demonstrate by chromatin immunoprecipitation that Bmal1 and Clock bind to regulatory regions in the promoter of the miR-23b/-27b/-24-1 cluster (Fig. 32 b, c), which has been charcaterized recently (Sun et al., 2009).

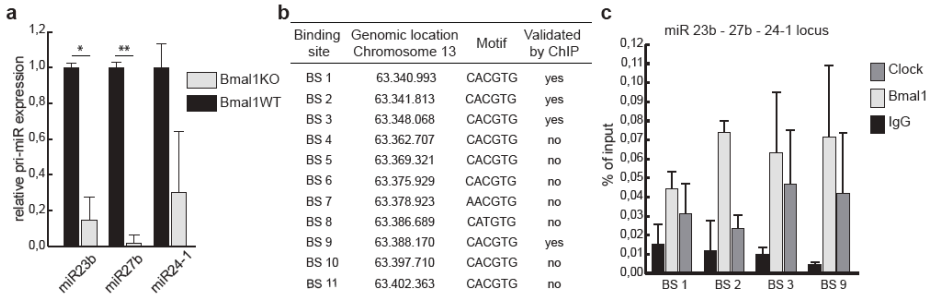

Figure 32: Clock controlled regulation of the miR-23b/-27b/-24-1 cluster.
a, Validation of microarray data by real time PCR (n = 2-3) shows differential abundance of the pri-miRNAs 23b, 27b and 24-1.. Fold-change values are displayed as relative expression to Bmal1WT cells after normalization to 18S-rRNA. Results are shown as mean ± s.e.m., * $p < 0.05$, ** $p < 0.01$ (two-tailed Student's t-test). **b**, Potential BMAL1/ CLOCK binding sites in the miR-23b/-27b/-24-1 promoter **c**, ChIP for Bmal1 and Clock from tail epidermis of WT mice (n = 2). Graphs show the percentage of immunoprecipitated DNA over the input. The result from one representative experiment is shown as mean ± s.e.m.

3.10 Loss of Bmal1 affects skin tumorigenesis

Since perturbation of the clock machinery affects the predisposition of certain tissues to carcinogenesis (Fu and Lee, 2003), we next studied whether epidermal deletion of Bmal1 had any impact over the development of cutaneous squamous tumors. To this end, we crossed Bmal1KO mice with a transgenic line expressing oncogenic SOS, an activator of Ras, under the regulation of the Keratin 5 promoter (K5-SOS) (Sibilia et al., 2000). K5-SOS mice spontaneously developed squamous tumors, primarily in the tail, with 100% penetrance, as previously described (Sibilia et al., 2000; Lichtenberger et al., 2010). Bmal1KO/K5-SOS mice developed significantly fewer neoplastic lesions on the tail at early-, mid-, and late-stages of carcinoma development than control mice (Fig. 33).

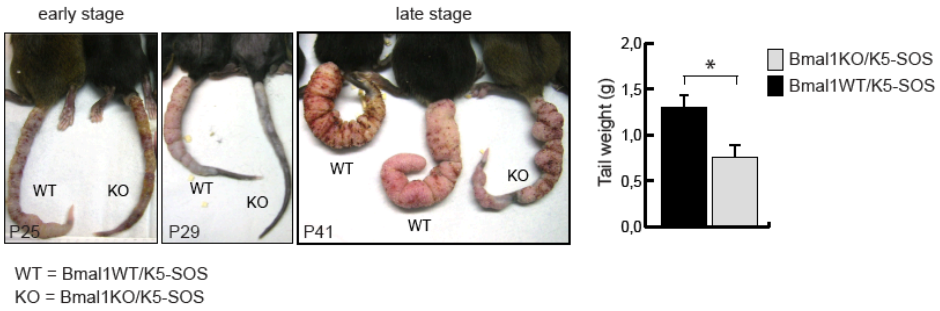

Figure 33: Loss of Bmal1 reduces the development of squamous tumors.
Bmal1KO/K5-SOS mice developed fewer neoplastic lesions compared to Bmal1WT/K5-SOS littermates at early and late stages. Results are shown as mean ± s.e.m., * $p < 0.05$ (two-tailed Student's t-test).

The skin lesions of Bmal1KO/K5-SOS mice were more differentiated, as determined by increased expression of Involucrin and Loricrin, contained large cornified areas, and a higher number of apoptotic areas, as compared to control tumors (Fig. 34). Control mice had to be sacrificed by two months of age, a time at which no Bmal1KO mice developed the number, or size of tumors.

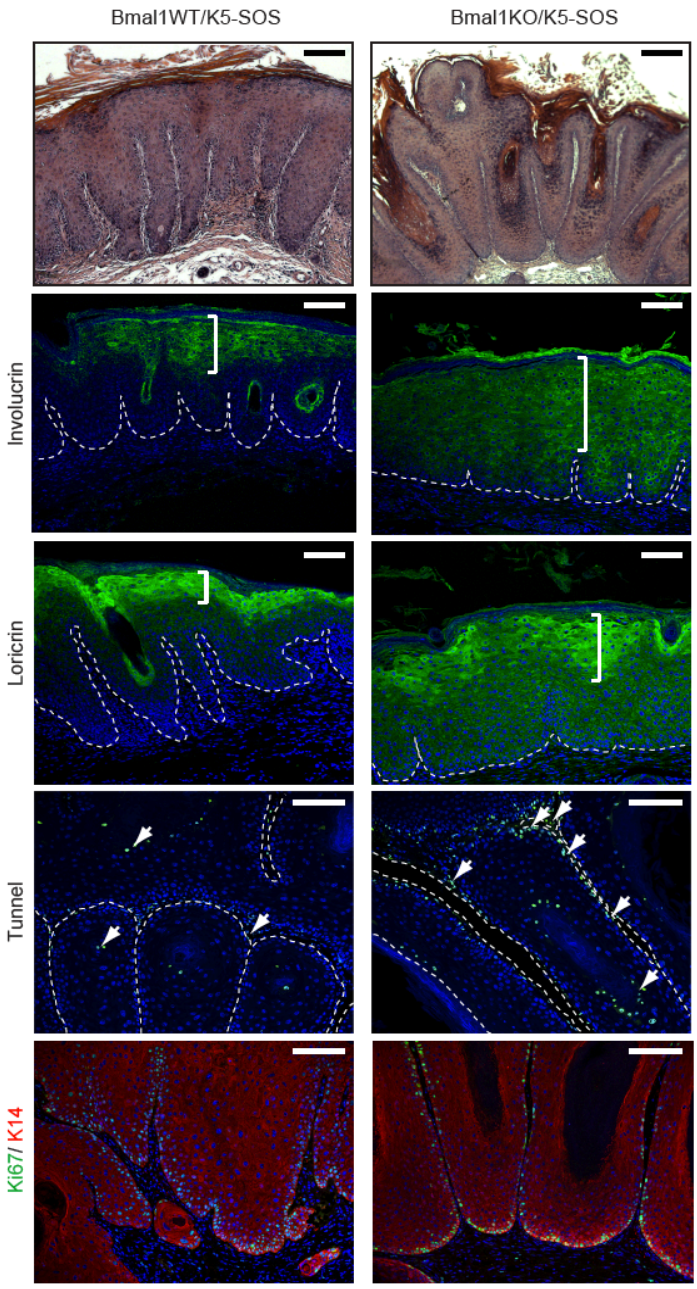

Figure 34: Histological analysis of squamous tumors.
Histological analysis and immunostaining of tumors from Bmal1WT/K5-SOS and Bmal1KO/K5-SOS mice for terminal differentiation (Involucrin, Loricrin), apoptosis (Tunnel; arrows) and proliferation (Ki67; green). Scale bars, 100 μm.

In a previous study, the growth of cutaneous squamous tumors has been shown to depend on Wnt activity in a population of CD34+ tumor-initiating cells (Malanchi et al., 2008). However, we could not detect any nuclear β-catenin, neither in control nor in Bmal1KO neoplastic lesions, suggesting that in our model tumor growth did not primarily depend on misregulated Wnt signaling (Fig. 35 a, b). Immunostaining for nuclear β-catenin in an anagen hair follicle served as positive control to verify the functionality of the staining protocol in order to detect nuclear localization of β-catenin (Fig. 35 a, b).

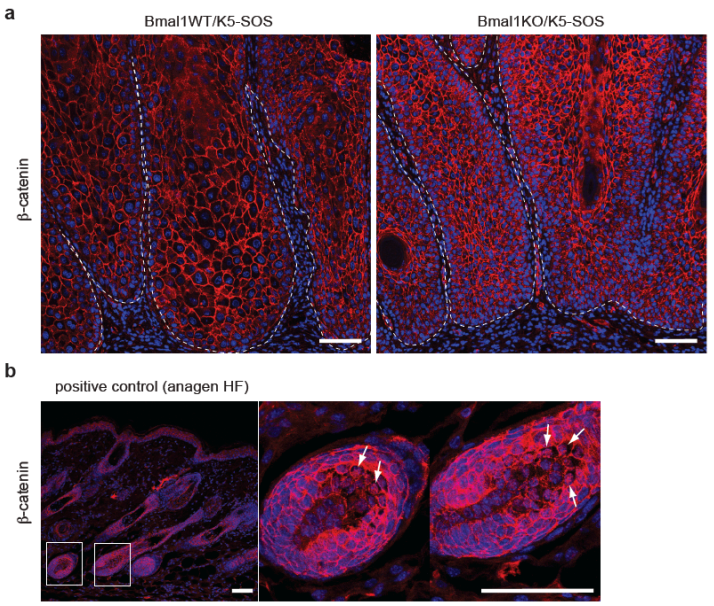

Figure 35: Absence of nuclear β–catenin in K5-SOS-induced tumors.
a, Immunostaining of sections from squamous tumors for β–catenin (red) shows no nuclear localization of β–catenin in K5-SOS tumors. **b**, Anagen hair follicle stained for nuclear β–catenin (arrow) was used as positive control to verify the staining protocol Scale bars, 75 μm.

Further, we compared the number $\alpha6^{bright}$/CD34+ tumor-initiating cells in the epithelial fraction of Bmal1WT and Bmal1KO/K5-SOS tumors by FACS (Fig. 36 a, b) (Beck et al., 2011). We observed a significant reduction in the percentage of $\alpha6^{bright}$/CD34+ tumor-initiating cells in BmalKO tumors with respect to WT tumors (Fig. 36 b). Notably, whereas WT tumors expressed α6-integrin in basal and suprabasal cells, which has been previously associated with increased malignancy (Owens, 2003), Bmal1KO tumors predominantly expressed it in cells of the basal layer (Fig. 36 c). The reduction in the percentage of tumor initiating cells, together with the high expression of tumor suppressors or low expression of oncogenes in Bmal1KO epidermal progenitors, including the non-coding RNA H19 (Yoshimizu et al., 2008) (top upregulated gene; Table3)[3], likely contribute to the reduced burden of squamous lesions in Bmal1KO mice.

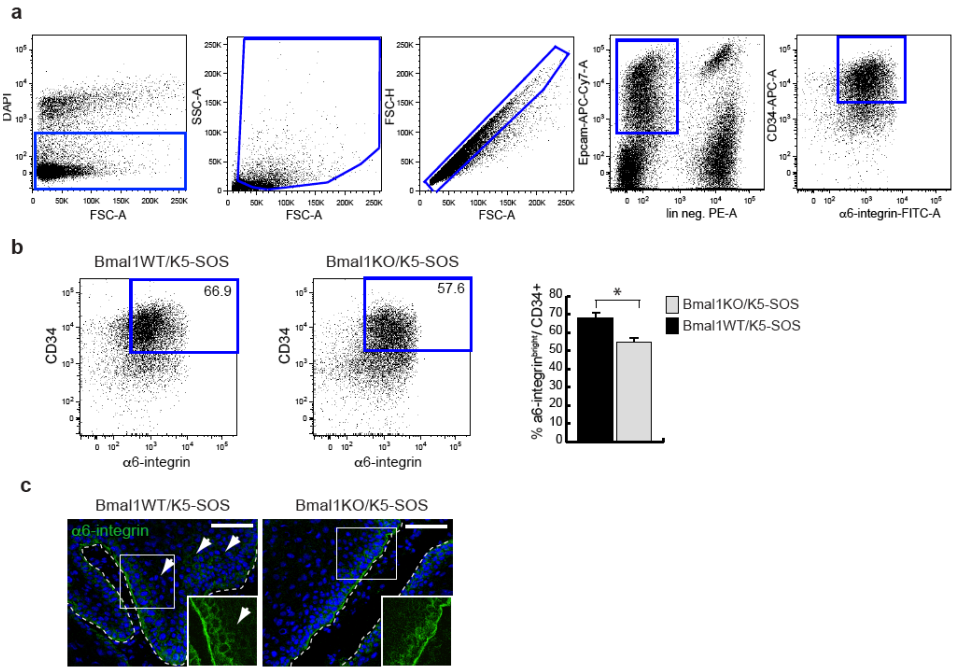

Figure 36: Bmal1KO/K5-SOS tumors have a reduced number of tumor initiating cells.
a, Gating strategy for FACS analysis of K5-SOS-induced tumors. Viable cells were selected by DAPI exclusion (gate 1), contaminating fibroblasts were excluded by forward and side scatter (gate 2), doublets were discarded in gate 3, epithelial cells were selected in gate 4 by a combination of lineage negative markers in PE (CD31, CD45 and CD140a) and a positive marker (Epcam APC-Cy7), and α6-integrin^{bright}/CD34+ tumor-initiating cells were selected in gate 5. **b**, FACS analysis and quantification of α6-integrin^{bright}/CD34+ tumor-initiating cells (P36 mice). Number represent percentage of α6-integrin^{bright}/CD34+ cells from gated epithelial cells ($n \geq 3$). Results are shown as mean ± s.e.m., * $p < 0.05$ (two-tailed Student's t-test). **c**, Immunostaining for α6-integrin (green; arrows indicate suprabasal expression). Scale bars, 50 μm.

3.11 Additional information provided on the enclosed CD (Tables 1-3):

1. Table 1.xls: excel document containing Affymetrix microarray data comparing Venus^{bright} and Venus^{dim} bulge cells of P19 Per1-Venus mice.

2. Table 2.pdf : pdf-document containing the promoter analysis of genes with putative BMAL1/CLOCK-binding sites within their proximal and distal promoters.

3. Table 3.xls : excel document containing Affymetrix microarray data comparing basal epidermal cells of 10 months old Bmal1WT and Bmal1KO mice.

DISCUSSION

IV DISCUSSION

In the present thesis we addressed the role of circadian rhythms in epidermal homeostasis and tumorigenesis. In particular, we were able to show for the first time, that on the one hand epSCs possess circadian rhythms, but that on the other hand epSCs are heterogeneous in their circadian clock. This heterogeneity fine-tunes epSC behavior by modulating their ability to respond to dormancy or activation signals from the microenvironment. Furthermore, we demonstrated that perturbation of this clock driven mechanism affects tissue homeostasis and predisposition to tumorigenesis.

4.1 Circadian clock heterogeneity in epSCs

Up to date, the role of circadian rhythms in adult stem cells has not yet been fully addressed. So far, only stem and progenitor cells of the hematopoietic system were shown to exhibit circadian fluctuations, which control the cyclical release of HSCs into the bloodstream (Méndez-Ferrer et al., 2008).

By means of two independent Per1 reporter mouse models we have shown that epSC of the interfollicular epidermis and the HF bulge contain two distinct SC populations with regard to their circadian clock activity. Both stem cell compartments harbor SCs that displayed robust circadian oscillations with a period of approximately 24 hours ($clock^{high}$ or $Venus^{bright}$ SCs) and stem cells that had no detectable clock reporter activity ($clock^{low}$ or $Venus^{dim}$ SCs). Interestingly, the ratio of 95% $clock^{high}$ to 5% $clock^{low}$ stem cells in the interfollicular epidermis remained constant at any given time point analyzed, whereas the ratio of $clock^{high}$ to $clock^{low}$ bulge SCs steadily increased from 50:50 to 90:10 when hair follicles transitioned from telogen into anagen.

But why would it be beneficial to have clock^{high} and clock^{low} SCs in the skin? SCs of the interfollicular epidermis are continuously activated in order to maintain integrity and functionality of the epidermis, because cells are constantly turned over and shed on the outside (Clayton et al., 2007). In contrast, the bulge was shown to contain mainly dormant SCs that under normal homeostatic conditions become only activated during a short period of the growth phase (Zhang et al., 2009; Greco et al., 2009). Although it has not yet been fully proven, it is believed that also the interfollicular epidermis contains a population of long term quiescent SCs that serve as backup SCs and are only activated under drastic conditions, e.g. wounding (Jones and Simons, 2008). Several studies have shown that dormant epSCs are indeed mobilized following injury, because wounding induced activation of bulge-derived stem cells and their migration into the interfollicular epidermis (Ito et al., 2005). Hence, clock^{low} SCs might represent this pool of long term quiescent SCs in the interfollicular epidermis and the bulge. This hypothesis is supported by our microarray data comparing the expression profiles of Venus^{bright} and Venus^{dim} bulge stem cells that revealed that Venus^{dim} stem cells possess a more dormant transcriptional signature, which renders them more refractory to activating signals than Venus^{bright} SCs, as also confirmed functionally in clonogenic assays.

There is emerging evidence that stem cells do not only differ in their transcriptome and epigenome from committed cells, but also in other aspects of cellular physiology, including cell cycle, metabolism, and signal transduction, which might explain differences in the response to metabolic signals, circadian rhythms and aging (Nakada et al., 2011). Knowing that there is a tight connection between circadian rhythms and metabolism,

differences in circadian rhythm or *vice versa* might also explain the heterogeneity within a stem cell population itself and account for the functional differences observed in Venus^{bright} and Venus^{dim} SCs. Interestingly, we observed that Venus^{bright} SCs show an upregulation of several metabolic pathways, including carbohydrate and lipid metabolism, whereas genes upregulated in Venus^{dim} SCs are involved in immune response (unpublished observations based on microarray data). The later observation might also indicate why dormant SCs are activated upon wounding.

Based on the observations obtained with the Per1-Venus reporter mouse model we conclude that Venus^{bright} and Venus^{dim} SCs correspond to stem cells with high or low circadian clock activity (clock^{high} and clock^{low} SCs), respectively. This assumption is partly supported by our microarray data, since several circadian core genes appear downregulated in Venus^{dim} SCs, including Per1, Cry2, and Dec2. Nevertheless, our statement might not be entirely correct, since it was shown that there is some functional redundancy between different Per and Cry proteins (van der Horst et al., 1999; Zheng et al., 2001). Therefore, Venus^{dim} SCs might indeed possess circadian rhythms that rely on the function of other circadian core members than in Venus^{bright} SCs. The laboratory that has generated the Per1-Venus reporter mouse has simultaneously generated a second fluorescent reporter line expressing DsRed under the Per2 promoter. Interestingly, cells in the SCN of Per1-Venus/Per2-DsRed double transgenic mice expressed Venus, DsRed or both transgenes, whereas other brain areas showed broad expression of Venus and only restricted expression of DsRed, which was mainly overlapping with Venus-positive cells (Cheng et al., 2009). Unfortunately, the authors did not elaborate or comment these

observations as to whether there might be functional differences between these individual cell populations differing in their expression of Per1 and Per2. Analysis of Per1-Venus/Per2-DsRed double transgenic mice could clarify whether Venus^{dim} SCs are indeed clock-less or whether these SCs contain a circadian clock that is operated by Per2 negative feedback loops.

Summarized, we know that Venus^{bright} and Venus^{dim} SCs are functionally different with regard to their circadian clock, but currently we are not able to distinguish whether Venus^{bright} and Venus^{dim} SCs represent two SC populations, in which one exhibits circadian oscillations and the other one not; or whether both populations contain circadian clocks, which are 'ticking' differently due to their varying combination of circadian core members.

4.2 Epidermal homeostasis genes are clock controlled

We analyzed promoters of genes known to regulate epSC fate in terms of quiescence and activation for sequence-specific BMAL1/CLOCK binding elements. Performing ChIP experiments we were able to show for the first time that multiple signaling components of the Wnt and TGF-β pathway are directly bound by BMAL1/CLOCK and that BMAL1 is recruited in a circadian manner to their promoters, which suggests a tight interconnection of the circadian rhythm with these pathways.

Nevertheless, it would be of broad interest to extend this analysis on a genome-wide scale by performing BMAL1-ChIP-seq in order to reveal the entire spectrum of clock-controlled genes in the epidermis. Specially, since recent studies suggest that the percentage of genes with an oscillatory pattern may approach up to 50% in certain tissues, it might be interesting to know how many of these are directly controlled by the circadian clock

machinery (Ptitsyn et al., 2006). Moreover, first ChIP-seq approaches in mouse fibroblasts identified yet another sequence element bound by BMAL1 in addition to E-boxes (Hatanaka et al., 2010). This and future ChIP-seq studies may help to decipher the network of circadian gene control and link it to fundamental physiological processes in many peripheral tissues.

4.3 Effects of clock perturbation on epidermal homeostasis

We have shown that epidermal deletion of Bmal1 affects keratinocyte proliferation and differentiation. Bmal1KO animals displayed a delay in hair follicle growth when challenged by depilation or treatment with TPA. In addition, KO animals showed an accumulation of dormant SCs and signs of increased aging at 10-12 months of age. We were able to demonstrate that this was due to the aberrant regulation of Wnt and TGFβ signaling pathways. Conversely, Per1/2 double mutant mice, which have elevated Bmal1 function, displayed the opposite phenotype, that is enhanced epidermal proliferation and depletion of dormant SCs. Interestingly, the Per1/2dKO phenotype was observed in animals as early as 10 weeks of age, whereas the phenotype of Bmal1KO animals was only apparent in older mice. This might be simply explained by the fact that the function of Per1/2 is lost in all tissues of the animal, whereas the knock out of Bmal1 is epidermal specific; because also the complete Bmal1KO has been shown to exhibit a delay in anagen entry at 3 weeks of age (Lin et al., 2009). Therefore, the epidermal phenotype observed in the conditional KO might be dampened or appear delayed due to the presence of intact circadian clocks in other tissues, which could partially help to entrain epidermal cells due to the cyclical release of hormones, growth factors, and cytokines. Moreover, similar to Per1 and Per2, there might be some functional redundancy between Bmal1 and Bmal2, because ectopic expression of

Bmal2 can rescue the phenotype of Bmal1 knock out mice (Shi et al., 2010). Although it was shown that, in mouse liver, Bmal2 is regulated by Bmal1 and that knock out of Bmal1 should result in a functional double knock out (Bunger et al., 2000), there might be some functional compensation in our conditional KO, since we did not observe significantly reduced transcript levels of Bmal2 in our microarray data.

Nevertheless, the phenotype observed in our epidermal-specific knock out is remarkable and shows the importance of circadian rhythms for tissue integrity. Similar, pancreas-specific deletion of Bmal1 results in reduced proliferation and insulin secretion of pancreatic islets that worsen with age (Marcheva et al., 2010). Moreover, loss of Clock function has been shown to affect pancreatic differentiation through deregulation cell cycle genes, Wnt and Notch signaling components (Li et al., 2007). And also retina-specific deletion impaired tissue function causing defects in electrical response to light (Storch et al., 2007). Unfortunately, information on how circadian rhythms affect the function of tissue specific stem and progenitor cells in this context is still missing.

Even though we have shown that deletion of Bmal1 in the epidermis affects cell proliferation and differentiation by modulating Wnt and TGFβ signaling, our microarray data of stem cells from aged Bmal1KO mice suggest that this is just a small fraction of the consequences caused by circadian arrhythmicity. Gene ontology analysis has shown that clock perturbation affects also metabolic processes, immune function, sensory perception, G-protein coupled receptor signaling, and chromatin assembly among others. Specially, since the circadian clock imposes rhythm on many metabolic pathways by controlling the cyclic expression and/or activity of certain

metabolic enzymes, nuclear receptors, and hormones (summarized in Froy and Miskin, 2010), more attention should be drawn on the role of metabolism in the regulation of stem cell fate.

Recently, it was shown that individual miRNAs can modulate the gene expression of key mRNAs in epSC that are important for stem cell self-renewal and lineage commitment (Lena et al., 2008; Yi et al., 2008; Zhang et al., 2011). Interestingly, we also observed that several miRNAs are deregulated upon deletion of Bmal1. Specially, the miRNA-23a/-27a/-24-2 and miR-23b/-27b/-24-1 cluster called our attention, since miRs of these clusters are predicted to target signaling components of the Wnt and TGFβ pathway (Chhabra et al., 2010). Moreover, the miRNA-23b cluster has been shown to regulate liver stem cell differentiation by targeting Smads (Rogler et al., 2009). Since we were able to demonstrate that BMAL1/CLOCK bind to regulatory regions in the promoter of the miR-23b cluster, it would be interesting to see whether the expression of these miRNAs is also cyclic and which are their targets in epSCs. Another interesting miRNA that was upregulated in Bmal1KO mice is miR-31. It has been shown to act as negative regulator of anagen progression, because inhibition of miR-31 activity accelerates anagen entry and affects hair shaft formation by regulating the expression of distinct components of the FGF, BMP and Wnt signaling pathways (Mardaryev et al., 2010).
In this sense, miRNAs add another layer of complexity in the fine-tuning of transcriptional regulated networks that ensure proper homeostasis and should therefore also be in the focus of follow-up studies.

4.4 Effects of clock perturbation on tumorigenesis

In this study we have shown that loss of Bmal1 function improves tumorigenic outcome. Neoplastic lesions of Bmal1KO/K5-SOS mice were not only smaller in size, and exhibited more differentiated and apoptotic cells, but also contained a lower amount of tumor initiating cells and reduced expression of suprabasal integrins. The effects on proliferation and differentiation are in line with the phenotype observed in the non-cancer background and may explain the reduced cancer burden. Nevertheless, effects of Bmal1 loss on cancer cell metabolism and other signaling cascades have not been shown, but are very likely to play an important role in tumorigenesis. Given that Bmal1KO mice had the opposite epidermal phenotype as Per1/2dKO mice, and since both, Per1 and Per2, have been shown to act as tumor suppressors (Fu et al., 2002; Gery et al., 2006), it would be interesting to see whether loss of Per1 and Per2 will enhance squamous tumor development in the K5-SOS background.

In general it seems, that there is a difference between positive and negative circadian clock regulators in the context of tumorigenesis. Mice with a gene knock out of a positive clock regulator, Bmal1 or Clock, do not display predisposition to tumor formation during normal life span or when challenged by γ-radiation, whereas Per and Cry mutant mice, that lack the negative limb of the circadian clock, develop spontaneous and radiation-induced tumors (Antoch et al., 2008; Lee et al., 2010). On the other hand, Bmal1 and Clock knock out mice display signs of premature aging (Kondratov et al., 2006; Antoch et al., 2008). Therefore, inconsistency in circadian rhythms seems to unbalance the homeostatic equilibrium and to promote cancer and aging. The molecular mechanisms whereby the circadian clock influences cancer and aging could be explained by its regulation of the cell cycle, metabolic pathways and DNA damage response

(summarized by Sahar and Sassone-Corsi, 2009). In the skin the main risk factor for cancer is exposure to UV radiation. Recently, in murine skin it was shown that components of the DNA damage response machinery, which mediate the response to UV-induced DNA damage, oscillate in a circadian manner with a peak during the day and that exposure to UV radiation during the night increases the risk to develop squamous cell carcinoma (Gaddameedhi et al., 2011). It is more likely to acquire *de novo* DNA mutations upon mutagenic UV radiation during the night than during the day, since a high percentage of epidermal proliferation occurs during the night, when the DNA is unprotected from the nuclear envelope and the DNA damage response machinery (Gaddameedhi et al., 2011).

So far, little is known about the role of circadian rhythms in human squamous cell carcinoma. It was reported that the expression of circadian genes is significantly reduced in head and neck squamous tumors (Hsu et al., 2011a), similar to what has been shown for other types of cancer. Interestingly, working night shifts, a major cause of circadian rhythm disruption, reduces the risk to develop skin cancer (Schernhammer et al., 2011), whereas breast and colon cancer risk is significantly increased (Schernhammer et al., 2003; Megdal et al., 2005). Even though, the molecular nature by which circadian rhythms influence tumorigenesis might be different in certain types of cancer, from a clinical point of view it seem clear that cancer prognosis is poorer in patients with an altered circadian rhythm than in patients with a normal rhythm (Lis et al., 2003).

Interestingly, it was shown that food intake plays an important role in the entrainment of circadian clocks in peripheral tissues, including liver, kidney, pancreas and heart (Stokkan et al., 2001). Normally, feeding-fasting

cycles are in phase with activity-rest cycles of an organism. Daytime restricted feeding during the resting period leads to the uncoupling of peripheral clocks from the SCN. Thus, peripheral clocks oscillate in anti-phase to clock of the SCN, which remains entrained by light and dark cycles (Damiola et al., 2000). Since shift work imposes similar changes in feeding-fasting cycles on humans, it could be speculated that tissue specific clocks are also out of phase with each other, which has consequences on health and well-being. In this context it would be interesting to know whether skin clocks will be entrained by feeding cues or by light and darkness via the SCN. If the latter is the case, this might explain why shift workers do not have a higher risk to develop skin cancer since clock-controlled protective mechanisms, e.g. DNA damage response, will still occur at the right time of day. This issue could be easily addressed by exposing Per1-Venus reporter mice to inverted feeding-fasting cycles.

Epidemiological studies have shown that the disruption of circadian rhythms is a major consequence of modern lifestyle in industrialized societies. This leads to several pathological conditions, including sleep disturbances, depression and increased susceptibility to cancer (Sahar and Sassone-Corsi, 2009). In the last years, chronotherapy (drug administration based on the patients biorhythm) has been attracting attention, since it has been shown that drug efficacy and toxicity can vary in a daytime dependent manner. Specially, in the field of oncology, chronotherapy helped to minimize side effects and maximize cancer-killing properties of drugs (summarized in Levi and Schibler, 2007). Altogether these observations indicate the importance of circadian physiology on human health.

4.5 Future directions

Although we found a functional link between circadian rhythms and epSC behavior, several interesting questions came across during this study, which might be worth addressing in the future.

1. When are the Venus^{bright} and Venus^{dim} stem cell states established during development?

2. Is there a transition from Venus^{bright} to Venus^{dim} stem cells or vice versa or are these SC states fixed once they have been established? How can the increase in the proportion of Venus^{bright} bulge SCs during anagen be explained? Is there a conversion of Venus^{dim} to Venus^{bright} SCs or an expansion of the Venus^{bright} SC population, or both? It has been shown that circadian gene expression persists during cell division and that daughter cells inherit the rhythms of mother cells (Nagoshi et al., 2004). But since the bulge compartment does not expand in size and activated SCs migrate out of the bulge area into the CD34^{negative} hair germ and ORS (Greco et al., 2009; Hsu et al., 2011b), cell division alone can not explain the increase of Venus^{bright} SCs from 50 to 90%, unless Venus^{dim} SC also leave the bulge.

3. Why are circadian rhythms affected during aging? It was reported that aging can lower the amplitude and/or change the phase of circadian rhythms, whereas a high oscillatory amplitude extends life span (Hurd and Ralph, 1998; Hofman and Swaab, 2006; Gibson et al., 2009). Therefore, aging related alterations in circadian rhythms might affect stem cell function and homeostasis.

4. What metabolic pathways are regulated by circadian rhythms in epSCs and how do they influence SC function?

5. What are the roles of clock-controlled miRNAs in epSCs?

6. To what extend do feeding-fasting cycles influence circadian rhythms in the skin?

7. Does chronotherapy improve the treatment of skin cancer?

SUMMARY

V SUMMARY OF SCIENTIFIC FINDINGS

1. Epidermal stem cells of the bulge and the interfollicular epidermis are heterogeneous in their circadian clock; they contain stem cells with high and low circadian clock activity.

2. Epidermal stem cells with high circadian clock activity exhibit oscillations with a period of approximately 24 hours.

3. Circadian clock heterogeneity creates two distinct stem cell predisposition states that respond differently to activation and dormancy cues.

4. These differences in responsiveness can be explained in part by the distinct regulation of Wnt and TGFβ pathways.

5. Several epidermal stem cell and homeostasis genes are directly clock-controlled.

6. Loss of circadian clock function leads to decreased responsiveness, accumulation of dormant stem cells and increased tissue aging.

7. Enhanced activation of the circadian clock machinery leads to a depletion of dormant stem cells.

8. The effects of clock perturbation can be partially attributed to the deregulation of Wnt and TGFβ pathways.

9. Loss of circadian clock function affects squamous tumor development.

MATERIALS & METHODS

VI MATERIALS AND METHODS

6.1 Chemicals

Commonly used chemicals and reagents were obtained from Sigma Aldrich, Merck, and Fluka. Distributors of specialty chemicals are indicated in the text. DNA-oligos were purchased from Sigma Aldrich and Thermo Scientific.

6.2 Consumables

Tissue culture dishes, plates and flasks were purchased from Nunc and BD Biosciences. Serological pipettes, pipette tips, syringes were purchased from VWR International. Filters were obtained from Millipore.

6.3 Animals

Bmal1$^{LoxP/LoxP}$ and Keratin14Cre mice were purchased from Jackson and were crossed together and with Keratin5-SOS mice (kindly donated by Erwin Wagner, CNIO, Madrid, Spain) to generate Bmal1$^{wt/wt}$K14Cre (Bmal1WT), Bmal1$^{LoxP/LoxP}$K14Cre (Bmal1KO), Bmal1$^{wt/wt}$K14Cre/K5-SOS (Bmal1WT/K5SOS) and Bmal1$^{LoxP/LoxP}$K14Cre/K5-SOS (Bmal1KO/K5SOS) littermate controls (Sibilia et al., 2000). Per1::GFP and mPer1-Venus mice (kindly donated by Douglas McMahon, Vanderbilt University, Nashville, Tennessee, USA and Karl Obrietan, Ohio State University, Columbus, Ohio, USA) have been described previously (LeSauter et al., 2003; Cheng et al., 2009). Bmal1$^{wt/wt}$K14Cre Per1-Venus and Bmal1$^{LoxP/LoxP}$K14Cre Per1-Venus mice were generated by crossing Bmal1$^{wt/wt}$K14Cre and Bmal1$^{LoxP/LoxP}$K14Cre animals with Per1-Venus mice, respectively. Period1 and Period2 double mutant mice (Per1/2dKO) have been described previously, and were compared to age and sex matched control animals(Zheng et al., 2001). Mice were housed in an AAALAC-I approved

animal unit under 12 h light/12 h dark (LD) or 12 h dark/12 h dark (DD) cycles, and SPF conditions, and all procedures were approved by the CEEA (Ethical Committee for Animal Experimentation) of the Government of Catalonia. For experiments in constant darkness, light was turned off at ZT12 and animals were housed in DD conditions for 5 days. For 5-Bromo-2-deoxyuridine (BrdU)-labeling experiments, 100 μg/g BrdU (Invitrogen) was injected intraperitoneally into the mice and chased for 10 weeks or up to 10 months, as indicated. To activate epidermal proliferation, backskin or tailskin of 10-week-old Bmal1WT and Bmal1KO mice was treated 3 times with 20 nM 12-O-tetradecanoylphorbol-13-acetate (TPA) (Sigma-Aldrich) during one week. For depilation experiments, dorsal skin of 15-month-old Bmal1WT and Bmal1KO mice in telogen phase was depilated with cold wax strips (Taky®).

6.4 Extraction of genomic DNA and genotyping

For genotyping genomic DNA was isolated from ear- or tail snips of transgenic mice. Tissue snips were digested over night in 200 μl 50 mM Tris-HCl pH 8.0, 100 mM EDTA, 100 mM NaCl, 1% SDS, and 0.5 mg/ml Proteinase K (Roche) at 55°C. Proteins were removed by addition of 80 μl 5 M NaCl and centrifugation at maximum speed in a tabletop centrifuge for 10 min. Genomic DNA was precipitated with isopropanol, washed with 70% ethanol, and the dried DNA pellet was re-suspended in 200 μl distilled water. PCR was performed in a 25 μl reaction volume using PCR Master Mix (Promega), 1 μl of transgenic mouse line specific primers (10 mM, Table 4) and 2 μl genomic DNA. DNA fragments were analyzed by agarose gel electrophoresis.

Alike, genomic DNA of keratinocytes from newborn skin of Bmal1$^{Wt/Wt}$K14Cre and Bmal1$^{LoxP/LoxP}$K14Cre mice was isolated. Multiplex PCR was performed using primers recognizing either the wild-type, conditional or disrupted allele in order to determine recombination efficiency in epidermal cells (Storch et al., 2007).

6.5 Culture of primary mouse keratinocytes

Primary mouse keratinocytes from newborn mice or tailskin of adult mice were isolated as described previously(Lichti et al., 2008; Jensen et al., 2010; Lichti et al., 2008; Jensen et al., 2010). Cells were plated on collagen I (Sigma Aldrich) coated dishes in EMEM medium (Lonza) containing 4% chelated FBS, 1% penicillin/ streptomycin and 0.2 mM calcium. After 24 hours medium was changed to growth medium (EMEM with 4% chelated FBS, 1% penicillin/ streptomycin, EGF (10 ng/ml) and 0.05 mM calcium). For time-course experiments of keratinocytes isolated from Bmal1$^{wt/wt}$K14Cre and Bmal1$^{LoxP/LoxP}$K14Cre mice, cells were synchronized by a serum shock with growth medium containing 50% chelated FBS for 2 hours (Balsalobre et al., 1998). After the serum shock cells were washed once with PBS and changed back to growth medium and cultured in the absence or presence of 2ng/ml TGFβ1 or TGFβ2 (PeproTech) for a period of 48 hours.

For clonogenic assays total keratinocytes or FACS sorted populations were seeded as triplicates into 6-well plates containing E-medium and mitomycin C (4 μg/ml) (Sigma-Aldrich) treated J2 3T3 feeder cells (Nowak and Fuchs, 2009). Keratinocytes were grown at 37ºC and 5% CO_2. Cells in clonogenic assays were fixed in neutral-buffered formalin (NBF) (Sigma Aldrich) for 30 min and stained with 0.5% crystal violet/0.5% rhodanile blue (Sigma Aldrich) for 30 min at room temperature. FBS and penicillin/ streptomycin were purchased from Invitrogen and EGF from PeproTech.

6.6 Plasmids

TOP-Flash (TCF reporter plasmid), FOP-Flash (containing mutant TCF binding sites) and pCMV-Renilla plasmids were kindly donated by the laboratory of Susana de la Luna. Plasmid preparations were carried out using QIAprep Miniprep and Maxiprep kits (Qiagen) according to the manufacturers instructions.

6.7 Whole mount immunofluorescence

Preparation of tailskin and whole mount stainings were done as described previously (Braun, 2003; 2003). Primary and secondary antibodies were incubated overnight at room temperature. The following primary and secondary antibodies were used: anti-GFP (1:1000, Invitrogen), anti-BrdU (1:250, Serotec), anti-Ki67 (1:250, Abcam), anti-rabbit, and anti-rat conjugated to AlexaFluor488 or AlexaFluor594 (1:500, Molecular Probes). Nuclei were stained with DAPI (1:5000, Roche) and epidermal sheets were mounted in Mowiol. Pictures were acquired using a Leica TCS SP5 confocal microscope.

6.8 Immunohistochemistry

Backskin and tailskin were fixed in 4% NBF (Sigma-Aldrich) at 4°C overnight or 2 h at room temperature and then either embedded in paraffin or incubated in 30% sucrose overnight at 4°C and embedded in OCT (Electron Microscopy Sciences). Paraffin sections were de-paraffinized in xylene (2 x 5 min) and rehydrated through graded ethanol down to water (2 x 5 min 100% EtOH, 2 x 5 min 96% EtOH, 2 x 5 min 70% EtOH, 10 min H_2O). Antigen retrieval was performed boiling the sections in 0.01M citric acid pH 6.0 for 10 min. Cryo- and paraffin sections were permeabilized for 25 min in 0.25% Triton X-100/PBS and blocked for 90 min in 0.25% gelatin/PBS.

Primary antibodies were incubated overnight at 4°C and secondary antibodies were incubated 2 h at room temperature in 0.25% gelatin/PBS. Nuclei were stained with DAPI (1:5000, Roche) and slides were mounted in Mowiol. Primary antibodies were used at the following dilutions: 1:50 for anti-p19 (M-167, Santa Cruz), anti-p16 (M-156, Santa Cruz); 1:100 for anti-Sox9 (H-90, Santa Cruz); 1:200 for anti-α6-integrin (CD49f clone NKI-GoH3, Serotec), anti-Keratin 14 (ab7800, Abcam); 1:250 for anti-Ki67 (ab15580, Abcam); 1:500 for anti-Keratin-5 (ab24647, Abcam); and 1:1000 for anti-GFP (ab290, Abcam; A11122, Invitrogen), anti-Involucrin (PRB-140C, Covance), anti-Filaggrin (ab24584, Abcam), and anti-Loricrin (PRB-145P, Covance), anti-phospho-Smad2 (#3101, Cell Signaling), anti-Lef1 (clone C12A5, Cell Signaling). Secondary antibodies were used at dilutions of 1:500: anti-rabbit, anti-mouse, or anti-rat, conjugated to AlexaFluor488 or AlexaFluor594 (Molecular Probes), or anti-rabbit biotin (GE Healthcare), followed by an incubation with ABC Kit (Vector Laboratories) and FAST 3,3 Diaminobenzidine tablets (Sigma-Aldrich).

For apoptosis measurements, tailskin was stained with the DeadEnd Fluorometric TUNEL System (Promega). Hematoxilin and eosin stainings were done according to a standard protocol. Pictures were acquired using a Leica DMI 6000B or a Leica TCS SP5 confocal microscope.

6.9 Time-lapse microscopy and quantification

For time-lapse confocal imaging backskin of Per1Venus mice was fixed with 0.5% agarose in an imaging dish (Ibidi) and over-layered with E-medium (Nowak and Fuchs, 2009). Images were taken every 15 minutes for a period of 48 hours using a Leica TCS SP5 confocal microscope equipped with a tempered chamber of 37°C and 5% CO_2. Mean fluorescence intensity of individual GFP positive nuclei was quantified using ImageJ software.

6.10 FACS

Epidermal cells from backskin of Per1-Venus, Bmal1$^{wt/wt}$K14Cre, and Bmal1$^{LoxP/LoxP}$K14Cre or tailskin of Bmal1$^{wt/wt}$K14Cre/K5-SOS and Bmal1$^{LoxP/LoxP}$K14Cre/K5-SOS mice were isolated as described previously (Jensen et al., 2010). Cell suspensions were incubated for 30 min on ice with the following antibodies in E-medium (Nowak and Fuchs, 2009) at the given dilutions: 1:100 for Biotin-, or APC-conjugated anti-CD34 (clone RAM34, BD Pharmingen), PE-conjugated anti-CD31 (clone MEC13.3, eBioscience), PE-conjugated anti-CD45 (clone 30F11, eBioscience), PE-conjugated anti-CD140a (clone APA5, BD Pharmingen), and APC-Cy7-conjugated anti-Epcam (clone G8.8, Biolegend); 1:200 for PE- or FITC-conjugated anti-α6-integrin (CD49f clone NKI-GoH3, Serotec); and 1:500 for APC-conjugated Streptavidin (BD Pharmingen). DAPI staining was used to exclude dead cells. Fluorescence-activated cell sorting was performed using FACSAriaII and FACSDiva software (BD Biosciences). Sorted cells were collected in E-medium and plated in culture or re-suspended in Trizol (Invitrogen) and further subjected to RNA isolation. FACS analysis was performed using LSRII FACS Analyzers (BD Biosciences) and Flowjo software.

6.11 Arrays

Total RNA was isolated from FACS sorted cells by Trizol/chloroform extraction followed by RNA clean up protocol of RNeasy Micro or Mini Kits (Qiagen). Transcriptional profiling was performed using GeneChip Mouse Gene 1.0 ST Array (Affymetrix). Arrays of Venus+ and Venus- bulge (α6-integrin^{bright}/CD34^{+}) cells of P19 Per1-Venus mice were done as triplicates from a pool of n = 64 mice. Arrays of bulge (α6-integrin^{bright}/CD34^{+}) cells from 10-11 months old Bmal1$^{wt/wt}$K14Cre and Bmal1$^{LoxP/LoxP}$K14Cre mice were done as triplicates from a pool of n = 4 mice in each group. Arrays of

epidermal (α6-integrin^{bright}/CD34^{-}) cells from 10 months old Bmal1$^{wt/wt}$K14Cre and Bmal1$^{LoxP/LoxP}$K14Cre mice were done as triplicates from 3 independent mice in each group. Functional analysis of microarray data was performed using DAVID Bioinformatics Resources 6.7.

6.12 Real time PCR

Total RNA from cultured or FACS sorted keratinocytes was purified as described above or using the RNeasy Micro and Mini Kit (Qiagen) or miRVana miRNA isolation Kit (Ambion) according to manufacturers instructions. Equal amounts of RNA were reverse transcribed using Superscript III (Invitrogen). Real time PCR with SYBR Green Master Mix (Roche) and gene specific primers (Table 5) was performed and analyzed using a Light Cycler 480 Instrument (Roche). Relative expression levels were determined by normalization to Pumilio 1 (Pum1) using $\Delta\Delta C_t$ method.

6.13 Chromatin immunoprecipitation

For ChIP assays from intact epidermis, mice were sacrificed at ZT0, and tails were incubated in 0.25% trypsin for 4h at 37°C to separate dermis from epidermis. Tail keratinocytes were extracted as described (Jensen et al., 2010). Cells in suspension were cross-linked for 10 min at room temperature in 1% formaldehyde. Cross-linking reactions were stopped adding 1.25 M glycine to a final concentration of 0.125 M. Cells were centrifuged for 10 min at 4ºC and washed in cold PBS. Initially, cell lysis, sonification and ChIP assay were performed using MAGnify Chromatin Immunoprecipitation System (Invitrogen). Per IP 2 x 10^5 cells were incubated with 2 µl of Bmal1 or Clock antibody (kindly provided by Jürgen Ripperger, University of Fribourg) (Ripperger and Schibler, 2006)

(Ripperger and Schibler, 2006)(Ripperger and Schibler, 2006)(Ripperger and Schibler, 2006)or 2 μl of rabbit IgG control antibody (Invitrogen).

Later ChIP assays were performed using a standard protocol (kindly provided by Elisabeth Simboeck from the laboratory of Luciano diCroce). Cross-linked cells were re-suspended in ice-cold lysis buffer I (5 mM PIPES pH8, 85 mM KCl, 0.5% NP40, 1.5mM $MgCl_2$) containing protease inhibitors (Complete protease inhibitor cocktail, Roche), incubated for 10 min on ice and centrifuged at 1200 rpm. The supernatant was discarded and the nuclei containing pellet was re-suspended in ice-cold lysis buffer II (50 mM Tris-HCl pH8, 1% SDS, 10mM EDTA pH8). After incubation on ice for 10 min, samples were sonicated 16 cycles (30 seconds "ON"/ 30 seconds "OFF") in 1.5 ml Eppendorf tubes at high power in a Bioruptor™ (Diagenode). Chromatin was cleared by centrifugation at 13000 rpm for 5 min at 4°C. An aliquot of sheared chromatin was analyzed by agarose gel electrophoresis to evaluate the fragment size. Chromatin samples were diluted 1:10 in dilution buffer (16.7 mM Tris-HCl pH8, 1.2 mM EDTA pH8, 167 mM NaCl, 1.1% Triton X-100, 0.01% SDS). Per IP diluted chromatin equal to 1 x 10^6 cells was used, in which 0.1 volume was stored as an input sample and the rest was incubated likewise with 2 μl of Bmal1 or Clock antibody or 2 μl of rabbit IgG control antibody (Invitrogen) at 4°C overnight with rotation. Immunocomplexes were collected with 30 μl Protein-G Dynabeads (Invitrogen) at 4°C for 2 h with rotation. Dynabeads were washed 2 x 5 min in low salt wash buffer (50 mM HEPES pH 7.5, 140 mM NaCl, 1% Triton X-100), 1 x 5 min in high salt wash buffer (50 mM HEPES pH 7.5, 500 mM NaCl, 1% Triton X-100) and again 1 x 5 min in low salt wash buffer. Immunocomplexes were eluted in 400 μl elution buffer (2% SDS, 0.1 M $NaHCO_3$) by shaking the samples for 1 h at 37°C and 1200 rpm in a thermo-

shaker. Input samples (diluted with 300 µl elution buffer) and eluted samples were reverse cross-linked by addition of 16 µl 5 M NaCl and incubation at 65°C overnight. Then, samples were incubated with 32 µl 0.5 M Tris-HCl pH 6.5, 8 µl 500 mM EDTA and 2 µl Proteinase K (10 mg/ml, Roche) for 2 h at 300 rpm. Genomic DNA was purified by phenol/chloroform/isoamyl alcohol (25:24:1) extraction and ethanol precipitation. Air-dried DNA pellets were resolved in 100 µl distilled water. Real time PCR was performed as described above using gene specific primers and 1µl of genomic DNA (Table 6).

6.14 Western blot

Keratinocyte cell pellets from freshly isolated or cultured cells were either directly re-suspended in 1 x Laemmli buffer or lysed in 1 x RIPA buffer (150 mM NaCl, 1% NP40, 0.5% DOC, 0.1% SDS, 50 mM Tris-HCl pH 8 and Complete protease inhibitor cocktail, Roche) and subjected to protein quantification using BCA protein assay kit (Pierce). Protein extracts from Bmal1 WT and KO keratinocytes were analyzed by SDS-PAGE and western blotting for Bmal1 (1:1000) (Ripperger and Schibler, 2006), anti-phospho-Smad2 (1:1000, #3101, Cell Signaling), anti-Lef1 (1:1000, clone C12A5, Cell Signaling), anti-Sox9 (1:400, H-90, Santa Cruz) and anti-Tubulin (1:5000, Sigma Aldrich).

6.15 Luciferase assay

Isolated primary mouse keratinocytes were grown in 6-well plates, and after 3 days culture in growth medium, cells were transiently transfected with either TOPflash or FOPflash and pCMV-Renilla plasmids using FuGENE6 (Roche) according to the manufacturers instructions. Cells were

treated in the absence or presence of Bromoindirubin-3-oxime (BIO, 1μM, Calbiochem) 48 h post-transfection for a period of 24 hours. Luciferase activity was measured in a Centro LB 960 luminometer (Berthold Technologies) using Dual-Luciferase Reporter Assay System (Promega).

6.16 Promoter analysis

Gene promoter analysis for potential Bmal1/Clock-binding sites (in general, from -5,000 to +1,000 bases from the transcriptional start site) were analyzed using Genomatix Software.

6.17 Statistics

Results are presented as mean ± s.e.m. Statistical significance was determined by two-tailed Student's t-test, one-way ANOVA, two-way ANOVA with Bonferroni post-test, or Cosinor analysis. A p-value of $p \leq 0.05$ was considered to be statistically significant.

Table 4 Genotyping primer

Mouse line	Forward/Reverse Primer
$Bmal1^{LoxP/LoxP}$	Fw: ACTGGAAGTAACTTTATCAAACTG Rv: CTGACCAACTTGCTAACAATTA
K14Cre_WT K14Cre_TG	Fw1: CAAATGTTGCTTGTCTGGTG Rv1: GTCAGTCGAGTGCACAGTTT Fw2: TTCCTCAGGAGTGTCTTCGC Rv2: GTCCATGTCCTTCCTGAAGC
K5-SOS_ Wa2	Fw: ATAACCTGACACTTGTCAGAGTAC Rv: TTTGCAATCTGCACACACCAGTTG
Per1::GFP	Fw: CCTGGTCGAGCTGGACGGCGACGTAAA Rv: CCGGCGGGAAGCCATGGCTAAGCTT
Per1-Venus	Fw: CCAGCAGATGCTGTGGGGTT Rv1: CCTGGACAAGGCCGGTGCTGC Rv2: CCTCGAACTTCACCTCGG
$Bmal1^{Wt/Wt/Lo}$	Fw: ACTGGAAGTAACTTTATCAAACTG Rv1: AATCCGCCTGCCTACTGCCTCC

$^{xP/LoxP}$K14Cre	Rv2: GGGTGGAGTATGATATGACC

Table 5 Real time PCR primer

Gene	Forward/Reverse Primer
Bhlhe41	Fw: CTGCCCGAACATCTGAAATTGA Rv: GCTGCTCAGTTAAGGCTGTTAG
Ccna2	Fw: CTTTACCCGCAGCAAGAAAAC Rv: ACGTTCACTGGCTTGTCTTCTA
Ccnb1	Fw: CTCAGGGTCACTAGGAACACG Rv: AGCTCTTCGCTGACTTTATTACC
Ccnd2	Fw: CTGTGCGCTACCGACTTCAA Rv: CACATCAGTGTGGGTGATCTTG
Cd34	Fw: AAGGCTGGGTGAAGACCCTTA Rv: TGAATGGCCGTTTCTGGAAGT
Cdkn2b (p15)	Fw: CCCTGCCACCCTTACCAGA Rv: CAGATACCTCGCAATGTCACG
Chek1	Fw: GTTAAGCCACGAGAATGTAGTGA Rv: GATACTGGATATGGCCTTCCCT
Dab2	Fw: AGGCCAAGCTAATCGGTATTGA Rv: AATGTTGACCCAGATTCTTTGCT
Dbp	Fw: CCTGATCCCGCTGATCTCG Rv: CAGGCACCTGGACTTTCCTT
Dkk3	Fw: CTCGGGGGTATTTTGCTGTGT Rv: TCCTCCTGAGGGTAGTTGAGA
Flg2	Fw: GCCAACTGTCCAGTCTTGTTT Rv: GCCTTTCATTAGGGCTGAATCC
Fzd2	Fw: GTTCTTCTCGCAAGAGGAGAC Rv: TCGCTGCATGTCCACTAAATAG
Gadd45b	Fw: CAACGCGGTTCAGAAGATGC Rv: GGTCCACATTCATCAGTTTGGC
H19	Fw: AGGATGACAGGTGTGGTCAA Rv: TGAGTGAGTGGGTGGACAAT
Itga6	Fw: TGCAGAGGGCGAACAGAAC Rv: GCACACGTCACCACTTTGC
Lef1	Fw: TGTTTATCCCATCACGGGTGG Rv: CATGGAAGTGTCGCCTGACAG
Lor	Fw: GATCGTCCCAACAGTATCAGTG Rv: TGCTGAGAGGAGTAATAGCCC

Ltbp2	Fw: CTGATGTCCAACGCTTTGCC Rv: GTGGGGGTGAAGACGACTTT
Mki67	Fw: ATCATTGACCGCTCCTTTAGGT Rv: GCTCGCCTTGATGGTTCCT
Nr1d1	Fw: TACATTGGCTCTAGTGGCTCC Rv: CAGTAGGTGATGGTGGGAAGTA
Per1	Fw: ACCAGGTCATTAAGTGTGTGC Rv: CTCTCCCGGTCTTGCTTCA
Per3	Fw: AAAAGCACCACGGATACTGGC Rv: GGGAGGCTGTAGCTTGTCA
Pum1	Fw: AGGCGTTAGCATGGTGGAGTA Rv: TCCATCAAACGTACCCTTGTTC
Rad9	Fw: CACTGCAAGTATGGGGTCAAG Rv: GCAATAAGTGAGGGCATGAGG
Smad3	Fw: CCCCCACTGGATGACTACAG Rv: TCCATCTTCACTCAGGTAGCC
Smad7	Fw: GAAACCGGGGGAACGAATTAT Rv: CGCGAGTCTTCTCCTCCCA
Sox9	Fw: GAGCCGGATCTGAAGAGGGA Rv: GCTTGACGTGTGGCTTGTTC
Tcf3	Fw: ACGAGCTGATCCCCTTCCA Rv: CAGGGACGACTTGACCTCAT
Tgfbr2	Fw: AGTGATGTCATGGCCAGCGAC Rv: CGCAGACTTCATGCGGCTTCTC
Tgm3	Fw: TCAGTGCTCCCATCGGATTG Rv: GGCGTGGTTACTCATAAAGACAT
Wnt10a	Fw: GCTCAACGCCAACACAGTG Rv: CGAAAACCTCGGCTGAAGATG
Wnt3a	Fw: CTCCTCTCGGATACCTCTTAGTG Rv: GCATGATCTCCACGTAGTTCCTG
miR primer sequence (Sun et al., 2009)	
Pri-miR-23b	Fw: TTCTAAAGGAGGCTGCACTGC Rv: AAATCAGCATGCCAGGAACCCAAGC
Pri-miR-27b	Fw: GTTCTAAAGAGGGATTACCA Rv: TGGTGAGCATCTTTGAAGGCTGTTG
Pri-miR-24-1	Fw: CTAAAGGGTCCAGGTCTCCATG Rv: CTGAGCCAGTGTGTGAAATGAGAAC
18sRNA	Fw: CCTGGATACCGCAGCTAGGA Rv: TCTAGCGGCGCAATACGAATG

Table 6 Chromatin immunoprecipitation primer

Gene	Primer name	Forward/Reverse Primer
Dbp	Dbp_P	Fw: ACACCCGCATCCGGTAGC Rv: CCACTTCGGGCCAATGAG
Dbp	Dbp_E3	Fw: CGTGGAGGTGCTTAATGACCTTT Rv: CATGGCCTGGAATGCTTGA
Dbp primer sequences (Ripperger and Schibler, 2006)		
Wnt3	Wnt3_UP	Fw: CAACCCCTTTGCTTTCTAG Rv: GACACCCCCTTCCCAGTC
Lef1	Lef1_farUP1	Fw: CAGTGTACTGTAACAGTG Rv: CTTCTTCCAGCCTGCTTC
Dab2	Dab2_farUP	Fw: CACTATGGAAAACGGGAC Rv: CTCTTTGTTATTACACTTC
Dab2	Dab2_UP	Fw: GAACCAGGACTGCACACT Rv: GGAGGACACAAAAGCATC
Notch2	Notch2_farUP	Fw: CACTCCAACAATTCAACAG Rv: ACCCAACTTTAACTTCTG
Itga6	Itga6_E1	Fw: GCTTCTAGCCCGGCTGGG Rv: GAACTCACAGCCGCTTGTC
Cdk4	Cdk4_UP1	Fw: CTTGTGCTCCACCCTCTC Rv: CTGACGGCCACGTGACCTG
Cdk4	Cdk4_I1	Fw: GTGATCCTCTTTGTGCCTAG Rv: GCCAACGCGATCAGCAAC
miR23b-27b-24-1 cluster	miR23_I11	Fw: GCACAGACGGACAGAGGTAC Rv: CTGCCAGCACCACCAAGG
	miR23_I12_1	Fw: CCAGCAAGAAAGCTTTAC Rv: GTGGGCCCATGTGCTGATG
	miR23_I12_2	Fw: CCTTCACCCTTTATCATG Rv: GTGCCAGTGTCCTGAGGTC
	miR23_I14_2	Fw: CCTAAGCCTTGATTTCCTG Rv: CATGTGCCTGACATGCGC
Lhx2	Lhx2-farUP1	Fw: CAGATCGCTGCAGGGAGAAG Rv: GGTCATACCATACAGAGAT
Tcf4	Tcf4_farUP	Fw: CCAAGAAGTCTGCGGTGA Rv: CCAGCGATCATTAGTTACC
Fzd2	Fzd2_farUP	Fw: GCTCTTGTACCTCAGAGG Rv: GCTCAGTCCGTGATTGCT
Smad7	Smad7_farUP	Fw: GGACATCAGCTCTGAATC Rv: AGGCTGGTATGATGATGG

Lefty	Lefty_UP	Fw: GCAGAGAACGTGAGACCTC Rv: TGTTAGCCATATACTTCACC
Dkk3	Dkk3_UP	Fw: TGCTGCAACGGACAGACC Rv: CTCTCCGCATCTCCTGATC
Sox9	Sox9_UP	Fw: ATCCGGTCCAATCAGCGAC Rv: CTCTCCGACTTCCAGCTCAG

Table 7 Facilities

Service	**Facility**
Animal housing	Animal Facility, PRBB, Barcelona
Confocal microscopy	Advanced Light Microscopy Unit, CRG, Barcelona
Fluorescent activated cell sorting (FACS)	FACS Unit, CRG-UPF, Barcelona
Affymetrix microarray	Functional Genomics Core Facility, IRB, Barcelona
Microarray data analysis	Bioinformatics Unit, CRG, Barcelona
Real time PCR	Microarray Unit, CRG, Barcelona
Sequencing	Genomics Unit, UPF, Barcelona
Tissue processing and sectioning	Histology Facility, CRG, Barcelona

REFERENCES

VII REFERENCES

Alam, M., and Ratner, D. (2001). Cutaneous squamous-cell carcinoma. N. Engl. J. Med. *344*, 975–983.

Amoh, Y., Li, L., Katsuoka, K., Penman, S., and Hoffman, R. M. (2005). Multipotent nestin-positive, keratin-negative hair-follicle bulge stem cells can form neurons. Proc Natl Acad Sci USA *102*, 5530–5534.

Andl, T., Reddy, S. T., Gaddapara, T., and Millar, S. E. (2002). WNT signals are required for the initiation of hair follicle development. Developmental Cell *2*, 643–653.

Annes, J. P. (2003). Making sense of latent TGFbeta activation. J. Cell. Sci. *116*, 217–224.

Antoch, M. P., Gorbacheva, V. Y., Vykhovanets, O., Toshkov, I. A., Kondratov, R. V., Kondratova, A. A., Lee, C., and Nikitin, A. Y. (2008). Disruption of the circadian clock due to the Clock mutation has discrete effects on aging and carcinogenesis. Cell Cycle *7*, 1197–1204.

Asher, G., Gatfield, D., Stratmann, M., Reinke, H., Dibner, C., Kreppel, F., Mostoslavsky, R., Alt, F. W., and Schibler, U. (2008). SIRT1 regulates circadian clock gene expression through PER2 deacetylation. Cell *134*, 317–328.

Asher, G., Reinke, H., Altmeyer, M., Gutierrez-Arcelus, M., Hottiger, M. O., and Schibler, U. (2010). Poly(ADP-Ribose) Polymerase 1 Participates in the Phase Entrainment of Circadian Clocks to Feeding. Cell, 1–11.

Bae, K., Jin, X., Maywood, E. S., Hastings, M. H., Reppert, S. M., and Weaver, D. R. (2001). Differential functions of mPer1, mPer2, and mPer3 in the SCN circadian clock. Neuron *30*, 525–536.

Balsalobre, A. (2000). Resetting of Circadian Time in Peripheral Tissues by Glucocorticoid Signaling. Science *289*, 2344–2347.

Balsalobre, A., Damiola, F., and Schibler, U. (1998). A serum shock induces circadian gene expression in mammalian tissue culture cells. Cell *93*, 929–937.

Barradas, M., Anderton, E., Acosta, J. C., Li, S., Banito, A., Rodriguez-Niedenfuhr, M., Maertens, G., Banck, M., Zhou, M. M., Walsh, M. J., et al. (2009). Histone demethylase JMJD3 contributes to epigenetic control of INK4a/ARF by oncogenic RAS. Genes Dev *23*, 1177–1182.

Barrandon, Y., and Green, H. (1987). Three clonal types of keratinocyte with different capacities for multiplication. Proc Natl Acad Sci USA *84*, 2302–2306.

Batard, P., Monier, M. N., Fortunel, N., Ducos, K., Sansilvestri-Morel, P., Phan, T., Hatzfeld, A., and Hatzfeld, J. A. (2000). TGF-(beta)1 maintains hematopoietic immaturity by a reversible negative control of cell cycle and induces CD34 antigen up-modulation. J. Cell. Sci. *113 (Pt 3)*, 383–390.

Beck, B., Driessens, G., Goossens, S., Youssef, K. K., Kuchnio, A., Caauwe, A., Sotiropoulou, P. A., Loges, S., Lapouge, G., Candi, A., et al. (2011). A vascular niche and a VEGF-Nrp1 loop regulate the initiation and stemness of skin tumours. Nature *478*, 399–403.

Bickenbach, J. R. (1981). Identification and behavior of label-retaining cells in oral mucosa and skin. J. Dent. Res. *60 Spec No C*, 1611–1620.

Blanpain, C., and Fuchs, E. (2009). Epidermal homeostasis: a balancing act of stem cells in the skin. Nat Rev Mol Cell Biol *10*, 207–217.

Blanpain, C., and Fuchs, E. (2006). Epidermal stem cells of the skin. Annu. Rev. Cell Dev. Biol. *22*, 339–373.

Blanpain, C., Lowry, W. E., Geoghegan, A., Polak, L., and Fuchs, E. (2004). Self-renewal, multipotency, and the existence of two cell populations within an epithelial stem cell niche. Cell *118*, 635–648.

Braun, K. M. (2003). Manipulation of stem cell proliferation and lineage commitment: visualisation of label-retaining cells in wholemounts of mouse epidermis. Development *130*, 5241–5255.

Bunger, M. K., Wilsbacher, L. D., Moran, S. M., Clendenin, C., Radcliffe, L. A., Hogenesch, J. B., Simon, M. C., Takahashi, J. S., and Bradfield, C. A. (2000). Mop3 is an essential component of the master circadian pacemaker in mammals. Cell *103*, 1009–1017.

Candi, E., Schmidt, R., and Melino, G. (2005). The cornified envelope: a model of cell death in the skin. Nat Rev Mol Cell Biol *6*, 328–340.

Cardone, L., Hirayama, J., Giordano, F., Tamaru, T., Palvimo, J. J., and Sassone-Corsi, P. (2005). Circadian clock control by SUMOylation of BMAL1. Science *309*, 1390–1394.

Celso, C. L. (2004). Transient activation of -catenin signalling in adult mouse epidermis is sufficient to induce new hair follicles but continuous activation is required to maintain hair follicle tumours. Development *131*, 1787–1799.

Chen, S.-T., Choo, K.-B., Hou, M.-F., Yeh, K.-T., Kuo, S.-J., and Chang, J.-G. (2005). Deregulated expression of the PER1, PER2 and PER3 genes in breast cancers. Carcinogenesis *26*, 1241–1246.

Cheng, H.-Y. M., Alvarez-Saavedra, M., Dziema, H., Choi, Y. S., Li, A., and Obrietan, K. (2009). Segregation of expression of mPeriod gene homologs in neurons and glia: possible divergent roles of mPeriod1 and mPeriod2 in the brain. *18*, 3110–3124.

Chhabra, R., Dubey, R., and Saini, N. (2010). Cooperative and individualistic functions of the microRNAs in the miR-23a~27a~24-2 cluster and its implication in human diseases. Mol Cancer *9*, 232.

Clayton, E., Doupé, D. P., Klein, A. M., Winton, D. J., Simons, B. D., and Jones, P. H. (2007). A single type of progenitor cell maintains normal epidermis. Nature *446*, 185–189.

Cotsarelis, G., Sun, T. T., and Lavker, R. M. (1990). Label-retaining cells reside in the bulge area of pilosebaceous unit: implications for follicular stem cells, hair cycle, and skin carcinogenesis. Cell *61*, 1329–1337.

Cui, W., Fowlis, D. J., Cousins, F. M., Duffie, E., Bryson, S., Balmain, A., and Akhurst, R. J. (1995). Concerted action of TGF-beta 1 and its type II receptor in control of epidermal homeostasis in transgenic mice. Genes Dev *9*, 945–955.

Damiola, F., Le Minh, N., Preitner, N., Kornmann, B., Fleury-Olela, F., and Schibler, U. (2000). Restricted feeding uncouples circadian oscillators in peripheral tissues from the central pacemaker in the suprachiasmatic nucleus. Genes Dev *14*, 2950–2961.

DasGupta, R., and Fuchs, E. (1999). Multiple roles for activated LEF/TCF transcription complexes during hair follicle development and differentiation. Development *126*, 4557–4568.

Davis, S., Mirick, D. K., and Stevens, R. G. (2001). Night shift work, light at night, and risk of breast cancer. J. Natl. Cancer Inst. *93*, 1557–1562.

DiTacchio, L., Le, H. D., Vollmers, C., Hatori, M., Witcher, M., Secombe, J., and Panda, S. (2011). Histone Lysine Demethylase JARID1a Activates CLOCK-BMAL1 and Influences the Circadian Clock. Science *333*, 1881–1885.

Doi, M., Hirayama, J., and Sassone-Corsi, P. (2006). Circadian regulator CLOCK is a histone acetyltransferase. Cell *125*, 497–508.

Duong, H. A., Robles, M. S., Knutti, D., and Weitz, C. J. (2011a). A Molecular Mechanism for Circadian Clock Negative Feedback. Science *332*, 1436–1439.

Duong, H. A., Robles, M. S., Knutti, D., and Weitz, C. J. (2011b). A Molecular Mechanism for Circadian Clock Negative Feedback. Science *332*, 1436–1439.

Ebisawa, T. (2001). Smurf1 Interacts with Transforming Growth Factor-beta Type I Receptor through Smad7 and Induces Receptor Degradation. Journal of Biological Chemistry *276*, 12477–12480.

Eckel-Mahan, K., and Sassone-Corsi, P. (2009). Metabolism control by the circadian clock and vice versa. Nat Struct Mol Biol *16*, 462–467.

Falk, S., Wurdak, H., Ittner, L. M., Ille, F., Sumara, G., Schmid, M.-T., Draganova, K., Lang, K. S., Paratore, C., Leveen, P., et al. (2008). Brain Area-Specific Effect of TGF-β Signaling on Wnt-Dependent Neural Stem Cell Expansion. Cell Stem Cell *2*, 472–483.

Foitzik, K., Lindner, G., Mueller-Roever, S., Maurer, M., Botchkareva, N., Botchkarev, V., Handjiski, B., Metz, M., Hibino, T., Soma, T., et al. (2000). Control of murine hair follicle regression (catagen) by TGF-beta1 in vivo. FASEB J. *14*, 752–760.

Froy, O., and Miskin, R. (2010). Effect of feeding regimens on circadian rhythms: implications for aging and longevity. Aging (Albany NY) *2*, 7–27.

Fu, L., and Lee, C. C. (2003). The circadian clock: pacemaker and tumour suppressor. Nat Rev Cancer *3*, 350–361.

Fu, L., Pelicano, H., Liu, J., Huang, P., and Lee, C. (2002). The circadian gene Period2 plays an important role in tumor suppression and DNA damage response in vivo. Cell *111*, 41–50.

Fuchs, E. (2007). Scratching the surface of skin development. Nature *445*, 834–842.

Fuchs, E. (2009). The Tortoise and the Hair: Slow-Cycling Cells in the Stem Cell Race. Cell *137*, 811–819.

Gaddameedhi, S., Selby, C. P., Kaufmann, W. K., Smart, R. C., and Sancar, A. (2011). Control of skin cancer by the circadian rhythm. Proceedings of the National Academy of Sciences.

Gallego, M., and Virshup, D. M. (2007). Post-translational modifications regulate the ticking of the circadian clock. Nat Rev Mol Cell Biol *8*, 139–148.

Gat, U., DasGupta, R., and Degenstein, L. (1998). De novo hair follicle morphogenesis and hair tumors in mice expressing a truncated [beta]-catenin in skin. Cell.

Gatfield, D., Le Martelot, G., Vejnar, C. E., Gerlach, D., Schaad, O., Fleury-Olela, F., Ruskeepaa, A. L., Oresic, M., Esau, C. C., Zdobnov, E. M., et al. (2009). Integration of microRNA miR-122 in hepatic circadian gene expression. Genes Dev *23*, 1313–1326.

Gery, S., and Koeffler, H. P. (2010). Circadian rhythms and cancer. Cell Cycle *9*.

Gery, S., Gombart, A. F., Yi, W. S., Koeffler, C., Hofmann, W.-K., and Koeffler, H. P. (2005). Transcription profiling of C/EBP targets identifies Per2 as a gene implicated in myeloid leukemia. Blood *106*, 2827–2836.

Gery, S., Komatsu, N., Baldjyan, L., Yu, A., Koo, D., and Koeffler, H. P. (2006).

The Circadian Gene Per1 Plays an Important Role in Cell Growth and DNA Damage Control in Human Cancer Cells. Molecular Cell *22*, 375–382.

Gery, S., Virk, R. K., Chumakov, K., Yu, A., and Koeffler, H. P. (2007). The clock gene Per2 links the circadian system to the estrogen receptor. Oncogene *26*, 7916–7920.

Gibson, E. M., Williams, W. P., and Kriegsfeld, L. J. (2009). Aging in the circadian system: considerations for health, disease prevention and longevity. Exp. Gerontol. *44*, 51–56.

Greco, V., Chen, T., Rendl, M., Schober, M., Pasolli, H. A., Stokes, N., Cruz-Racelis, dela, J., and Fuchs, E. (2009). A Two-Step Mechanism for Stem Cell Activation during Hair Regeneration. Stem Cell *4*, 155–169.

Haegebarth, A., and Clevers, H. (2010). Wnt Signaling, Lgr5, and Stem Cells in the Intestine and Skin. Am. J. Pathol. *174*, 715–721.

Hatanaka, F., Matsubara, C., Myung, J., Yoritaka, T., Kamimura, N., Tsutsumi, S., Kanai, A., Suzuki, Y., Sassone-Corsi, P., Aburatani, H., et al. (2010). Genome-Wide Profiling of the Core Clock Protein BMAL1 Targets Reveals a Strict Relationship with Metabolism. Molecular and Cellular Biology *30*, 5636–5648.

Hirayama, J., Sahar, S., Grimaldi, B., Tamaru, T., Takamatsu, K., Nakahata, Y., and Sassone-Corsi, P. (2007). CLOCK-mediated acetylation of BMAL1 controls circadian function. Nature *450*, 1086–1090.

Hoffman, A. E., Zheng, T., Stevens, R. G., Ba, Y., Zhang, Y., Leaderer, D., Yi, C., Holford, T. R., and Zhu, Y. (2009). Clock-Cancer Connection in Non-Hodgkin's Lymphoma: A Genetic Association Study and Pathway Analysis of the Circadian Gene Cryptochrome 2. Cancer Research *69*, 3605–3613.

Hofman, M. A., and Swaab, D. F. (2006). Living by the clock: the circadian pacemaker in older people. Ageing Res. Rev. *5*, 33–51.

Horsley, V., O'Carroll, D., Tooze, R., and Ohinata, Y. (2006). Blimp1 defines a progenitor population that governs cellular input to the sebaceous gland. Cell.

Hsu, C.-M., Lin, S.-F., Lu, C.-T., Lin, P.-M., and Yang, M.-Y. (2011a). Altered expression of circadian clock genes in head and neck squamous cell carcinoma. Tumor Biol.

Hsu, Y.-C., Pasolli, H. A., and Fuchs, E. (2011b). Dynamics between Stem Cells, Niche, and Progeny in the Hair Follicle. Cell *144*, 92–105.

Huelsken, J., Vogel, R., Erdmann, B., Cotsarelis, G., and Birchmeier, W. (2001). beta-Catenin controls hair follicle morphogenesis and stem cell differentiation in the skin. Cell *105*, 533–545.

Hurd, M. W., and Ralph, M. R. (1998). The significance of circadian organization for longevity in the golden hamster. J Biol Rhythms *13*, 430–436.

Ikushima, H., and Miyazono, K. (2010). TGFβ signalling: a complex web in cancer progression. 1–10.

Ito, M., Liu, Y., Yang, Z., Nguyen, J., Liang, F., Morris, R. J., and Cotsarelis, G. (2005). Stem cells in the hair follicle bulge contribute to wound repair but not to homeostasis of the epidermis. Nat Med *11*, 1351–1354.

Ito, M., Yang, Z., Andl, T., Cui, C., Kim, N., Millar, S. E., and Cotsarelis, G. (2007). Wnt-dependent de novo hair follicle regeneration in adult mouse skin after wounding. Nature *447*, 316–320.

Jaks, V., Barker, N., Kasper, M., van Es, J. H., Snippert, H. J., Clevers, H., and Toftgård, R. (2008). Lgr5 marks cycling, yet long-lived, hair follicle stem cells. Nat Genet *40*, 1291–1299.

Jensen, K. B., Collins, C. A., Nascimento, E., Tan, D. W., Frye, M., Itami, S., and Watt, F. M. (2009). Lrig1 expression defines a distinct multipotent stem cell population in mammalian epidermis. Cell Stem Cell *4*, 427–439.

Jensen, K. B., Driskell, R. R., and Watt, F. M. (2010). Assaying proliferation and differentiation capacity of stem cells using disaggregated adult mouse epidermis. Nat Protoc *5*, 898–911.

Jensen, U. B., Yan, X., Triel, C., Woo, S.-H., Christensen, R., and Owens, D. M. (2008). A distinct population of clonogenic and multipotent murine follicular keratinocytes residing in the upper isthmus. J. Cell. Sci. *121*, 609–617.

Jones, P., and Simons, B. D. (2008). Epidermal homeostasis: do committed progenitors work while stem cells sleep? Nat Rev Mol Cell Biol *9*, 82–88.

Jones, P.H., Harper, S., and Watt, F.M. (1995). Stem cell patterning and fate in human epidermis. Cell *80,* 83-93.

Kameda, T., and Sugiyama, T. (2005). Application of genetically modified feeder cells for culture of keratinocytes. Methods Mol. Biol. *289*, 29–38.

Karlsson, G., Blank, U., Moody, J. L., Ehinger, M., Singbrant, S., Deng, C. X., and Karlsson, S. (2007). Smad4 is critical for self-renewal of hematopoietic stem cells. Journal of Experimental Medicine *204*, 467–474.

Kemp, C. J. (2005). Multistep skin cancer in mice as a model to study the evolution of cancer cells. Semin. Cancer Biol. *15*, 460–473.

Kim, D.-S., Park, S.-H., and Park, K.-C. (2004). Transforming growth factor-β1 decreases melanin synthesis via delayed extracellular signal-regulated kinase activation. Int J Biochem Cell Biol *36*, 1482–1491.

Klaus, A., and Birchmeier, W. (2008). Wnt signalling and its impact on development and cancer. Nat Rev Cancer *8*, 387–398.

Kojima, S., Gatfield, D., Esau, C. C., and Green, C. B. (2010). MicroRNA-122 Modulates the Rhythmic Expression Profile of the Circadian Deadenylase Nocturnin in Mouse Liver. PLoS ONE *5*, e11264.

Kondratov, R. V., Kondratova, A. A., Gorbacheva, V. Y., Vykhovanets, O. V., and Antoch, M. P. (2006). Early aging and age-related pathologies in mice deficient in BMAL1, the core componentof the circadian clock. Genes Dev *20*, 1868–1873.

Kubo, T. (2006). Prospective Cohort Study of the Risk of Prostate Cancer among Rotating-Shift Workers: Findings from the Japan Collaborative Cohort Study. American Journal of Epidemiology *164*, 549–555.

Kuhlman, S. J., Quintero, J. E., and McMahon, D. G. (2000). GFP fluorescence reports Period 1 circadian gene regulation in the mammalian biological clock. Neuroreport *11*, 1479–1482.

Kuo, S.-J., Chen, S.-T., Yeh, K.-T., Hou, M.-F., Chang, Y.-S., Hsu, N. C., and Chang, J.-G. (2009). Disturbance of circadian gene expression in breast

cancer. Virchows Arch *454*, 467–474.

Lako, M., Armstrong, L., Cairns, P. M., Harris, S., Hole, N., and Jahoda, C. A. B. (2002). Hair follicle dermal cells repopulate the mouse haematopoietic system. J. Cell. Sci. *115*, 3967–3974.

Lamia, K. A., Storch, K.-F., and Weitz, C. J. (2008). Physiological significance of a peripheral tissue circadian clock. Proceedings of the National Academy of Sciences *105*, 15172–15177.

Larsson, J. (2003). TGF- signaling-deficient hematopoietic stem cells have normal self-renewal and regenerative ability in vivo despite increased proliferative capacity in vitro. Blood *102*, 3129–3135.

Lee, S., Donehower, L. A., Herron, A. J., Moore, D. D., and Fu, L. (2010). Disrupting circadian homeostasis of sympathetic signaling promotes tumor development in mice. PLoS ONE *5*, e10995.

Lena, A. M., Shalom-Feuerstein, R., di Val Cervo, P. R., Aberdam, D., Knight, R. A., Melino, G., and Candi, E. (2008). miR-203 represses "stemness" by repressing ΔNp63. Cell Death Differ. *15*, 1187–1195.

LeSauter, J., Yan, L., Vishnubhotla, B., Quintero, J. E., Kuhlman, S. J., McMahon, D. G., and Silver, R. (2003). A short half-life GFP mouse model for analysis of suprachiasmatic nucleus organization. Brain Res *964*, 279–287.

Levi, F., and Schibler, U. (2007). Circadian rhythms: mechanisms and therapeutic implications. *47*, 593–628.

Levy, V., Lindon, C., Harfe, B. D., and Morgan, B. A. (2005). Distinct Stem Cell Populations Regenerate the Follicle and Interfollicular Epidermis. Developmental Cell *9*, 855–861.

Levy, V., Lindon, C., Zheng, Y., Harfe, B. D., and Morgan, B. A. (2007). Epidermal stem cells arise from the hair follicle after wounding. The FASEB Journal *21*, 1358–1366.

Li, Z., Ruan, L., Lin, S., and Gittes, G. K. (2007). Clock controls timing of mouse pancreatic differentiation through regulation of Wnt- and Notch-based and cell division components. Biochem Biophys Res Commun *359*, 491–496.

Lichtenberger, B. M., Tan, P. K., Niederleithner, H., Ferrara, N., Petzelbauer, P., and Sibilia, M. (2010). Autocrine VEGF Signaling Synergizes with EGFR in Tumor Cells to Promote Epithelial Cancer Development. Cell *140*, 268–279.

Lichti, U., Anders, J., and Yuspa, S. H. (2008). Isolation and short-term culture of primary keratinocytes, hair follicle populations and dermal cells from newborn mice and keratinocytes from adult mice for in vitro analysis and for grafting to immunodeficient mice. Nat Protoc *3*, 799–810.

Lin, K. K., Kumar, V., Geyfman, M., Chudova, D., Ihler, A. T., Smyth, P., Paus, R., Takahashi, J. S., and Andersen, B. (2009). Circadian Clock Genes Contribute to the Regulation of Hair Follicle Cycling. PLoS Genet *5*, e1000573.

Lis, C. G., Grutsch, J. F., Wood, P., You, M., Rich, I., and Hrushesky, W. J. M. (2003). Circadian timing in cancer treatment: the biological foundation for an integrative approach. Integr Cancer Ther *2*, 105–111.

Liu, X., Alexander, V., Vijayachandra, K., Bhogte, E., Diamond, I., and Glick, A. (2001). Conditional epidermal expression of TGFbeta 1 blocks neonatal lethality but causes a reversible hyperplasia and alopecia. Proc Natl Acad Sci USA *98*, 9139–9144.

Lowry, W. E., Blanpain, C., Nowak, J. A., Guasch, G., Lewis, L., and Fuchs, E. (2005). Defining the impact of beta-catenin/Tcf transactivation on epithelial stem cells. Genes Dev *19*, 1596–1611.

MacDonald, B. T., Tamai, K., and He, X. (2009). Wnt/β-Catenin Signaling: Components, Mechanisms, and Diseases. Developmental Cell *17*, 9–26.

Mackenzie, I. C. (1970). Relationship between mitosis and the ordered structure of the stratum corneum in mouse epidermis. Nature *226*, 653–655.

Malanchi, I., Peinado, H., Kassen, D., Hussenet, T., Metzger, D., Chambon, P., Huber, M., Hohl, D., Cano, A., Birchmeier, W., et al. (2008). Cutaneous cancer stem cell maintenance is dependent on β-catenin signalling. Nature *452*, 650–653.

Marcheva, B., Ramsey, K. M., Buhr, E. D., Kobayashi, Y., Su, H., Ko, C. H.,

Ivanova, G., Omura, C., Mo, S., Vitaterna, M. H., et al. (2010). Disruption of the clock components CLOCK and BMAL1 leads to hypoinsulinaemia and diabetes. Nature, 1–5.

Mardaryev, A. N., Ahmed, M. I., Vlahov, N. V., Fessing, M. Y., Gill, J. H., Sharov, A. A., and Botchkareva, N. V. (2010). Micro-RNA-31 controls hair cycle-associated changes in gene expression programs of the skin and hair follicle. The FASEB Journal *24*, 3869–3881.

Massagué, J., and Gomis, R. (2006). The logic of TGFβ signaling. FEBS Lett *580*, 2811–2820.

Matsuo, T., Yamaguchi, S., Mitsui, S., Emi, A., Shimoda, F., and Okamura, H. (2003). Control mechanism of the circadian clock for timing of cell division in vivo. Science *302*, 255–259.

Megdal, S. P., Kroenke, C. H., Laden, F., Pukkala, E., and Schernhammer, E. S. (2005). Night work and breast cancer risk: A systematic review and meta-analysis. Eur J Cancer *41*, 2023–2032.

Merrill, B. J. (2001). Tcf3 and Lef1 regulate lineage differentiation of multipotent stem cells in skin. Genes Dev *15*, 1688–1705.

Méndez-Ferrer, S., Lucas, D., Battista, M., and Frenette, P. S. (2008). Haematopoietic stem cell release is regulated by circadian oscillations. Nature *452*, 442–447.

Moon, R. T., Kohn, A. D., Ferrari, G. V. D., and Kaykas, A. (2004). WNT and β-catenin signalling: diseases and therapies. Nature Publishing Group *5*, 691–701.

Morris, R. J., Liu, Y., Marles, L., Yang, Z., Trempus, C., Li, S., Lin, J. S., Sawicki, J. A., and Cotsarelis, G. (2004). Capturing and profiling adult hair follicle stem cells. Nat Biotechnol *22*, 411–417.

Nagoshi, E., Saini, C., Bauer, C., Laroche, T., Naef, F., and Schibler, U. (2004). Circadian gene expression in individual fibroblasts: cell-autonomous and self-sustained oscillators pass time to daughter cells. Cell *119*, 693–705.

Nakada, D., Levi, B. P., and Morrison, S. J. (2011). Integrating physiological regulation with stem cell and tissue homeostasis. Neuron *70*, 703–718.

Nguyen, H., Merrill, B. J., Polak, L., Nikolova, M., Rendl, M., Shaver, T. M., Pasolli, H. A., and Fuchs, E. (2009). Tcf3 and Tcf4 are essential for long-term homeostasis of skin epithelia. Nat Genet *41*, 1068–1075.

Nijhof, J. G. W. (2006). The cell-surface marker MTS24 identifies a novel population of follicular keratinocytes with characteristics of progenitor cells. Development *133*, 3027–3037.

Nishimura, E. K., Granter, S. R., and Fisher, D. E. (2005). Mechanisms of hair graying: incomplete melanocyte stem cell maintenance in the niche. Science *307*, 720–724.

Nishimura, E. K., Suzuki, M., Igras, V., Du, J., Lonning, S., Miyachi, Y., Roes, J., Beermann, F., and Fisher, D. E. (2010). Key Roles for Transforming Growth Factor β in Melanocyte Stem Cell Maintenance. Stem Cell *6*, 130–140.

Nowak, J. A., and Fuchs, E. (2009). Methods in Molecular Biology J. M. Walker, J. Audet, and W. L. Stanford, eds. (Totowa, NJ: Humana Press).

Nowak, J. A., Polak, L., Pasolli, H. A., and Fuchs, E. (2008). Hair follicle stem cells are specified and function in early skin morphogenesis. Cell Stem Cell *3*, 33–43.

Owens, D. M. (2003). Suprabasal 6 4 integrin expression in epidermis results in enhanced tumourigenesis and disruption of TGF signalling. J. Cell. Sci. *116*, 3783–3791.

Panda, S. (2007). Multiple Photopigments Entrain the Mammalian Circadian Oscillator. Neuron *53*, 619–621.

Panda, S., Antoch, M. P., Miller, B. H., Su, A. I., Schook, A. B., Straume, M., Schultz, P. G., Kay, S. A., Takahashi, J. S., and Hogenesch, J. B. (2002). Coordinated transcription of key pathways in the mouse by the circadian clock. Cell *109*, 307–320.

Pincelli, C., and Marconi, A. (2010). Keratinocyte stem cells: Friends and foes. J. Cell. Physiol. *225*, 310–315.

Potten, C. S. (1974). The epidermal proliferative unit: the possible role of the central basal cell. Cell Tissue Kinet *7*, 77–88.

Ptitsyn, A. A., Zvonic, S., Conrad, S. A., Scott, L. K., Mynatt, R. L., and Gimble, J. M. (2006). Circadian clocks are resounding in peripheral tissues. PLoS Comput Biol *2*, e16.

Rhee, H., Polak, L., and Fuchs, E. (2006). Lhx2 maintains stem cell character in hair follicles. Science *312*, 1946–1949.

Ripperger, J. A., and Schibler, U. (2006). Rhythmic CLOCK-BMAL1 binding to multiple E-box motifs drives circadian Dbp transcription and chromatin transitions. Nat Genet *38*, 369–374.

Ripperger, J. A., Jud, C., and Albrecht, U. (2011). The daily rhythm of mice. FEBS Lett, 1–9.

Rogler, C. E., LeVoci, L., Ader, T., Massimi, A., Tchaikovskaya, T., Norel, R., and Rogler, L. E. (2009). MicroRNA-23b cluster microRNAs regulate transforming growth factor-beta/bone morphogenetic protein signaling and liver stem cell differentiation by targeting Smads. Hepatology *50*, 575–584.

Sahar, S., and Sassone-Corsi, P. (2009). Metabolism and cancer: the circadian clock connection. Nat Rev Cancer *9*, 886–896.

Schernhammer, E. S., Laden, F., Speizer, F. E., Willett, W. C., Hunter, D. J., Kawachi, I., Fuchs, C. S., and Colditz, G. A. (2003). Night-shift work and risk of colorectal cancer in the nurses' health study. J. Natl. Cancer Inst. *95*, 825–828.

Schernhammer, E. S., Razavi, P., Li, T. Y., Qureshi, A. A., and Han, J. (2011). Rotating Night Shifts and Risk of Skin Cancer in the Nurses' Health Study. J. Natl. Cancer Inst. *103*, 602–606.

Schneider, M. R., Schmidt-Ullrich, R., and Paus, R. (2009). The Hair Follicle as a Dynamic Miniorgan. Curr Biol *19*, R132–R142.

Shi, S., Hida, A., Mcguinness, O. P., Wasserman, D. H., Yamazaki, S., and Johnson, C. H. (2010). Circadian Clock Gene Bmal1 Is Not Essential; Functional Replacement with its Paralog, Bmal2. Current Biology, 1–6.

Sibilia, M., Fleischmann, A., Behrens, A., Stingl, L., Carroll, J., Watt, F. M., Schlessinger, J., and Wagner, E. F. (2000). The EGF receptor provides an essential survival signal for SOS-dependent skin tumor development.

Cell *102*, 211–220.

Siegel, P. M., and Massagué, J. (2003). Cytostatic and apoptotic actions of TGF-β in homeostasis and cancer. Nat Rev Cancer *3*, 807–820.

Snippert, H. J., Haegebarth, A., Kasper, M., Jaks, V., van Es, J. H., Barker, N., van de Wetering, M., van den Born, M., Begthel, H., Vries, R. G., et al. (2010). Lgr6 marks stem cells in the hair follicle that generate all cell lineages of the skin. Science *327*, 1385–1389.

Spencer, J. M., Kahn, S. M., Jiang, W., DeLeo, V. A., and Weinstein, I. B. (1995). Activated ras genes occur in human actinic keratoses, premalignant precursors to squamous cell carcinomas. Arch Dermatol *131*, 796–800.

Steingrímsson, E., Copeland, N. G., and Jenkins, N. A. (2005). Melanocyte stem cell maintenance and hair graying. Cell *121*, 9–12.

Stokkan, K. A., Yamazaki, S., Tei, H., Sakaki, Y., and Menaker, M. (2001). Entrainment of the circadian clock in the liver by feeding. Science *291*, 490–493.

Storch, K.-F., Lipan, O., Leykin, I., Viswanathan, N., Davis, F. C., Wong, W. H., and Weitz, C. J. (2002). Extensive and divergent circadian gene expression in liver and heart. Nature *417*, 78–83.

Storch, K.-F., Paz, C., Signorovitch, J., Raviola, E., Pawlyk, B., Li, T., and Weitz, C. J. (2007). Intrinsic circadian clock of the mammalian retina: importance for retinal processing of visual information. Cell *130*, 730–741.

Sun, F., Wang, J., Pan, Q., Yu, Y., Zhang, Y., Wan, Y., Wang, J., Li, X., and Hong, A. (2009). Characterization of function and regulation of miR-24-1 and miR-31. Biochem Biophys Res Commun *380*, 660–665.

Tajima, Y. (2003). Chromosomal Region Maintenance 1 (CRM1)-dependent Nuclear Export of Smad Ubiquitin Regulatory Factor 1 (Smurf1) Is Essential for Negative Regulation of Transforming Growth Factor-beta Signaling by Smad7. Journal of Biological Chemistry *278*, 10716–10721.

Tani, H., Morris, R. J., and Kaur, P. (2000). Enrichment for murine keratinocyte stem cells based on cell surface phenotype. Proc Natl Acad Sci USA *97*, 10960–10965.

Toh, K. L. (2001). An hPer2 Phosphorylation Site Mutation in Familial Advanced Sleep Phase Syndrome. Science *291*, 1040–1043.

Törnqvist, G., Sandberg, A., and Hägglund, A. (2010). Cyclic Expression of Lhx2 Regulates Hair Formation. PLoS Genet.

Tumbar, T., Guasch, G., Greco, V., Blanpain, C., Lowry, W. E., Rendl, M., and Fuchs, E. (2004). Defining the epithelial stem cell niche in skin. Science *303*, 359–363.

Turek, F. W., Joshu, C., Kohsaka, A., Lin, E., Ivanova, G., McDearmon, E., Laposky, A., Losee-Olson, S., Easton, A., Jensen, D. R., et al. (2005). Obesity and metabolic syndrome in circadian Clock mutant mice. Science *308*, 1043–1045.

Uchugonova, A., Duong, J., Zhang, N., König, K., and Hoffman, R. M. (2011). The bulge area is the origin of nestin-expressing pluripotent stem cells of the hair follicle. J. Cell. Biochem. *112*, 2046–2050.

van der Horst, G. T., Muijtjens, M., Kobayashi, K., Takano, R., Kanno, S., Takao, M., de Wit, J., Verkerk, A., Eker, A. P., van Leenen, D., et al. (1999). Mammalian Cry1 and Cry2 are essential for maintenance of circadian rhythms. Nature *398*, 627–630.

van der Schroeff, J. G., Evers, L. M., Boot, A. J., and Bos, J. L. (1990). Ras oncogene mutations in basal cell carcinomas and squamous cell carcinomas of human skin. J Invest Dermatol *94*, 423–425.

van Genderen, C., Okamura, R. M., Farinas, I., Quo, R. G., Parslow, T. G., Bruhn, L., and Grosschedl, R. (1994). Development of several organs that require inductive epithelial-mesenchymal interactions is impaired in LEF-1-deficient mice. Genes Dev *8*, 2691–2703.

Van Mater, D. (2003). Transient activation of beta -catenin signaling in cutaneous keratinocytes is sufficient to trigger the active growth phase of the hair cycle in mice. Genes Dev *17*, 1219–1224.

Vidal, V. P. I., Chaboissier, M.-C., Lützkendorf, S., Cotsarelis, G., Mill, P., Hui, C.-C., Ortonne, N., Ortonne, J.-P., and Schedl, A. (2005). Sox9 is essential for outer root sheath differentiation and the formation of the hair stem cell compartment. Curr Biol *15*, 1340–1351.

Wang, X.-J., Greenhalgh, D. A., Bickenbach, J. R., Jiang, A., Bundman, D. S., Krieg, T., Derynck, R., and Roop, D. R. (1997). Expression of a dominant-negative type II transforming growth factor beta (TGF-beta) receptor in the epidermis of transgenic mice blocks TGF-beta-mediated growth inhibition. Proc Natl Acad Sci USA *94*, 2386–2391.

Wang, X.-J., Liefer, K. M., Tsai, S., O'Malley, B. W., and Roop, D. R. (1999). Development of gene-switch transgenic mice that inducibly express transforming growth factor beta1 in the epidermis. Proc Natl Acad Sci USA *96*, 8483–8488.

Winter, S. L., Bosnoyan-Collins, L., Pinnaduwage, D., and Andrulis, I. L. (2007). Expression of the circadian clock genes Per1 and Per2 in sporadic and familial breast tumors. Neoplasia *9*, 797–800.

Xu, Y., Toh, K. L., Jones, C. R., Shin, J. Y., Fu, Y.-H., and Ptáček, L. J. (2007). Modeling of a Human Circadian Mutation Yields Insights into Clock Regulation by PER2. Cell *128*, 59–70.

Yamazaki, S., Iwama, A., Takayanagi, S. I., Eto, K., Ema, H., and Nakauchi, H. (2009). TGF- as a candidate bone marrow niche signal to induce hematopoietic stem cell hibernation. Blood *113*, 1250–1256.

Yang, M.-Y., Chang, J.-G., Lin, P.-M., Tang, K.-P., Chen, Y.-H., Lin, H. Y.-H., Liu, T.-C., Hsiao, H.-H., Liu, Y.-C., and Lin, S.-F. (2006a). Downregulation of circadian clock genes in chronic myeloid leukemia: alternative methylation pattern of hPER3. Cancer Sci *97*, 1298–1307.

Yang, X., Downes, M., Yu, R. T., Bookout, A. L., He, W., Straume, M., Mangelsdorf, D. J., and Evans, R. M. (2006b). Nuclear receptor expression links the circadian clock to metabolism. Cell *126*, 801–810.

Yang, X., Wood, P. A., Ansell, C. M., Quiton, D. F. T., Oh, E.-Y., Du-Quiton, J., and Hrushesky, W. J. M. (2011). THE CIRCADIAN CLOCK GENE PER1 SUPPRESSES CANCER CELL PROLIFERATION AND TUMOR GROWTH AT SPECIFIC TIMES OF DAY. Chronobiol. Int. *26*, 1323–1339.

Yi, R., Poy, M. N., Stoffel, M., and Fuchs, E. (2008). A skin microRNA promotes differentiation by repressing “stemness.” Nature *452*, 225–229.

Yoshimizu, T., Miroglio, A., Ripoche, M.-A., Gabory, A., Vernucci, M., Riccio, A.,

Colnot, S., Godard, C., Terris, B., Jammes, H., et al. (2008). The H19 locus acts in vivo as a tumor suppressor. Proceedings of the National Academy of Sciences *105*, 12417–12422.

Zhang, L., Stokes, N., Polak, L., and Fuchs, E. (2011). Specific MicroRNAs Are Preferentially Expressed by Skin Stem Cells To Balance Self-Renewal and Early Lineage Commitment. Stem Cell *8*, 294–308.

Zhang, S., Fei, T., Zhang, L., Zhang, R., Chen, F., Ning, Y., Han, Y., Feng, X. H., Meng, A., and Chen, Y. G. (2007). Smad7 Antagonizes Transforming Growth Factor Signaling in the Nucleus by Interfering with Functional Smad-DNA Complex Formation. Molecular and Cellular Biology *27*, 4488–4499.

Zhang, Y. V., Cheong, J., Ciapurin, N., McDermitt, D. J., and Tumbar, T. (2009). Distinct Self-Renewal and Differentiation Phases in the Niche of Infrequently Dividing Hair Follicle Stem Cells. Stem Cell *5*, 267–278.

Zheng, B., Albrecht, U., Kaasik, K., Sage, M., Lu, W., Vaishnav, S., Li, Q., Sun, Z. S., Eichele, G., Bradley, A., et al. (2001). Nonredundant roles of the mPer1 and mPer2 genes in the mammalian circadian clock. Cell *105*, 683–694.

Zheng, B., Larkin, D. W., Albrecht, U., Sun, Z. S., Sage, M., Eichele, G., Lee, C. C., and Bradley, A. (1999). The mPer2 gene encodes a functional component of the mammalian circadian clock. Nature *400*, 169–173.

Zhu, Y., Stevens, R. G., Hoffman, A. E., Tjonneland, A., Vogel, U. B., Zheng Tongzhang, and Hansen, J. (2011). Epigenetic Impact of Long-Term Shiftwork: Pilot Evidence From Circadian Genes and Whole-Genome Methylation Analysis. Chronobiol. Int. *28*, 852–861.

VIII ACKNOWLEDGEMENTS

I have to admit that on the one hand I think acknowledgements are very important but on the other hand it is so difficult to please everybody. What is the best way to thank people? For some people the order seems to be crucial. But who decides actually whether the first or the last person mentioned is the most important one? To avoid this problem, there is always the possibility to list people chronologically according to the time you got to know them, or very simplistic in alphabetical order. But honestly I don't favor any of those, because unfortunately my memory is not the best and it is very likely that I will forget someone. Then I have to deal with my guilty conscience next time I run into someone realizing that I should have mentioned this person. For this reason I decided to keep this section rather short. I just want to thank all the wonderful people that I met in Barcelona during the last five years. And I hope that those who are my close friends know either way what they mean to me. You are deep inside my heart and I appreciate all the wonderful time we spen(t)d together!

However, I want to thank one person in particular, because I realized that the way he supported us people from the lab was quite unique.
Salva, thank you for all the confidence, encouragement and support you gave me in the last five years. You were always listening to my problems and tried to solve them as good as you could even though you have lost a lot of hair sometimes. Thank you also for providing me the opportunity to work on this amazing project. Although it was sometimes quite difficult you never lost the faith in it and encouraged me to continue. Thank you for the ideas, suggestions and fruitful discussions that we had in our weekly meetings. I really enjoyed working with you. Gracias!

ACKNOWLEDGEMENTS

Special thanks go to following people for their help in this project:
Gloria who assisted me with the mouse work and did the analysis of the K5-SOS mice.
Lilli for her advice for the ChIP experiments. Ohne deine Hilfe wären die nie so schön geworden!
Nuno for discussing, sharing and solving problems.

Ein grosses Dankeschön an Gunther dafür, dass du so bist wie du bist, denn das gibt mir das Gefühl alles erreichen zu können.